ON THE CYCLOSTATIONARITY OF ORTHOGONAL FREQUENCY DIVISION MULTIPLEXING AND SINGLE CARRIER LINEAR DIGITAL MODULATIONS: THEORETICAL DEVELOPMENTS AND APPLICATIONS

ANJANA PUNCHIHEWA

On the Cyclostationarity of Orthogonal Frequency Division Multiplexing and Single Carrier Linear Digital Modulations: Theoretical Developments and Applications

by

© Anjana Punchihewa

A thesis submitted to the School of Graduate Studies
in partial fulfillment of the requirements for the degree of
Master of Engineering

Faculty of Engineering and Applied Science
Memorial University of Newfoundland

January 2008

St John's Newfoundland

Abstract

In recent years, new technologies for wireless communications have emerged. The wireless industry has shown great interest in orthogonal frequency division multiplexing (OFDM) technology, due to the efficiency of OFDM schemes to convey information in a frequency selective fading channel without requiring complex equalizers. On the other hand, the emerging OFDM wireless communication technology raises new challenges for the designers of intelligent radios, such as discriminating between OFDM and single-carrier modulations. To achieve this objective we study the cyclostationarity of OFDM and single carrier linear digital (SCLD) modulated signals.

In this thesis, we first investigate the *n*th-order cyclostationarity of OFDM and SCLD modulated signals embedded in additive white Gaussian noise (AWGN) and subject to phase, frequency and timing offsets. We derive the analytical closed-form expressions for the *n*th-order (*q*-conjugate) cyclic cumulants (CCs) and cycle frequencies (CFs), and the *n*th-order (*q*-conjugate) cyclic cumulant polyspectra (CCPs) of OFDM signal, and obtain a necessary and sufficient condition on the oversampling factor (per subcarrier) to avoid cycle aliasing. An algorithm based on a second-order CC is proposed to recognize OFDM against SCLD modulations in AWGN channel, as an application of signal cyclostationarity to modulation recognition problem.

We further study the *n*th-order cyclostationarity of OFDM and SCLD modulated signals, affected by a time dispersive channel, AWGN, carrier phase, and frequency and timing offsets. The analytical closed-form expressions for the *n*th-order (*q*-conjugate) CCs and

CFs, the nth-order (q-conjugate) CCPs of such signals are derived, and a necessary and sufficient condition on the oversampling factor (per subcarrier) is obtained to eliminate cycle aliasing for both OFDM and SCLD signals. We extend the applicability of the proposed algorithm in AWGN channel to time dispersive channels to recognize OFDM against SCLD modulations. The proposed algorithm obviates the preprocessing tasks; such as symbol timing, carrier and waveform recovery, and signal and noise power estimation. This is of practical significance, as algorithms that rely less on preprocessing are of crucial interest for receivers that operate with no prior information in a non-cooperative environment. It is shown that the recognition performance of the proposed algorithm in time dispersive channel is close to that in AWGN channel. In addition, we have noticed that the performance of recognizing both OFDM and SCLD signals does not depend on the modulation format used on each subcarrier for OFDM and for SCLD signals respectively.

Acknowledgements

I am deeply indebted to my supervisor, Dr. Octavia Dobre, from Memorial University of Newfoundland, whose help, suggestions and encouragements helped me throughout my master's program.

I would also like to acknowledge the generous financial support form the Defence Research Development Canada, Ottawa.

I would like to thank the people in the Computer Engineering Research Laboratory (CERL) at Memorial University of Newfoundland, for the pleasant working environment. Especially, I would like to thank Reza Shahidi for his help.

I would also like to give special thanks to my elder brother and sister-in-law, on whose constant encouragement and love I have relied through my life.

Lastly, and most important, I wish to thank my parents. They borne, raised, supported, and loved me. I dedicate this thesis to them, and my elder brother.

Table of Contents

List of Tables

List of Figures

List of Abbreviations

AWGN	Additive white Gaussian noise
BPSK	Binary Phase-Shift-Keying
CC	Cyclic cumulant
CF	Cycle frequency
CM	Cyclic moment
CCP	Cyclic cumulant polyspectrum
DSP	Digital signal processor
FB	Feature-based
FT	Fourier transform
IFFT	Inverse fast Fourier transform
ISI	Inter symbol interference
i.i.d.	Independent and identically distributed
LB	Likelihood-based
MR	Blind modulation recognition
OFDM	Orthogonal Frequency Division Multiplexing
PSK	Phase-Shift-Keying
QAM	Quadrature Amplitude Modulation
QPSK	Quadrature Phase-Shift-Keying
RRC	Root raised cosine
SCLD	Single carrier linear digital modulations
SNR	Signal-to-noise ratio

List of Symbols

a	Amplitude factor
$\tilde{\alpha}$	A CF for the CM of $r(t)$
$\otimes$	Convolution operator
β	A CF for the CC of $r(u)$, for the case when the CC order equals twice the number of conjugations
$\tilde{c}_r(t;\tilde{\boldsymbol{\tau}})_{n,q}$	The nth-order (q-conjugate) time-varying cumulant of $r(t)$
$\tilde{c}_r(\tilde{\gamma};\tilde{\boldsymbol{\tau}})_{n,q}$	The nth-order (q-conjugate) CC of $r(t)$ at CF $\tilde{\gamma}$ and delay vector $\tilde{\boldsymbol{\tau}}$
$c_r(\gamma;\boldsymbol{\tau})_{n,q}$	The nth-order (q-conjugate) CC of $r(u)$ at CF γ and delay vector $\boldsymbol{\tau}$
$\tilde{c}_{r_{\mathrm{SCLD}}}(t;\tilde{\boldsymbol{\tau}})_{n,q}$	The nth-order (q-conjugate) time-varying cumulant of $r_{\mathrm{SCLD}}(t)$
$\tilde{c}_{r_{\mathrm{SCLD}}}(\tilde{\gamma};\tilde{\boldsymbol{\tau}})_{n,q}$	The nth-order (q-conjugate) CC of $r_{\mathrm{SCLD}}(t)$ at CF $\tilde{\gamma}$ and delay vector $\tilde{\boldsymbol{\tau}}$
$c_{r_{\mathrm{SCLD}}}(\gamma;\boldsymbol{\tau})_{n,q}$	The nth-order (q-conjugate) CC of $r_{\mathrm{SCLD}}(u)$ at CF γ and delay vector $\boldsymbol{\tau}$
$\tilde{c}_{r_{\mathrm{OFDM}}}(t;\tilde{\boldsymbol{\tau}})_{n,q}$	The nth-order (q-conjugate) time-varying cumulant of $r_{\mathrm{OFDM}}(t)$
$\tilde{c}_{r_{\mathrm{OFDM}}}(\tilde{\gamma};\tilde{\boldsymbol{\tau}})_{n,q}$	The nth-order (q-conjugate) CC of $r_{\mathrm{OFDM}}(t)$ at CF $\tilde{\gamma}$ and delay vector $\tilde{\boldsymbol{\tau}}$
$c_{r_{\mathrm{OFDM}}}(\gamma;\boldsymbol{\tau})_{n,q}$	The nth-order (q-conjugate) CC of $r_{\mathrm{OFDM}}(u)$ at CF γ and delay vector $\boldsymbol{\tau}$
$c_w(\beta;\tau)_{2,1}$	The second-order (one-conjugate) CC of $w(u)$ at CF β and delay τ
$\lvert c_{r_i}(\beta;\tau)_{2,1}\rvert$	The magnitude of the second-order (one-conjugate) CC of a discrete-time signal with modulation i, at CF β and delay τ
$\lvert \hat{c}_{r_i}(\beta;\tau)_{2,1}\rvert$	The estimated second-order (one-conjugate) CC magnitude of a discrete-time signal with modulation i, at CF β and delay τ
$\tilde{C}_{r_{\mathrm{OFDM}}}(\tilde{\gamma};\tilde{\mathbf{f}})_{n,q}$	The nth-order (q-conjugate) CCP of $r_{\mathrm{OFDM}}(t)$ at CF $\tilde{\gamma}$ and spectral frequency vector $\tilde{\mathbf{f}}$
$C_{r_{\mathrm{OFDM}}}(\gamma;\mathbf{f})_{n,q}$	The nth-order (q-conjugate) CCP of $r_{\mathrm{OFDM}}(u)$ at CF γ and spectral frequency vector $\mathbf{f}$
$\tilde{C}_{r_{\mathrm{SCLD}}}(\tilde{\gamma};\tilde{\mathbf{f}})_{n,q}$	The nth-order (q-conjugate) CCP of $r_{\mathrm{SCLD}}(t)$ at CF $\tilde{\gamma}$ and spectral frequency vector $\tilde{\mathbf{f}}$
$C_{r_{\mathrm{SCLD}}}(\gamma;\mathbf{f})_{n,q}$	The nth-order (q-conjugate) CCP of $r_{\mathrm{SCLD}}(u)$ at CF γ and spectral frequency vector $\mathbf{f}$
$\hat{\mathbf{c}}_{21}$	Vector containing the real and imaginary parts of estimated second-order (one-conjugate) CC at CF β and delay τ
Cum[·]	Cumulant operator
$c_{s,n,q}$	The nth-order (q-conjugate) cumulant of the signal constellation

Δf_c	Carrier frequency offset
Δf_K	Frequency separation between two adjacent subcarriers
ε	Normalized timing offset
$\mathrm{E}[\cdot]$	Statistical expectation
f_s	Sampling frequency
$f_{2,1}(u;\tau)$	Second-order (one-conjugate) lag product of $r(u)$
$g(t)$	Overall impulse response
$g^{tr}(t)$	Transmit pulse shape
$g^{rec}(t)$	Receive filter impulse response
$h(t)$	Impulse response of the channel
$h(\tilde{\zeta}_m)$	Coefficient in the channel model, at delay $\tilde{\zeta}_m$
$\tilde{\gamma}$	A CF for the CC of $r(t)$
γ	A CF for the CC of $r(u)$
$\Psi_{2,1}$	Test statistic used in the cyclostationarity test
Γ	Threshold value used in the cyclostationarity test
$\Im\{\cdot\}$	Fourier transform
i	Modulation format, i = OFDM, SCLD
$\tilde{\kappa}^m_{n,q}$	CFs for the CM of $r(t)$
$\tilde{\kappa}^c_{n,q}$	CFs for the CC of $r(t)$
$\kappa^m_{n,q}$	CFs for the CM of $r(u)$
$\kappa^c_{n,q}$	CFs for the CC of $r(u)$
$\kappa^{\tilde{\beta}}_H$	The domain of $\tilde{\beta}$ values for bad channels
$\kappa^{\tilde{\gamma}}_H$	The domain of $\tilde{\gamma}$ values for bad channels
L	Number of samples available at the receive-side
$m_r(\alpha;\boldsymbol{\tau})_{n,q}$	The nth-order (q-conjugate) CM of $r(u)$ at CF α and delay vector $\boldsymbol{\tau}$
$\hat{m}_r(\alpha;\boldsymbol{\tau})_{n,q}$	The nth-order (q-conjugate) CM estimate at CF α and delay vector $\boldsymbol{\tau}$
n	Order of the statistic
K	Number of subcarriers
$K_{\min}$	Minimum number of subcarriers
$K_{\max}$	Maximum number of subcarriers
$P^{(i\|i)}_{cr}$	Probability of correct recognition for modulation i

P_f	Probability of false alarm
q	Number of conjugations
$Q_{2,0}$	Components of the covariance matrix used in the cyclostationarity test
$Q_{2,1}$	Components of the covariance matrix used in the cyclostationarity test
$\hat{Q}_{2,0}$	Estimator of $Q_{2,0}$
$\hat{Q}_{2,1}$	Estimator of $Q_{2,1}$
$r(t)$	Continuous-time received baseband signal
$r_{\text{SCLD}}(t)$	Continuous-time received baseband SCLD signal
$r_{\text{SCLD}}(u)$	Discrete-time received baseband SCLD signal
$r_{\text{OFDM}}(t)$	Continuous-time received baseband OFDM signal
$r_{\text{OFDM}}(u)$	Discrete-time received baseband OFDM signal
r_o	Roll-off factor
ρ	Oversampling factor (per subcarrier)
s_l	Symbol transmitted within the lth symbol period
$s_{k,l}$	Symbol transmitted within the lth symbol period and on the kth subcarrier
T	Symbol period
T_{cp}	Cyclic prefix period
T_u	Useful time period
θ	Carrier phase
$w(t)$	Continuous-time baseband Gaussian noise
$w(u)$	Discrete-time baseband Gaussian noise
$x_{\text{OFDM}}(t)$	Transmitted baseband OFDM signal
$\Sigma_{2,1}$	Covariance matrix used in the cyclostationarity test

Chapter 1

Introduction

1.1. Modulation Recognition: Problem Formulation

In recent years, new technologies for wireless communications have emerged. The wireless industry has shown great interest in OFDM, due to several advantages of OFDM, such as high capacity data transmission, immunity to multipath fading and impulsive noise and, simplicity in equalization [1]-[2]. OFDM has been adopted in a variety of applications, such as wireless local area network (WLAN) IEEE 802.11a [3] and wireless metropolitan area network (WMAN) IEEE 802.16a [4]. On the other hand, the emerging OFDM wireless communication technology raises new challenges for the designers of intelligent radios, such as discrimination of OFDM against single-carrier modulations. Solutions to tackle such new signal recognition problems need to be sought [5]. Blind modulation recognition (MR) for single carrier signals has been studied for at least a decade (see [5] and references herein). Algorithms for discriminating between OFDM and single-carrier signals have been recently started to be investigated by the research community [6]-[8]. However, algorithms proposed in the literature to recognize the OFDM require either carrier or timing recovery [6]-[10], or estimation of signal-to-noise ratio [8], before the recognition algorithm is applied. This effort explores the applicability of signal cyclostationarity to distinguish OFDM against the class of single carrier linear digital (SCLD) modulations.

MR is an intermediate step between signal interception and data demodulation. This is a difficult task, especially in a non-cooperative environment, in which no prior knowledge on the detected signal is available at the receive-side. Once the modulation format is correctly identified, other operations, such as signal demodulation and information extraction can be subsequently performed. The design of a modulation classifier essentially involves two steps; a signal preprocessing and proper selection of a modulation recognition algorithm. A simplified block diagram of an intelligent receiver is depicted in Fig. 1.1.

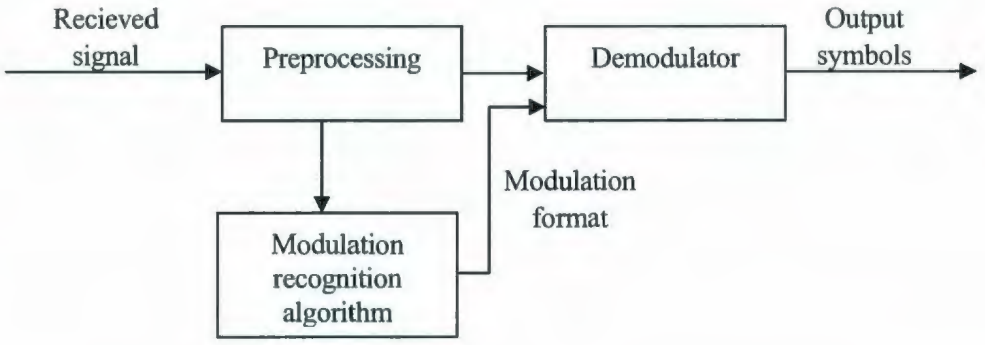

Figure 1.1: Simplified block diagram of an intelligent receiver

Preprocessing tasks includes, but not limited to, perform some or all of, noise removal, estimation of carrier frequency, symbol period and signal power, equalization, etc. The required accuracy in preprocessing depends on the recognition algorithm chosen in the second step. For example, some recognition methods need more precise estimates, whereas some are less sensitive to unknown parameters [5].

Generally, two approaches are proposed to tackle the MR problem, i.e., the likelihood-based (LB) and the feature-based (FB) methods (see [5] and references herein). The LB approach is based on the likelihood function of the received signal and the

likelihood ratio test is used for decision making. This can provide an optimal solution, in the sense that it maximizes the probability of false recognition. However, a complete mathematical representation of an optimal classifier is very complex even for simple modulation formats [5]. With the latter approach, features are extracted from the received signal, and a decision on the modulation format is made based on their differences. Several signal features have been investigated in the open literature, such as moments and cumulants, cyclic moments and cyclic cumulants, and wavelet transform [5]. The FB approach can have the advantage of implementation simplicity for an appropriately chosen feature set, and can provide near optimal performance.

Here we exploit signal cyclostationarity to distinguish OFDM against SCLD modulations. In general, cyclostationary signals are present in communications, signal processing, telemetry, radar, sonar, and control systems. Signal cyclostationarity can be exploited for several purposes, including signal identification, blind equalization, synchronization, parameter estimation and modulation recognition [6]-[22]. Communication signals exhibit cyclostationarity in connection with the symbol period, carrier frequency, chip rate and combination of these [6]-[7] and [11]-[22]. First-, second- and higher-order cyclostationarity of single carrier signals is employed for the aforementioned applications in [11]-[17], [21]-[22]. In particular, second-order cyclostationarity of the OFDM signal is exploited for blind estimation of symbol timing and carrier frequency offset, extraction of channel allocation information in a spectrum poling system, and blind channel identification [18]-[20].

1.2. Thesis Objectives

The main objective of this research is to find a feature-based blind recognition algorithm to identify OFDM against SCLD modulations, which is easy to implement, and still can provide good recognition performance. To achieve this objective, we investigate the cyclostationarity of OFDM and SCLD signals. Firstly, we study the nth-order cyclostationarity of OFDM and SCLD modulated signals embedded in additive white Gaussian noise (AWGN) and subject to phase, frequency and timing offsets. The analytical closed-form expressions for the nth-order (q-conjugate) cyclic cumulants (CCs) and cycle frequencies (CFs), and nth-order (q-conjugate) cyclic cumulant polyspectra (CCPs) of OFDM signals are derived. Such expressions for the SCLD signals are presented in [11]. An algorithm based on a second-order CC is proposed to recognize OFDM against SCLD modulations in AWGN channel. In addition, we obtain a necessary and sufficient condition on the oversampling factor (per subcarrier) to avoid cycle aliasing for OFDM signals. Note that such a condition for SCLD signals is obtained in [11]. Secondly, we investigate the nth-order cyclostationarity of OFDM and SCLD modulated signal affected by a time dispersive channel, AWGN, carrier phase, and frequency and timing offsets. We derive the analytical closed-form expressions for the nth-order (q-conjugate) CCs and CFs, and the nth-order (q-conjugate) CCPs of these signals, and obtain a necessary and sufficient condition on the oversampling factor (per subcarrier) to eliminate cycle aliasing for both OFDM and SCLD. We extend the applicability of the algorithm proposed for AWGN channel to time dispersive channel, to discriminate OFDM against SCLD. The proposed algorithm has the advantage that it does not require

preprocessing tasks, such as symbol timing, carrier and waveform recovery, and signal and noise power estimation. This is of practical significance, as algorithms that rely less on preprocessing are of crucial interest for receivers that operate with no prior information in non-cooperative environments. Both recognition performance and complexity of the proposed algorithm are investigated for AWGN and time dispersive channels.

1.3. Thesis Organization

The rest of the thesis is organized as follows. Fundamental concepts of signal cyclostationarity are introduced in Chapter 2. Single carrier linearly digitally modulated and OFDM signal models, along with corresponding signal cyclostationarity, and proposed recognition algorithm in AWGN and time dispersive channels are presented in Chapter 3 and Chapter 4, respectively. Finally, conclusions are drawn in Chapter 5.

Chapter 2

Signal Cyclostationarity: Fundamental Concepts

2.1. Introduction

Signal cyclostationarity has been used as a statistical tool for several applications, including signal identification, blind equalization, synchronization, parameter estimation and modulation recognition [6]-[22]. In communications, signals exhibit cyclostationarity in connection with symbol period, carrier frequency, chip rate and combination of these [6]-[7]. The cyclostationary signals have been studied either within a stochastic [23]-[24] or a fraction-of-time probability framework [22], [25]. Here, we first introduce the fundamental concepts of continuous-time cyclostationary processes, using the stochastic framework. Then, we briefly review the fundamental concepts of discrete-time cyclostationary processes. For the modulation recognition application, we employed discrete-time processes obtained by sampling continuous-time cyclostationary processes.

2.2. Signal Cyclostationarity

A signal exhibits *n*th-order cyclostationarity if its *n*th- and lower-order time-variant cumulants are almost-periodic functions[1] of time [22]-[25]. For a complex-valued

[1] A function $r(t)$, real or complex, defined for all real arguments t, is said to possess a translation number τ_ε pertaining to the positive number ε, if for all values of t from $-\infty$ to ∞, $|r(t+\tau_\varepsilon)-r(t)|\leq\varepsilon$. The continuous function $r(t)$ is then said to be almost periodic if, whenever ε is given, there exists a finite number l_ε, such that if v is any real number, the interval $(v, v+l_\varepsilon)$ contains at least one translation number τ_ε pertaining to ε.

continuous-time nth-order cyclostationary process, $r(t)$, the nth-order (q-conjugate) time-varying cumulant,

$$\tilde{c}_r(t;\tilde{\boldsymbol{\tau}})_{n,q} = \mathrm{Cum}[r^{(*)_1}(t+\tilde{\tau}_1), r^{(*)_2}(t+\tilde{\tau}_2), \ldots, r^{(*)_n}(t+\tilde{\tau}_n)], \tag{2.1}$$

is an almost periodic function of time. Here $\mathrm{Cum}[\cdot]$ represents the cumulant operator (for the definition one can see, e.g. [22]), $\tilde{\boldsymbol{\tau}} = [\tilde{\tau}_1, \ldots, \tilde{\tau}_n]^{\dagger}\big|_{\tilde{\tau}_n = 0}$ is the delay vector and $(*)_i$, $i = 1, \ldots, n$, is a possible conjugation, with the total number of conjugations equal to q and $\dagger$ as the transpose. This time-varying cumulant can be expressed as a Fourier series [22]-[25]

$$\tilde{c}_r(t,\tilde{\boldsymbol{\tau}})_{n,q} = \sum_{\tilde{\gamma} \in \tilde{\kappa}^c_{n,q}} \tilde{c}_r(\tilde{\gamma};\tilde{\boldsymbol{\tau}})_{n,q} e^{j2\pi\tilde{\gamma}t}, \tag{2.2}$$

where $\tilde{\kappa}^c_{n,q} = \{\tilde{\gamma} \mid \tilde{c}_r(\tilde{\gamma};\tilde{\boldsymbol{\tau}})_{n,q} \neq 0\}$ represents the nth-order cycle frequencies (CFs) (for cyclic cumulants) and the coefficient $\tilde{c}_r(\tilde{\gamma};\tilde{\boldsymbol{\tau}})_{n,q}$ is the nth-order (q-conjugate) cyclic cumulant (CC) at CF $\tilde{\gamma}$ and delay vector $\tilde{\boldsymbol{\tau}}$, which can be expressed as [22]-[25]

$$\tilde{c}_r(\tilde{\gamma};\tilde{\boldsymbol{\tau}})_{n,q} = \lim_{I \to \infty} I^{-1} \int_{-I/2}^{I/2} \tilde{c}_r(t;\tilde{\boldsymbol{\tau}})_{n,q} e^{-j2\pi\tilde{\gamma}t} dt. \tag{2.3}$$

For the nth-order cyclostationarity process $r(t)$, the nth-order (q-conjugate) time-varying moment function

$$\tilde{m}_r(t;\tilde{\boldsymbol{\tau}})_{n,q} = \mathrm{E}[r^{(*)_1}(t+\tilde{\tau}_1), r^{(*)_2}(t+\tilde{\tau}_2), \ldots, r^{(*)_n}(t+\tilde{\tau}_n)], \tag{2.4}$$

is also an almost periodic function of time [22]-[25]. Here $\mathrm{E}[\cdot]$ denotes the statistical expectation. This time-varying moment can also be expressed as a Fourier series [22]-[25]

$$\tilde{m}_r(t,\tilde{\boldsymbol{\tau}})_{n,q} = \sum_{\tilde{\alpha} \in \tilde{\kappa}^m_{n,q}} \tilde{m}_r(\tilde{\alpha};\tilde{\boldsymbol{\tau}})_{n,q} e^{j2\pi\tilde{\alpha}t}, \tag{2.5}$$

where $\tilde{\kappa}_{n,q}^{m} = \{\tilde{\alpha} \mid \tilde{m}_r(\tilde{\alpha};\tilde{\tau})_{n,q} \neq 0\}$ represents the nth-order CFs (for cyclic moments), and the coefficient $\tilde{m}_r(\tilde{\alpha};\tilde{\tau})_{n,q}$ is the nth-order (q-conjugate) cyclic moment (CM) at CF $\tilde{\alpha}$ and delay vector $\tilde{\tau}$, given by [22]-[25]

$$\tilde{m}_r(\tilde{\alpha};\tilde{\tau})_{n,q} = \lim_{I\to\infty} I^{-1} \int_{-I/2}^{I/2} \tilde{m}_r(t;\tilde{\tau})_{n,q} e^{-j2\pi\tilde{\alpha}t} dt. \tag{2.6}$$

The nth-order (q-conjugate) cumulant can be expressed in terms of the nth- and lower-order moments by using the moment-to-cumulant formula [25],

$$\tilde{c}_r(t;\tilde{\tau})_{n,q} = \sum_{\{\wp_1,\ldots,\wp_Z\}} (-1)^{(Z-1)}(Z-1)! \prod_{z=1}^{Z} \tilde{m}_r(t;\tilde{\tau}_z)_{n_z,q_z}, \tag{2.7}$$

where $\{\wp_1,\ldots,\wp_Z\}$ is a partition of $\wp = \{1,2,\ldots,n\}$, with $\wp_z$, $z = 1,\ldots,Z$, as a non-empty disjoint subset of $\wp$, so that the reunion of these subsets is $\wp$, Z is the number of subsets in a partition $(1 \le Z \le n)$, τ_z is a delay vector whose components are elements of $\{\tau_u\}_{u=1}^{n}$, with indices specified by $\wp_z$, and n_z is the number of elements in the subset $\wp_z$, from which q_z corresponds to conjugate terms, with $\sum_{z=1}^{Z} n_z = n$ and $\sum_{z=1}^{Z} q_z = q$.

By combining (2.2), (2.5) and (2.7), the nth-order (q-conjugate) CC of $r(t)$ at CF $\tilde{\gamma}$ and delay vector $\tilde{\tau}$ can be expressed using the nth- and lower-order CMs as [25]

$$\tilde{c}_r(\tilde{\gamma};\tilde{\tau})_{n,q} = \sum_{\{\wp_1,\ldots,\wp_Z\}} (-1)^{(Z-1)}(Z-1)! \sum_{\tilde{\boldsymbol{\alpha}}^{\dagger}\mathbf{1}=\tilde{\gamma}} \prod_{z=1}^{Z} \tilde{m}_r(\tilde{\alpha};\tilde{\tau}_z)_{n_z,q_z}, \tag{2.8}$$

where $\tilde{\boldsymbol{\alpha}} = [\tilde{\alpha}_1,\ldots,\tilde{\alpha}_Z]^{\dagger}$ is a vector of CFs and $\mathbf{1} = [1,\ldots,1]^{\dagger}$ is a Z-dimensional one vector. Equation (2.8) is referred to as the cyclic moment-to-cumulant formula [25].

The nth-order (q-conjugate) cyclic cumulant polyspectrum (CCP) of the cyclostationary process, $r(t)$, at CF $\tilde{\gamma}$ and spectral frequency vector $\tilde{\mathbf{f}}$, is defined as the $(n-1)$-dimensional Fourier transform of the nth-order (q-conjugate) CC [23], [25]

$$\tilde{C}_r(\tilde{\gamma};\tilde{\mathbf{f}})_{n,q} = \int_{-\infty}^{\infty} \tilde{c}_r(\tilde{\gamma};\tilde{\boldsymbol{\tau}})_{n,q} e^{-j2\pi\tilde{\mathbf{f}}^{\dagger}\tilde{\boldsymbol{\tau}}} d\tilde{\boldsymbol{\tau}}, \tag{2.9}$$

where $\tilde{\mathbf{f}} = [\tilde{f}_1,\ldots,\tilde{f}_{n-1}]^{\dagger}$.

A discrete-time signal $r(u) = r(t)\big|_{t=uf_s^{-1}}$ is obtained by periodically sampling the continuous-time signal $r(t)$ at rate f_s. The nth-order (q-conjugate) CCP of the discrete-time signal, $r(u)$, at CF γ and spectral frequency vector $\mathbf{f}$, is given by [26]

$$C_r(\gamma;\mathbf{f})_{n,q} = f_s^{n-1} \sum_{v\in Z} \sum_{\mathbf{v}\in Z^{n-1}} \tilde{C}_r(\tilde{\gamma} - vf_s;\tilde{\mathbf{f}} - \mathbf{v}f_s)_{n,q} \tag{2.10}$$

where $\gamma = \tilde{\gamma} f_s^{-1}$, $\mathbf{f} = \tilde{\mathbf{f}} f_s^{-1}$, with components $f_u = \tilde{f}_u f_s^{-1}$, $u = 1,\ldots,n-1$, Z is the set of all integers, and $\mathbf{v} = [v_1 \ldots v_{n-1}]^{\dagger}$, with v_u, $u = 1,\ldots,n-1$, as an integer. One can notice that the nth-order CCP of the sampled signal consists of the periodic extension of the nth-order CCP of the original continuous signal, in both spectral $(\tilde{\mathbf{f}} - \mathbf{v}f_s)$ and cycle frequency $(\tilde{\gamma} - vf_s)$ domains. Two kinds of aliasing effects can appear due to sampling, i.e., spectral aliasing, which is overlapping of images of CCP with the same CF, and cycle aliasing, which is the overlapping of images of the CCP with different CFs. Sampling has to be carried out such that both spectral and cycle aliasing are eliminated. Apparently, for a band-limited signal, the Nyquist condition has to be fulfilled to eliminate aliasing in the spectral frequency domain. For the cycle frequency domain, the support of $\tilde{\gamma}$ has to be found in order to obtain a condition to eliminate cycle aliasing.

Under the assumption of no aliasing, the nth-order (q-conjugate) CC of the discrete-time signal, $r(u)$, the nth-order (q-conjugate) CCP, and the corresponding CFs, are respectively given by [26]

$$c_r(\gamma;\boldsymbol{\tau})_{n,q} = \tilde{c}_r(\gamma f_s;\boldsymbol{\tau} f_s^{-1})_{n,q}, \tag{2.11}$$

$$C_r(\gamma;\mathbf{f})_{n,q} = f_s^{n-1}\tilde{C}_r(\gamma f_s;\mathbf{f} f_s)_{n,q}, \tag{2.12}$$

and

$$\kappa^c_{n,q} = \{\gamma \in [-1/2, 1/2) |\ \gamma = \tilde{\gamma} f_s^{-1},\ c_r(\gamma;\boldsymbol{\tau})_{n,q} \neq 0\}, \tag{2.13}$$

where $\boldsymbol{\tau} = \tilde{\boldsymbol{\tau}} f_s$, with components $\tau_u = \tilde{\tau}_u f_s$, $u = 1,\ldots,n$.

Similar expressions can be written for the nth-order (q-conjugate) CM of the discrete-time signal, $m_r(\alpha;\boldsymbol{\tau})_{n,q}$, cycle moment polyspectrum, and corresponding CFs, $\kappa^m_{n,q}$ [23].

The estimator for the nth-order (q-conjugate) CM at a CF α and delay vector $\boldsymbol{\tau}$, based on L samples, is given by [24]

$$\hat{m}_r(\alpha;\boldsymbol{\tau})_{n,q} = L^{-1}\sum_{u=1}^{L}\prod_{p=1}^{n} r^{(*)_p}(u+\tau_p)e^{-j2\pi\alpha u}. \tag{2.14}$$

Furthermore, the estimator for the nth-order (q-conjugate) CC at a CF γ and delay vector $\boldsymbol{\tau}$, based on L samples, $\hat{c}_r(\gamma;\boldsymbol{\tau})_{n,q}$, can be obtained by applying the cyclic moment-to-cumulant formula given in (2.8), with CMs replaced by their estimates given in (2.14) [24]. For the estimator of the nth-order (q-conjugate) CCP one can see, for example, [23].

Chapter 3

Cyclostationarity-Based Recognition of OFDM Against SCLD in AWGN Channel

3.1. Introduction

Blind recognition of the modulation format of a received signal is of importance in a variety of military and commercial applications, such as electronic warfare, surveillance and control of broadcasting activities, spectrum monitoring and management, and cognitive radio. Although this topic has been extensively studied (see the comprehensive survey [5] and reference herein), less attention has been paid to the identification of OFDM signals. In recent years OFDM has been adopted in a variety of applications, such as WLANs and WMANs. Algorithms to recognize OFDM against SCLD signals have been reported in [8]-[9]. The algorithms proposed in [8], [9] and [10] require estimation of signal-to-noise ratio, carrier frequency recovery, and both carrier frequency and timing recovery as preprocessing tasks. In this Chapter, we investigate the cyclostationarity of OFDM signals with a view to recognizing OFDM against SCLD. The analytical closed-form expressions for the nth-order (q-conjugate) CCs and CFs, and CCPs of an OFDM signal embedded in additive white Gaussian noise and subject to phase, frequency and timing offsets are derived. In addition, a necessary and sufficient condition on the oversampling factor (per subcarrier) to eliminate cycle aliasing is derived for OFDM signals. An algorithm based on a second-order CC is proposed to recognize OFDM against

SCLD modulations. The proposed recognition algorithm obviates the need for preprocessing tasks, such as symbol timing estimation, carrier and waveform recovery, and signal and noise power. The performance of the proposed recognition algorithm is evaluated through simulations. The average probability of correct recognition, P_{cr}, is used as a performance measure for performance evaluation.

3.2. Cyclostationarity of Single Carrier Linearly Digitally Modulated Signals

3.2.1. Signal Model

Let us assume that a single carrier linearly digitally modulated signal is transmitted through a channel, which corrupts the signal by adding white Gausian noise. The output of the matched filter at the receive-side is a baseband waveform, given by [27]

$$r_{\mathrm{SCLD}}(t) = a e^{j\theta} e^{j2\pi\Delta f_c t} \sum_{l=-\infty}^{\infty} s_l g(t - lT - \varepsilon T) + w(t), \tag{3.1}$$

where a is the amplitude factor, θ is the phase, Δf_c is the carrier frequency offset, T is the symbol period, $0 \le \varepsilon \le 1$ is the normalized timing offset, s_l represents the symbol transmitted within the lth symbol period drawn either from a quadrature amplitude modulation (QAM) or phase shift keying (PSK) constellation, $g(t)$ is the overall impulse response of the transmit and receive filters and $w(t)$ is the zero-mean complex Gaussian noise. The overall impulse response of the transmit and receive filters in cascade is given by $g(t) = g^{tr}(t) \otimes g^{rec}(t)$, with $g^{tr}(t)$ and $g^{rec}(t)$ as the impulse response of the transmit and

receive filters, respectively and $\otimes$ as the convolution operator. The data symbols $\{s_l\}$ are assumed to be zero-mean independent and identically distributed (i.i.d.) random variables.

The discrete-time baseband signal $r_{\text{SCLD}}(u)$, obtained by oversampling $r_{\text{SCLD}}(t)$ at rate $f_s = \rho T^{-1}$, with ρ as the number of samples per symbol (oversampling factor), is given by

$$r_{\text{SCLD}}(u) = ae^{j\theta} e^{j\frac{2\pi}{\rho}\Delta f_c T u} \sum_{l=-\infty}^{\infty} s_l g(u - l\rho - \varepsilon\rho) + w(u), \tag{3.2}$$

where $w(u)$ is wide-sense stationary zero-mean complex Gaussian noise.

3.2.2. Cyclostationarity of Received SCLD Modulated Signals

For the continuous-time baseband received signal, $r_{\text{SCLD}}(t)$, the nth-order (q-conjugate) time-varying cumulant at delay vector $\tilde{\tau}$ is given by [11]

$$\tilde{c}_{r_{\text{SCLD}}}(t;\tilde{\boldsymbol{\tau}})_{n,q} = a^n c_{s,n,q} e^{j(n-2q)\theta} e^{j2\pi\Delta f_c \sum_{p=1}^{n}(-)_p \tilde{\tau}_p} e^{j2\pi(n-2q)\Delta f_c t}$$
$$\times \prod_{p=1}^{n} g^{(*)_p}(t + \tilde{\tau}_p) \otimes \sum_{l=-\infty}^{\infty} \delta(t - lT - \varepsilon T) + \tilde{c}_w(t;\tilde{\boldsymbol{\tau}})_{n,q}, \tag{3.3}$$

where $c_{s,n,q}$ is the nth-order (q-conjugate) cumulant of the signal constellation, $\tilde{c}_w(t;\tilde{\boldsymbol{\tau}})_{n,q}$ [2] is the nth-order (q-conjugate) time-varying cumulant of $w(t)$, $(-)_p$ is the optional minus sign associated with the optional conjugation $(*)_p$, $p = 1,...,n$, $\delta(t)$ is the Dirac delta function. The values of delays, $\tilde{\tau}$, are defined within the symbol interval (for rectangular pulse shape). At zero-delays, the cumulant magnitude reaches a maximum, and as the delay

[2] For $n = 1$ and $n \geq 3$ there is no additive contribution of the wide-sense stationary zero-mean Gaussian noise to the cumulant of the received signal. For n=2, the cumulant corresponding to the noise does not depend on time, due to the wide- sense stationarity of the noise.

values increase towards the symbol duration, the cumulant magnitude reduces to zero. The delay values for which the CCs are non-zero can exceed the symbol period for a non-rectangular pulse shape.

The nth-order (q-conjugate) CC at CF $\tilde{\gamma}$ and delay vector $\tilde{\boldsymbol{\tau}}$, the nth-order (q-conjugate) CCP at CF $\tilde{\gamma}$ and spectral frequency vector $\tilde{\mathbf{f}}$, and the CFs for the continuous-time signal $r_{\mathrm{SCLD}}(t)$ are respectively given by [11], [13]

$$\tilde{c}_{r_{\mathrm{SCLD}}}(\tilde{\gamma};\tilde{\boldsymbol{\tau}})_{n,q} = a^n c_{s,n,q} T^{-1} e^{j(n-2q)\theta} e^{-j2\pi\tilde{\beta}\varepsilon T} e^{j2\pi\Delta f_c \sum_{p=1}^{n}(-)_p \tilde{\tau}_p} \times \int_{-\infty}^{\infty} \prod_{p=1}^{n} g^{(*)_p}(t+\tilde{\tau}_p) e^{-j2\pi\tilde{\beta}t} dt + \tilde{c}_w(\tilde{\gamma};\tilde{\boldsymbol{\tau}})_{n,q}, \tag{3.4}$$

$$\tilde{C}_{r_{\mathrm{SCLD}}}(\tilde{\gamma};\tilde{\mathbf{f}})_{n,q} = a^n c_{s,n,q} T^{-1} e^{j(n-2q)\theta} e^{j2\pi\tilde{\beta}\varepsilon T} \prod_{p=1}^{n-1} G^{(*)_p}((-)_p \tilde{f}_p - \Delta f_c) \times G^{(*)_n}((-)_n(\tilde{\beta} - \sum_{p=1}^{n-1}(-)_p((-)_p \tilde{f}_p - \Delta f_c))) + \tilde{C}_w(\tilde{\gamma};\tilde{\mathbf{f}})_{n,q}, \tag{3.5}$$

and

$$\tilde{\kappa}_{n,q}^{\mathrm{SCLD}} = \{\tilde{\gamma} \mid \tilde{\gamma} = \tilde{\beta} + (n-2q)\Delta f_c,\ \tilde{\beta} = lT^{-1},\ l \text{ integer},\ \tilde{c}_{r_{\mathrm{SCLD}}}(\tilde{\gamma};\tilde{\boldsymbol{\tau}})_{n,q} \neq 0\}, \tag{3.6}$$

where $\tilde{c}_w(\tilde{\gamma};\tilde{\boldsymbol{\tau}})_{n,q}$ and $\tilde{C}_w(\tilde{\gamma};\tilde{\mathbf{f}})_{n,q}$ are the nth-order (q-conjugate) CC and CCP of $w(t)$, respectively.

A necessary and sufficient condition on the oversampling factor, ρ, to eliminate cycle aliasing has been derived in [11] for a raised cosine pulse shape as

$$\rho \geq n(1+r_o), \tag{3.7}$$

where r_o is the roll-off factor.

One can easily show that (3.7) is valid for any SCLD signal, which is band-limited to $W=(1+r_0)(2T)^{-1}$. As an example, with $n=2$ and $r_0=0.35$, a necessary and sufficient condition on the oversampling factor, ρ, is $\rho \geq 3$.

Under the assumption of no aliasing, the expressions for the *n*th-order (*q*-conjugate) CC, CCP, and CFs for the discrete-time SCLD signal, $r_{\text{SCLD}}(u)$, can be easily obtained based on (3.4)-(3.6) and by using (2.11)-(2.13). Note that the cumulant $c_{s,n,q}$ of odd order (*n* odd) is zero for symmetric signal constellatioins, in which case the lowest order non-zero CC and CCP are of second-order [11]. For numerical values of $c_{s,n,q}$ for diverse orders, *n*, number of conjugations, *q*, and SCLD modulations, one can see [11], [13].

3.3. Cyclostationarity of OFDM Signals

3.3.1. Signal Model

The continuous-time baseband equivalent of a transmitted OFDM signal is given by [18],

$$x_{\text{OFDM}}(t)=\frac{1}{\sqrt{K}}\sum_{k=0}^{K-1}\sum_{l=-\infty}^{\infty}s_{k,l}\ e^{j2\pi k\Delta f_K(t-lT)}g^{tr}(t-lT), \tag{3.8}$$

where K is the number of subcarriers, Δf_K is the frequency separation between two adjacent subcarriers, T is the OFDM symbol period, given by $T=T_u+T_{cp}$, with $T_u=1/\Delta f_K$ as the useful symbol duration and T_{cp} as the length of the cyclic prefix, $s_{k,l}$ is the symbol transmitted within the *l*th symbol period and the *k*th subcarrier, and $g^{tr}(t)$ is the transmit pulse shaping window [2]. The data symbols $\{s_{k,l}\}$ are assumed to be zero-mean i.i.d. random variables, drawn either from a QAM or PSK constellation.

At the receiver-side, the continuous-time baseband equivalent is given by

$$r_{\text{OFDM}}(t)= ae^{j\theta}e^{j2\pi\Delta f_c t}\sum_{k=0}^{K-1}\sum_{l=-\infty}^{\infty} s_{k,l}\ e^{j2\pi k\Delta f_K (t-lT-\varepsilon T)}g(t-lT-\varepsilon T)+w(t), \qquad (3.9)$$

where $g(t)=g^{tr}(t)\otimes g^{rec}(t)$.

A discrete-time baseband OFDM signal, $r_{\text{OFDM}}(u)$, is obtained by oversampling $r_{\text{OFDM}}(t)$ at a rate $f_s=\rho K T_u^{-1}$, where ρK is a positive integer, which represents the oversampling factor per subcarrier in the useful symbol duration, with ρ as the number of samples per symbol per subcarrier (oversampling factor per subcarrier). For SCLD signals, the number of (sub)carriers is one and ρ simply represents the oversampling factor (the number of samples per symbol). The expression for the discrete-time baseband OFDM signal can be easily written as,

$$r_{\text{OFDM}}(u) = ae^{j\theta}e^{j\frac{2\pi}{\rho K}\Delta f_c T_u u}\sum_{k=0}^{K-1}\sum_{l=-\infty}^{\infty} s_{k,l}\ e^{j\frac{2\pi}{\rho K}k(u-lD-\varepsilon D)}g(u-lD-\varepsilon D)+w(u), \qquad (3.10)$$

where $D=\rho K(1+T_{cp}T_u^{-1})$ is the number of samples over an OFDM symbol.

Note that equations (3.1) and (3.2) represent particular cases of (3.9) and (3.10), respectively, $K=1$ and no cyclic prefix, $T_{cp}=0$ ($T=T_u$).

3.3.2. Cyclostationarity Of Received OFDM Signals

Results derived in Appendices A and B for the *n*th-order cyclostationarity of the received OFDM signal are presented in the following. The *n*th-order (*q*-conjugate) time-varying cumulant of the continuous-time baseband received OFDM signal, $r_{\text{OFDM}}(t)$, at delay vector $\tilde{\boldsymbol{\tau}}$ (see Appendix A for the comments on the delay values) is given by [2]

$$\tilde{c}_{r_{\mathrm{OFDM}}}(t;\tilde{\boldsymbol{\tau}})_{n,q} = a^n c_{s,n,q} e^{j(n-2q)\theta} e^{j2\pi\Delta\Delta f_c \sum_{p=1}^{n}(-)_p \tilde{\tau}_p} e^{j2\pi(n-2q)\Delta f_c t} \sum_{k=0}^{K-1} e^{j2\pi k\Delta f_K \sum_{p=1}^{n}(-)_p \tilde{\tau}_p}$$

$$\times e^{j2\pi(n-2q)k\Delta f_K t} \prod_{p=1}^{n} g^{(*)_p}(t+\tilde{\tau}_p) \otimes \sum_{l=-\infty}^{\infty} \delta(t-lT-\varepsilon T) + \tilde{c}_w(t;\tilde{\boldsymbol{\tau}})_{n,q}. \quad (3.11)$$

The nth-order (q-conjugate) CC at CF $\tilde{\gamma}$ and delay vector $\tilde{\boldsymbol{\tau}}$, the nth-order (q-conjugate) CCP at CF $\tilde{\gamma}$ and spectral frequency vector $\tilde{\mathbf{f}}$, and the CFs for the continuous-time baseband received OFDM signal, $r_{\mathrm{OFDM}}(t)$, are respectively given as

$$\tilde{c}_{r_{\mathrm{OFDM}}}(\tilde{\gamma};\tilde{\boldsymbol{\tau}})_{n,q} = a^n c_{s,n,q} T^{-1} e^{j(n-2q)\theta} e^{-j2\pi\tilde{\beta}\varepsilon T} e^{j2\pi\Delta f_c \sum_{p=1}^{n}(-)_p \tilde{\tau}_p} \sum_{k=0}^{K-1} e^{j2\pi k\Delta f_K \sum_{p=1}^{n}(-)_p \tilde{\tau}_p}$$

$$\times \int_{-\infty}^{\infty} e^{j2\pi(n-2q)k\Delta f_K t} \prod_{p=1}^{n} g^{(*)_p}(t+\tilde{\tau}_p) e^{-j2\pi\tilde{\beta}t} dt + \tilde{c}_w(\tilde{\gamma};\tilde{\boldsymbol{\tau}})_{n,q}, \quad (3.12)$$

$$\tilde{C}_{r_{\mathrm{OFDM}}}(\tilde{\gamma};\tilde{\mathbf{f}})_{n,q} = a^n c_{s,n,q} T^{-1} e^{j(n-2q)\theta} e^{-j2\pi\tilde{\beta}\varepsilon T} \sum_{k=0}^{K-1} \prod_{p=1}^{n-1} G^{(*)_p}((-)_p \tilde{f}_p - \Delta f_c - k\Delta f_K)$$

$$\times G^{(*)_n}((-)_n(\tilde{\beta} - (\sum_{p=1}^{n-1}(-)_p((-)_p \tilde{f}_p - \Delta f_c - k\Delta f_K)) - (n-2q)k\Delta f_K))$$

$$+\tilde{C}_w(\tilde{\gamma};\tilde{\mathbf{f}})_{n,q}, \quad (3.13)$$

and

$$\tilde{\kappa}_{n,q}^{\mathrm{OFDM}} = \{\tilde{\gamma} \mid \tilde{\gamma} = \tilde{\beta} + (n-2q)\Delta f_c,\ \tilde{\beta} = lT^{-1},\ l \text{ integer}\}. \quad (3.14)$$

A necessary and sufficient condition on the oversampling factor (per subcarrier), ρ, to eliminate cycle aliasing in AWGN channel is derived in Appendix C, which will be presented in the subsequent section. Under the assumption of no aliasing, the expressions for the nth-order (q-conjugate) CC, CCP, and CFs for the discrete-time OFDM signal, $r_{\mathrm{OFDM}}(u)$, can be easily derived based on (3.12)-(3.14) and by using (2.11)-(2.13).

Note that (3.4), (3.12) and (3.5), (3.13) give the analytical expressions for the CC and CCP, respectively, only at CFs and certain delays (see Appendix A for comment on the delay). At other frequencies and delays, the CC and CCP equal to zero. It is also to be noted that (3.4)-(3.6) are particular cases of (3.12)-(3.14) for a single carrier ($K=1$) and no cyclic prefix ($T_{cp}=0$, $T=T_u$). This is expected from the comments on the signal models. From (3.4) and (3.12) one can see that the *n*th-order (*q*-conjugate) CCs of both SCLD and OFDM signals depend on the *n*th power of the signal amplitude, the *n*th-order (*q*-conjugate) cumulant of the signal constellation, phase, timing offset, carrier frequency offset, pulse shape, and symbol period. In addition, the CC of the OFDM signal depends on the number of subcarriers, K , and frequency separation between two adjacent subcarriers, Δf_K . However, the CC magnitude of the signal component does not depend on phase, and timing and carrier frequency offsets. Owing to the nature of the noise, $c_w(\gamma;\boldsymbol{\tau})_{n,q}$ is non-zero only for $n=2$ and $q=1$, at zero CF and for zero delay vector. From (3.5) and (3.13) it can be noticed that the *n*th-order (*q*-conjugate) CCP of SCLD and OFDM signals depends on the *n*th power of the signal amplitude, the *n*th-order (*q*-conjugate) cumulant of the signal constellation, phase, timing offset, carrier frequency offset, symbol period, and the Fourier transform of the pulse shape. In addition, the CCP of the OFDM signal depends on the number of subcarriers, K , and frequency separation between two adjacent subcarriers, Δf_K . According to (3.6) and (3.14), if $n=2q$, the CFs are integer multiples of the inverse of the SCLD and OFDM symbol period, respectively. Otherwise, there is a shift of these values due to the carrier frequency offset, Δf_c .

3.3.3. A Necessary and Sufficient Condition on the Oversampling Factor (per Subcarrier) to Eliminate Cycle Aliasing for OFDM Signals

In several signal processing applications, cyclostationary continuous-time signals are subject to sampling operations. This leads to aliasing in both cycle and spectral frequency domains [26]. In our analysis, the continuous-time signal, $r_i(t)$, $i = \text{OFDM, SCLD}$ is oversampled at the output of the receive lowpass filter. Therefore, it is important to find a condition to eliminate aliasing.

As mentioned in Chapter 2, the Nyquist condition has to be fulfilled to eliminate spectral aliasing. On the other hand, we show that to eliminate cycle aliasing, a necessary and sufficient condition on the oversampling factor (per subcarrier), ρ, has to be fulfilled. This is as follows (see Appendix C for derivations):

$$\rho \geq |n-2q| + \left\lceil K^{-1}(2nT_u T^{-1} - |n-2q|) \right\rceil, \tag{3.15}$$

where $\lceil . \rceil$ denotes the nearest largest integer.

Note that this result is valid for n even. For n odd we cannot derive such a condition, as the nth-order (q-conjugate) CPP equals zero.

From (3.15) one can see that the oversampling factor per subcarrier, ρ, depends on the order n, number of conjugations, q, number of subcarriers, K, and the product $T_u T^{-1}$. As an example, with $n=2$, $q=1$, $K=128$, and $T_{cp} = T_u / 4$, the necessary and sufficient condition on the oversampling factor (per subcarrier), ρ, given by (3.15), becomes $\rho \geq 1$.

3.4. Recognition of OFDM Against SCLD by Exploiting Signal Cyclostationarity

Results presented in previous sections are employed here to develop an algorithm for the classification of OFDM and SCLD in AWGN channel.

3.4.1. Discriminating Signal Feature

We investigate the lowest-order non-zero CC to recognize OFDM against SCLD signals; this is of second-order (one-conjugate); the first-order and second-order (zero-conjugate) CCs equal zero due to zero values of $c_{s,1,0}$ and $c_{s,2,0}$, respectively, for PSK and QAM signals with more than four points in the signal constellation [5], [11]. Under the assumption of no aliasing, with $n=2$, $q=1$, and $\tau=[\tau\ 0]^{\dagger}$, and by using (2.11), (2.13), (3.4), (3.6), (3.12) and (3.14), one can easily obtain the second-order (one-conjugate) CCs and sets of CFs for the discrete-time SCLD and OFDM signals respectively, as[3]

$$c_{r_{\mathrm{SCLD}}}(\beta;\tau)_{2,1} = a^2 c_{s,2,1}\rho^{-1}e^{-j2\pi\beta\varepsilon\rho}e^{j\frac{2\pi}{\rho}\Delta f_c T\tau}\sum_{u} g(u+\tau)g^*(u)e^{-j2\pi\beta u} + c_w(\beta;\tau)_{2,1}, \quad (3.16)$$

$$c_{r_{\mathrm{OFDM}}}(\beta;\tau)_{2,1} = a^2 c_{s,2,1}D^{-1}e^{-j2\pi\beta\varepsilon D}e^{j\frac{2\pi}{\rho K}\Delta f_c T_u\tau}\sum_{k=0}^{K-1}e^{j\frac{2\pi}{\rho K}k\tau}\sum_{u} g(u+\tau)g^*(u)e^{-j2\pi\beta u}$$

$$+c_w(\beta;\tau)_{2,1}. \quad (3.17)$$

$$\kappa_{n,q}^{\mathrm{SCLD}} = \{\beta \mid \beta = l\rho^{-1},\ l \text{ integer}\}, \quad (3.18)$$

and

[3] Note that according to (2.11) and (3.6), if $n=2q$ (in this case $n=2$ and $q=1$), the CF γ is equal to β. This result will be used for the CF notation throughout the thesis.

$$\kappa_{n,q}^{\text{OFDM}} = \{\beta \,|\, \beta = lD^{-1},\ l \ \text{integer}\}\,. \tag{3.19}$$

One can easily show that $\Xi_K(\tau) = \sum_{k=0}^{K-1} e^{j\frac{2\pi}{\rho K}k\tau} = e^{j\frac{\pi}{\rho K}(K-1)\tau}\frac{\sin(\pi\tau/\rho)}{\sin(\pi\tau/\rho K)}$, and write (3.17) as

$$c_{r_{\text{OFDM}}}(\beta;\tau)_{2,1} = a^2 c_{s,2,1} D^{-1} e^{-j2\pi\beta\varepsilon D} e^{j\frac{2\pi}{\rho K}\Delta f_c T_u \tau}\Xi_K(\tau)\sum_u g(u)g^*(u+\tau)e^{-j2\pi\beta u} + c_{w'}(\beta;\tau)_{2,1}. \tag{3.20}$$

According to the analysis carried out in Appendix A, these results are valid for specific ranges of the delay values. For SCLD and OFDM, these delay values belong to the interval zero to that corresponding to symbol period of SCLD and OFDM, respectively (for rectangular pulse shape). At zero delay, the second-order (one-conjugate) CC magnitude reaches maximum, and approaches zero at delay corresponding to the symbol period for both SCLD and OFDM signals (rectangular pulse shape). If the pulse shape is non-rectangular, non-zero CC magnitude values can appear also at delays beyond that corresponding to the symbol period. For the OFDM signal, a significant non-zero value of the second-order (one-conjugate) CC magnitude can be noticed at delays corresponding to the useful symbol period, $\pm\rho K$. This is due to the existence of the cyclic prefix. The magnitude of the second-order (one-conjugate) CC of SCLD and OFDM signals (in the absence of noise) is plotted versus CF and delay in Fig. 3.1 a) and b), respectively (for parameter setting see Section 3.5.1). In addition to the peak at zero delay, CC magnitude peaks are visible for the OFDM signal at $\tau = \pm\rho K$ and for different CFs. With sufficiently large K, these peaks do not occur in the vicinity of zero delay, and this represents a distinctive characteristic of OFDM in comparison with the SCLD signals. The existence of such a peak in the magnitude of the second-order (one-conjugate) CC of

the OFDM signal (at zero CF, $\beta = 0$, and delay $\tau = \rho K$) is employed here as discriminating feature to identify OFDM against SCLD signals.

3.4.2. Proposed Recognition Algorithm

At the receive-side, the bandwidth of the signal is roughly estimated, and a low-pass filter is used to remove the out-of-band noise. The signal is down-converted and (over)sampled at a rate equal to ρ times the signal bandwidth estimate. Discrimination between OFDM and SCLD signals is performed by applying the following algorithm, which consists of two steps.

Step 1:

Based on the observation interval available at the receive-side (L samples), the magnitude of the second-order (one-conjugate) CC of the baseband received signal is estimated at zero CF, $\beta = 0$, and over a range of positive delay values. This range is chosen to cover possible peaks at $\rho K_{\min}$ and $\rho K_{\max}$, with $K_{\min}$ and $K_{\max}$ as the minimum and maximum number of subcarriers that we consider (the number of subcarriers is assumed unknown at the receive-side and a range of possible values considered). The peak $\rho K_{\min}$ has to be far enough from zero delay to serve as an unambiguous discriminating feature between OFDM and SCLD signals. Over the considered delay range, we select that delay value for which the CC magnitude reaches a maximum.

Step 2:

With $n = 2$ and $q = 1$, the cyclostationarity test developed in [28] is used to check whether or not $\beta = 0$ is indeed a CF for the delay selected in Step 1. This test consists in comparing a statistic against a threshold (see Appendix G for the test description). If $\beta = 0$ is found to be a CF, then we decide that the signal is OFDM, otherwise we declare it as SCLD.

As one can notice, the algorithm proposed here to recognize OFDM against SCLD does not require symbol timing, carrier and waveform recovery, or estimation of signal and noise powers.

3.5. Simulation Results

Simulations are performed to confirm theoretical developments, and results of these simulations are presented in the following.

3.5.1. Simulation Setup

For SCLD modulations, we consider a pool consisting of BPSK, QPSK, 8-PSK, 16-QAM and 64-QAM. Without any loss of generality, we simulate unit variance constellations. The transmit filter is a root-raised cosine with 0.35 roll-off factor [27], and the signal bandwidth is 40 kHz. At the receive-side, a low-pass filter is used to eliminate the out-of-band noise, and the signal is sampled at a rate $f_s = 160$ kHz. For the OFDM signal, we set the parameters as follows. The signal bandwidth is set to 800 kHz, the number of subcarriers to 128, the useful time period to 160 μs, and the cyclic prefix period to 40 μs. All subcarriers are modulated either using QPSK or 16-QAM. Unit variance constellations

are also used in this case. The transmit pulse-shaping window is chosen as raised cosine, with 0.025 roll-off factor [2]. At the receive-side, the signal is low-pass filtered and sampled at a rate of 3.2 MHz. For both OFDM and SCLD, we consider an oversampling factor of 4. Unless otherwise mentioned, the observation interval available at the receive-side is 0.1 s. This interval corresponds to $L = 320{,}000$ and 16,000 samples for OFDM and SCLD, respectively. In addition, we set a to one, ε to 0.75, θ as a random variable uniformly distributed over $[-\pi, \pi)$, and Δf_c to 16 kHz and 320 kHz for SCLD and OFDM signals, respectively. The signal-to-noise ratio (SNR) is defined as the signal power to the noise power at the output of receive filter. For the cyclostationarity test, a Kaiser window of length 61 and parameter 10 is employed to compute the estimates of covariances used in the test, and a threshold of 23.0258 is employed for decision making (see Appendix G for the description of the test and parameters involved in it). This threshold value corresponds to a probability of false alarm $P_f = 10^{-5}$ [29]. The probability of false alarm represents the probability to decide that $\beta = 0$ is a CF for the delay $\tau = \rho K$, when it is actually not; in other words, that the received signal is OFDM, when this is SCLD. The probability to correctly decide that the modulation format of the received signal is i, when indeed the modulation format i is transmitted, $P_{cr}^{(i|i)}$, $i = \text{OFDM}, \text{SCLD}$, is used to evaluate the performance of the proposed recognition algorithm. This is calculated based on 100 trials.

3.5.2. Numerical Results

The estimated magnitude of the second-order (one-conjugate) CC of OFDM and SCLD signals is plotted versus cycle frequency and delay in Fig. 3.2 a) and b), respectively, for 20dB SNR and 0.1s observation interval. When comparing results presented in Figs. 3.1 and 3.2, one can notice the existence of non-zero spikes in the estimated magnitude at frequencies different than CFs, and over the whole delay range. This is due to the finite length of the observation interval. The magnitude of the second-order (one-conjugate) CC at zero CF ($\beta = 0$), is plotted versus delay (positive values) in Fig. 3.3 a) and b), for OFDM and SCLD signals, respectively. The peak corresponding to $\tau = \rho K$ is to be noticed in the results presented for OFDM; no such peak appears for SCLD.

Fig. 3.4 shows the estimated magnitude of the second-order (one-conjugate) CC of OFDM versus delay, for zero CF and at different SNRs. From Fig. 3.4 one can notice the significant peak at delay $\tau = \rho K$. In addition, it is to be noted that the CC value at zero delay increases with a decrease in the SNR, which can be explained by the noise contribution to the CC, at zero CF and zero delay. Fig. 3.5 shows the estimated magnitude of the second-order (one-conjugate) CC of SCLD versus delay, for zero CF, and at different SNRs. From Fig. 3.5 one can notice that there is no significant peak along the delay axis, even at lower SNR values. As the SNR decreases, the same behavior of the CC at zero CF and zero delay can be noticed for SCLD signals as well.

Recognition performance of the proposed algorithm is shown in Fig. 3.6. The probability of correct recognition, $P_{cr}^{(i|i)}$, is plotted versus SNR, for $i = \text{OFDM, SCLD}$. It can be noticed

that with 0.1 s and 0.05 s observation intervals, $P_{cr}^{(\mathrm{OFDM}|\mathrm{OFDM})}$ equals one for SNR above –9 dB and –7 dB respectively; these results do not depend on the modulation type within the OFDM signal (4-PSK or 16-QAM). On the other hand, $P_{cr}^{(\mathrm{SCLD}|\mathrm{SCLD})}$ is always one for the whole investigated SNR range; these results hold regardless the SCLD modulation format. This can be easily explained, as for SCLD there is no statistically significant peak in the second-order (one-conjugate) CC magnitude at zero CF and over the searched delay range. Thus, the local maximum in the CC magnitude, which is selected in Step 1 of the classification algorithm, is due only to the finite length of the observation interval, and does not pass the cyclostationarity test in Step 2 of the algorithm. Hence, a correct decision is made when recognizing SCLD modulations. This is in agreement with the value set for the probability of false alarms, which actually represents the probability to decide that the modulation format is OFDM when this is SCLD. Simulations have been performed for different pulse shapes at the transmit-side, such as rectangular for both SCLD and OFDM signals, root-raised cosine with roll-off factor 1 for SCLD signals, and raised cosine with 0.1 roll-off factor for OFDM signals. The same recognition performance is practically obtained, regardless the change in the pulse shape.

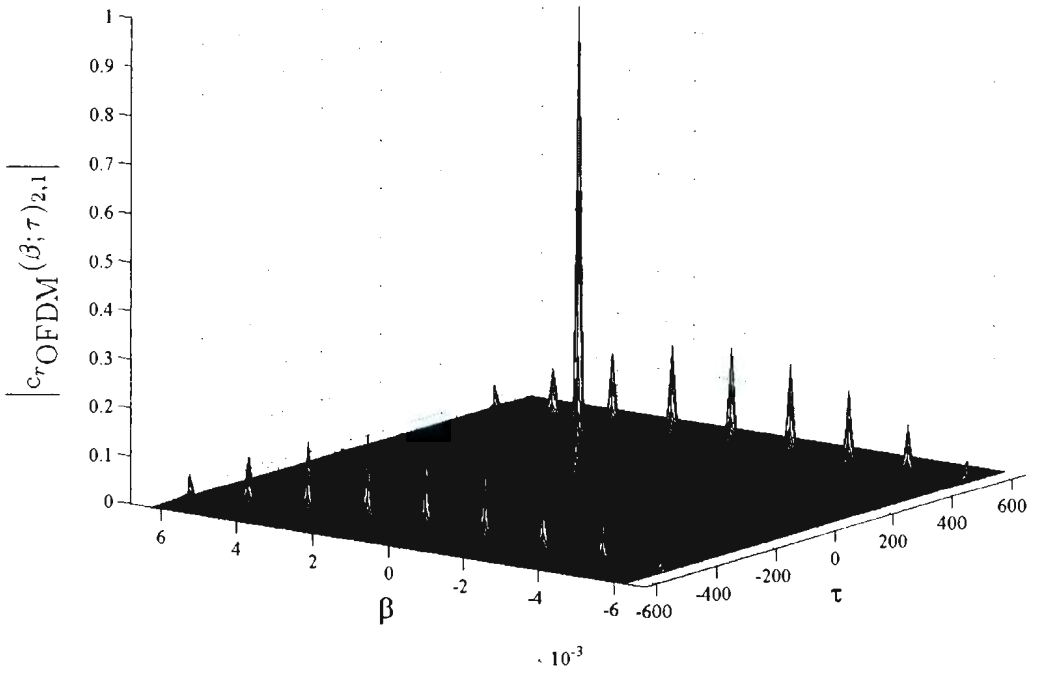

a)

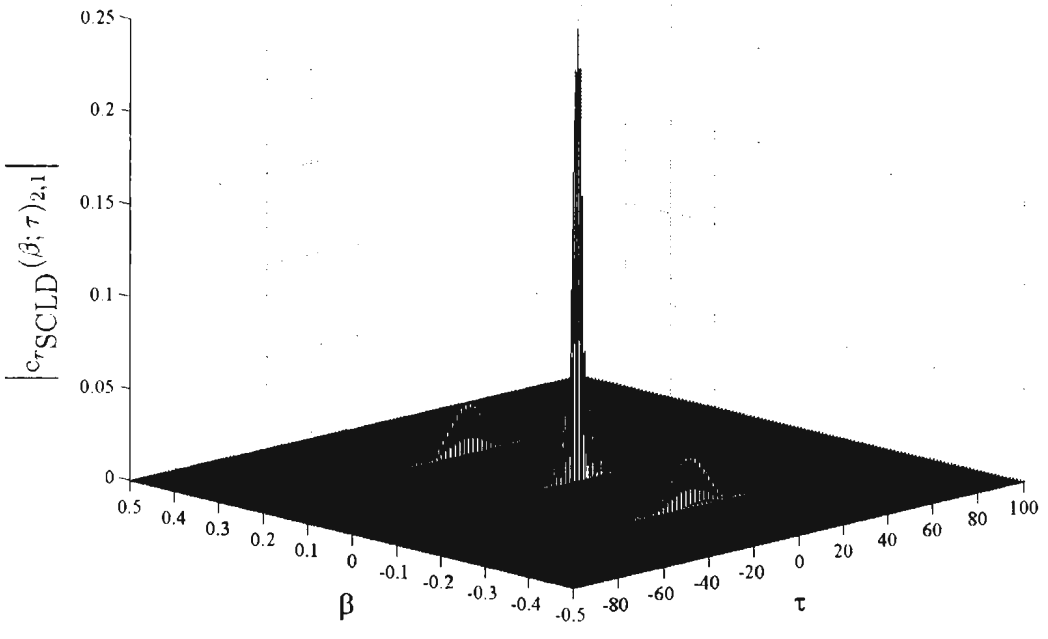

b)

Figure 3.1: The magnitude of second-order (one-conjugate) CC versus cycle frequency and delay (in absence of noise), for a) OFDM and b) SCLD signals in AWGN channel

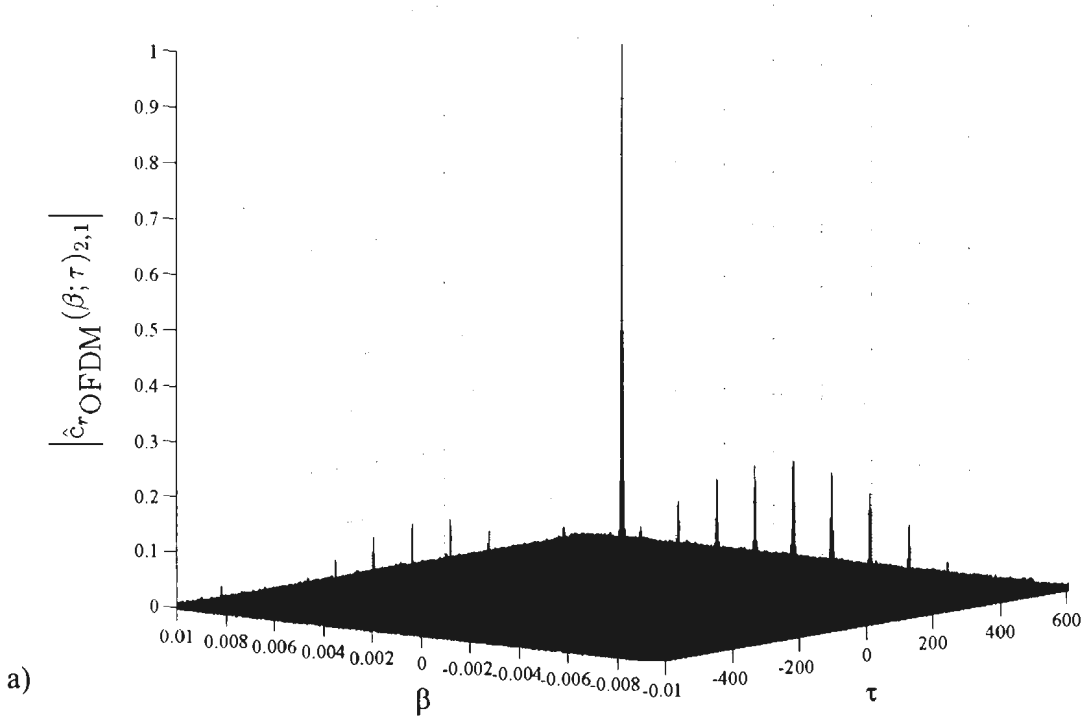

a)

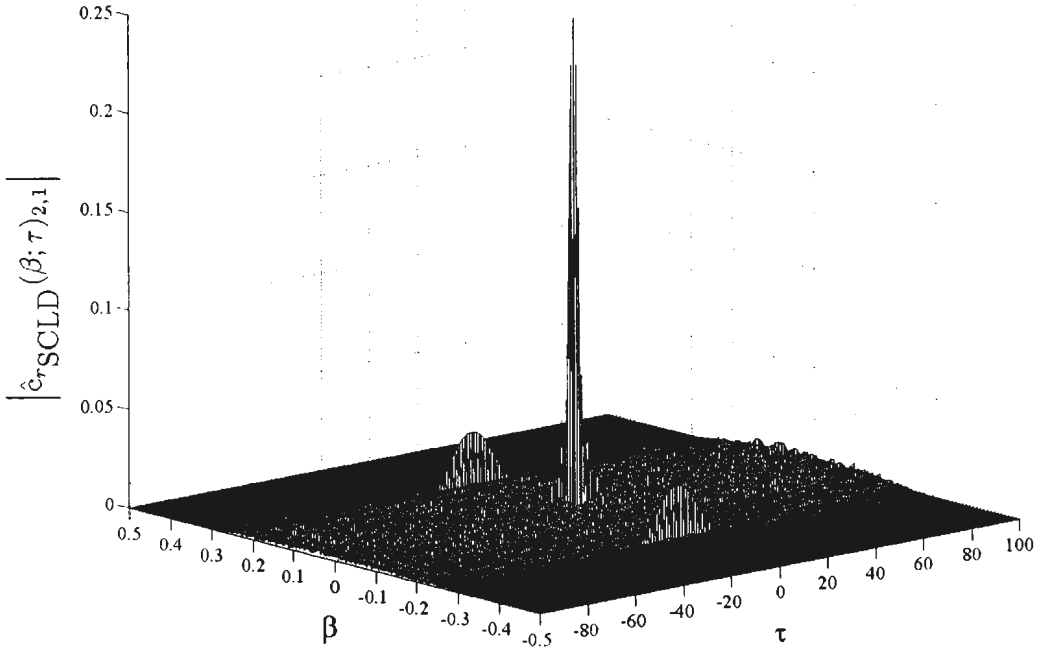

b)

Figure 3.2: The estimated second-order (one-conjugate) CC magnitude versus cycle frequency and delay (at 20 dB SNR), for a) OFDM and b) SCLD signals in AWGN channel

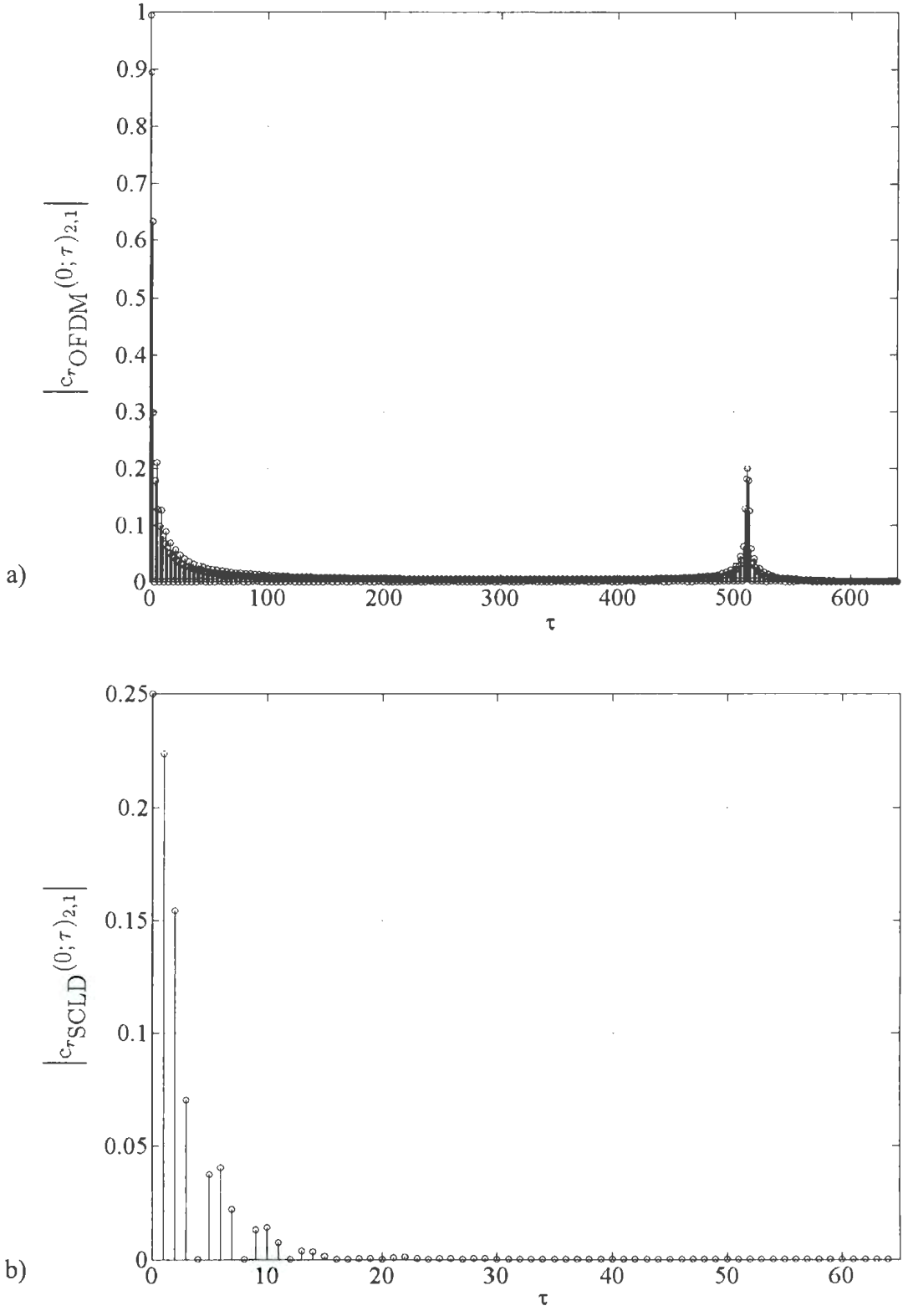

Figure 3.3: The magnitude of second-order (one-conjugate) CC at zero CF versus positive delays (in absence of noise), for a) OFDM and b) SCLD signals in AWGN channel

a)

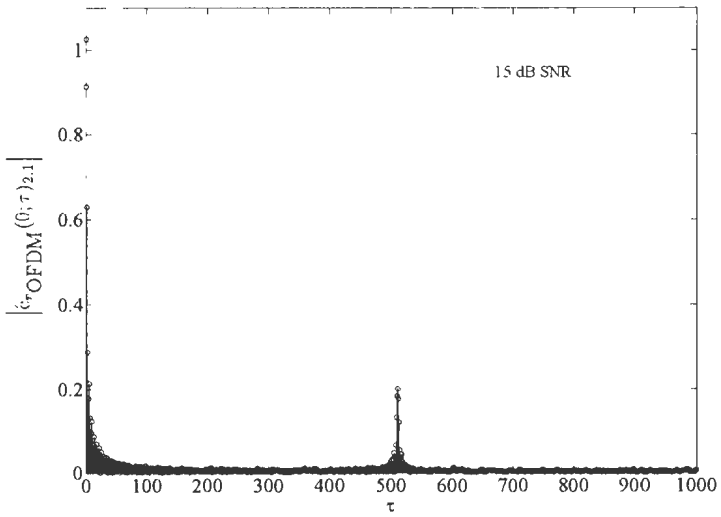

b)

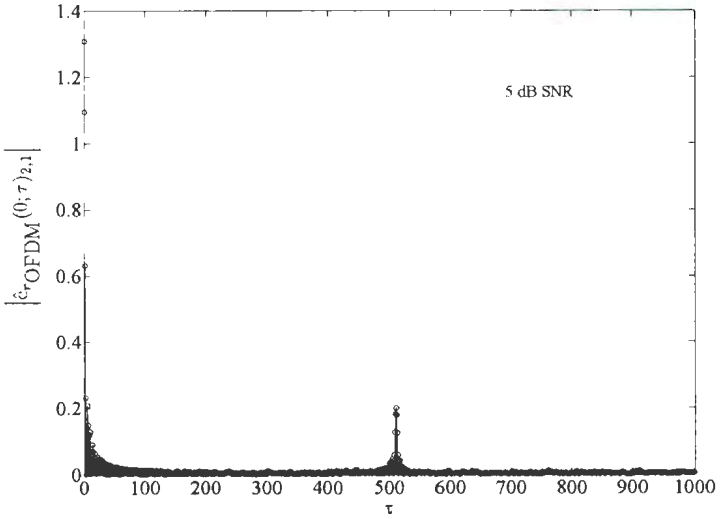

c)

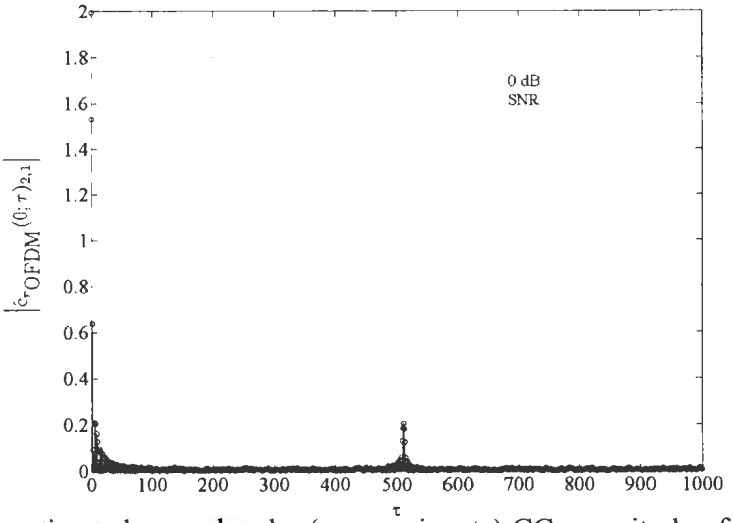

Figure 3.4: The estimated second-order (one-conjugate) CC magnitude of OFDM signals (in AWGN channel) versus delay, at zero CF and a) 15 dB SNR, b) 5 dB SNR, and c) 0 dB SNR

a)

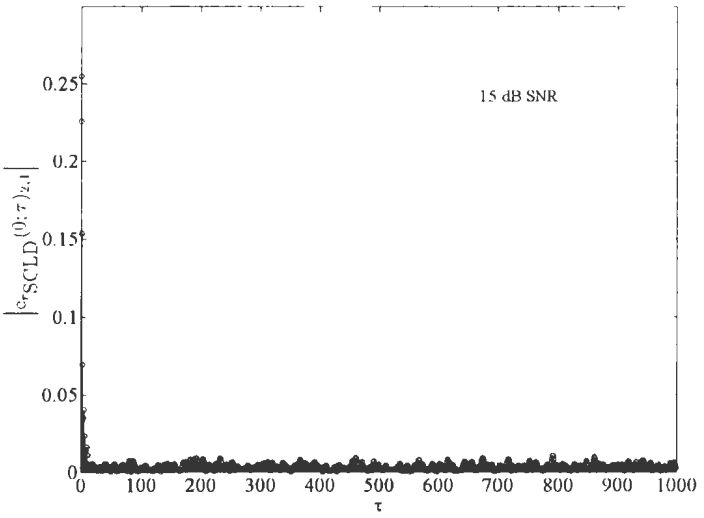

b)

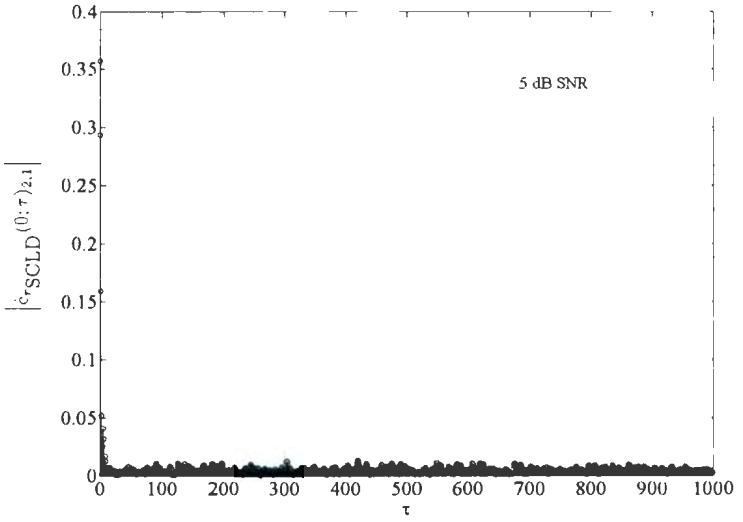

c)

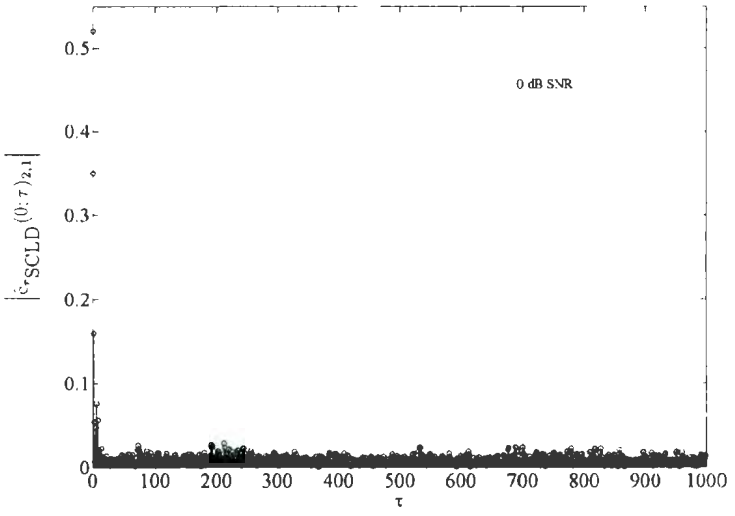

Figure 3.5: The estimated second-order (one-conjugate) CC magnitude of SCLD signals (in AWGN channel) versus delay, at zero CF and a) 15 dB SNR, b) 5 dB SNR, and c) 0 dB SNR

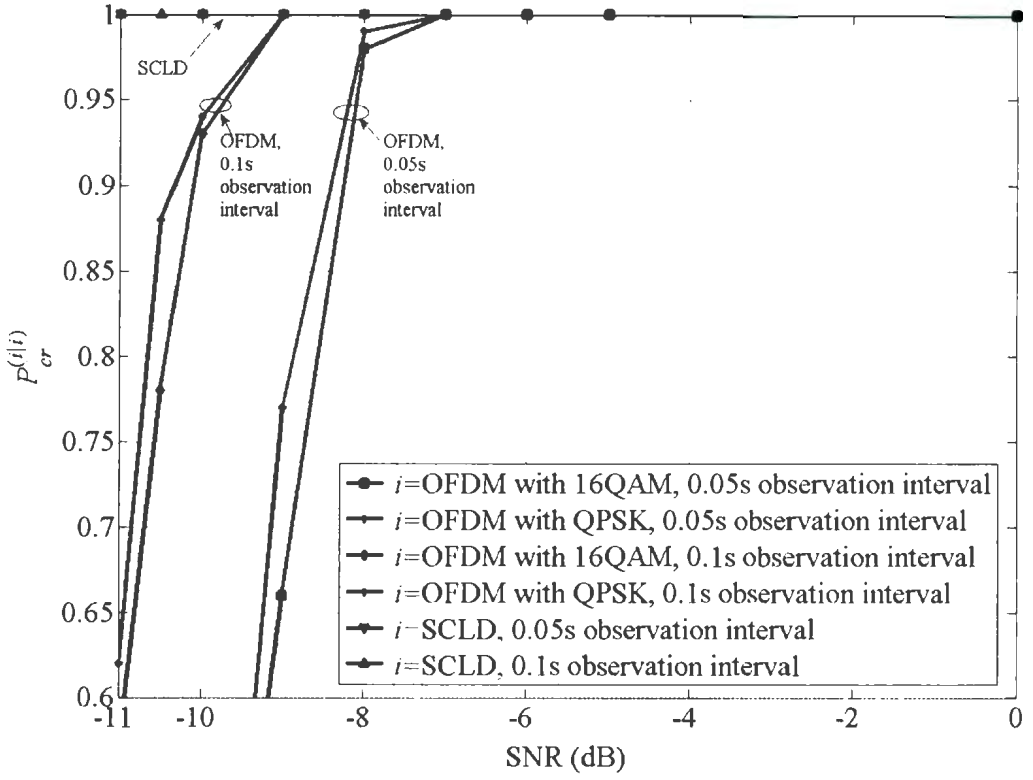

Figure 3.6: The average probability of correct recognition $P_{cr}^{(i|i)}$, i = OFDM, SCLD, versus SNR in AWGN channel

3.6. Summary

In this Chapter, we investigate signal cyclostationarity of OFDM, and apply the results to recognize OFDM against SCLD modulations in AWGN channel. We derive the analytical closed-form expressions for the *n*th-order cyclic (*q*-conjugate) CC, CCP, and CFs for an OFDM signal embedded in AWGN and affected by phase, frequency offset and timing errors, and obtain a necessary and sufficient condition on the oversampling factor (per subcarrier) to avoid cycle aliasing. Furthermore, based on the second-order (one-conjugate) CC, we propose an algorithm to discriminate OFDM against SCLD

modulations. The proposed recognition algorithm has the advantage that is devoid of preprocessing tasks, such as symbol timing, carrier and waveform recovery, and signal and noise power estimation.

Chapter 4

Cyclostationarity-Based Recognition of OFDM Against SCLD in Time Dispersive Channel

4.1. Introduction

The algorithm proposed in Chapter 3 is applicable to the recognition of OFDM against SCLD signals in AWGN channel. Here we extend the applicability of this algorithm to time dispersive channels. We study the nth-order cyclostationarity of OFDM and SCLD signals affected by a time dispersive channel, AWGN, carrier phase, and frequency and timing offsets. We derive analytical closed-form expressions for the nth-order (q-conjugate) CCs, nth-order (q-conjugate) CFs, nth-order (q-conjugate) CCPs of such signals. Then, we obtain a necessary and sufficient condition on the oversampling factor (per subcarrier) to eliminate cycle aliasing for OFDM and SCLD signals. Second-order CCs are finally employed to develop the recognition algorithm. In addition, we investigate the computational complexity of the proposed recognition algorithm.

4. 2. Cyclostationarity of Signals of Interest

4.2.1. Channel and Signal Models

Channel Model

Let us assume that the signals of interest are transmitted through a time dispersive channel, which also corrupts the signal by adding white Gaussian noise. The impulse response of the time dispersive channel is

$$h(t) = \sum_{m=1}^{M} h(\tilde{\zeta}_m)\delta(t - \tilde{\zeta}_m), \tag{4.1}$$

with $h(\tilde{\zeta}_m)$ as the channel coefficient at delay $\tilde{\zeta}_m$, $m = 1,\ldots M$.

SCLD Signal Model

If an SCLD signal is transmitted through the above channel, the output of the matched filter at the receive-side is a baseband waveform, given by [27]

$$r_{\text{SCLD}}(t) = ae^{j\theta}e^{j2\pi\Delta f_c t}\sum_{l=-\infty}^{\infty}\sum_{m=1}^{M} s_l h(\tilde{\zeta}_m)g(t - \tilde{\zeta}_m - lT - \varepsilon T) + w(t). \tag{4.2}$$

The discrete-time baseband signal, $r_{\text{SCLD}}(u)$, obtained by oversampling $r_{\text{SCLD}}(t)$ at a rate $f_s = \rho T^{-1}$, with ρ as the number of samples per symbol (oversampling factor), is given by

$$r_{\text{SCLD}}(u) = ae^{j\theta}e^{j\frac{2\pi}{\rho}\Delta f_c T u}\sum_{l=-\infty}^{\infty}\sum_{m=1}^{M} s_l h(u_m)g(u - u_m - l\rho - \varepsilon\rho) + w(u), \tag{4.3}$$

where $w(u)$ is wide-sense stationary zero-mean complex Gaussian noise and $u_m = \tilde{\zeta}_m f_s$ (not necessarily an integer).

OFDM Signal Model

The continuous-time baseband equivalent of a transmitted OFDM signal is given by [18],

$$x_{\text{OFDM}}(t) = \frac{1}{\sqrt{K}} \sum_{k=0}^{K-1} \sum_{l=-\infty}^{\infty} s_{k,l}\ e^{j2\pi k \Delta f_K (t-lT)} g^{tr}(t-lT). \tag{4.4}$$

At the receive-side, the continuous-time baseband equivalent is given by

$$r_{\text{OFDM}}(t) = a e^{j\theta} e^{j2\pi \Delta f_c t} \sum_{k=0}^{K-1} \sum_{l=-\infty}^{\infty} \sum_{m=1}^{M} s_{k,l} h(\tilde{\zeta}_m) e^{j2\pi k \Delta f_K (t-\tilde{\zeta}_m - lT - \varepsilon T)} g(t-\tilde{\zeta}_m - lT - \varepsilon T) + w(t). \tag{4.5}$$

A discrete-time baseband OFDM signal, $r_{\text{OFDM}}(u)$, is obtained by oversampling $r_{\text{OFDM}}(t)$ at a rate $f_s = \rho K T_u^{-1}$, with ρK as a positive integer which represents the number of samples in the useful symbol duration, and ρ as the number of samples per symbol per subcarrier (oversampling factor per subcarrier). Note that for the SCLD signals there is a single carrier $(K=1)$ and, thus, ρ simply becomes the number of samples per symbol (oversampling factor). The expression for the discrete-time baseband OFDM signal can be easily written as,

$$r_{\text{OFDM}}(u) = a e^{j\theta} e^{j\frac{2\pi}{\rho K} \Delta f_c T_u u} \sum_{k=0}^{K-1} \sum_{l=-\infty}^{\infty} \sum_{m=1}^{M} s_{k,l} h(u_m)\, e^{j\frac{2\pi}{\rho K} k(u-u_m-lD-\varepsilon D)} g(u-u_m-lD-\varepsilon D) + w(u), \tag{4.6}$$

where $D = \rho K (1 + T_{cp} T_u^{-1})$ is the number of samples over an OFDM symbol.

Note that equations (4.2) and (4.3) represent particular cases of (4.5) and (4.6), respectively, for $K=1$ and $T_{cp}=0$ $(T=T_u)$. In addition, if $h(t)=\delta(t)$, (the channel is AWGN) (3.1), (3.2), (3.9) and (3.10) represents particular cases of (4.2), (4.3), (4.5) and (4.6), respectively.

4.2.2. Cyclostationarity of SCLD Signals

Results obtained from the analysis performed in Appendices D, E and F for the nth-order cyclostationarity of the SCLD signals are presented as follows. For the continuous-time baseband received signal, $r_{\text{SCLD}}(t)$, the nth-order (q-conjugate) time-varying cumulant at delay vector $\tilde{\boldsymbol{\tau}}$ (see Appendix D for the comments on the delay values), is obtained as[2]

$$\tilde{c}_{r_{\text{SCLD}}}(t;\tilde{\boldsymbol{\tau}})_{n,q} = a^n c_{s,n,q} e^{j(n-2q)\theta} e^{j2\pi(n-2q)\Delta f_c t} e^{j2\pi\Delta f_c \sum_{p=1}^{n}(-)_p \tilde{\tau}_p} \times \prod_{p=1}^{n}\sum_{m_p=1}^{M} h^{(*)_p}(\tilde{\zeta}_{m_p}) g^{(*)_p}(t-\tilde{\zeta}_{m_p}+\tilde{\tau}_p) \otimes \sum_{l=-\infty}^{\infty}\delta(t-lT-\varepsilon T) + \tilde{c}_w(t;\tilde{\boldsymbol{\tau}})_{n,q}, \tag{4.7}$$

where $c_{s,n,q}$ is the nth-order (q-conjugate) cumulant of the signal constellation, $\tilde{c}_w(t;\tilde{\boldsymbol{\tau}})_{n,q}$[2] is the nth-order (q-conjugate) time-varying cumulant of $w(t)$, and $(-)_p$ is the optional minus sign associated with the optional conjugation $(*)_p$, $p=1,\ldots,n$.

The nth-order (q-conjugate) CC at CF $\tilde{\gamma}$ and delay vector $\tilde{\boldsymbol{\tau}}$, the nth-order (q-conjugate) CCP at CF $\tilde{\gamma}$ and spectral frequency vector $\tilde{\mathbf{f}}$, and the CFs for the continuous-time signal, $r_{\text{SCLD}}(t)$, are respectively given as

$$\tilde{c}_{r_{\text{SCLD}}}(\tilde{\gamma};\tilde{\boldsymbol{\tau}})_{n,q} = a^n c_{s,n,q} T^{-1} e^{j(n-2q)\theta} e^{-j2\pi\tilde{\beta}\varepsilon T} e^{j2\pi\Delta f_c \sum_{p=1}^{n}(-)_p \tilde{\tau}_p} \times \int_{-\infty}^{\infty}\prod_{p=1}^{n}\sum_{m_p=1}^{M} h^{(*)_p}(\tilde{\zeta}_{m_p}) g^{(*)_p}(t-\tilde{\zeta}_{m_p}+\tilde{\tau}_p) e^{-j2\pi\tilde{\beta}t} dt + \tilde{c}_w(\tilde{\gamma};\tilde{\boldsymbol{\tau}})_{n,q}, \tag{4.8}$$

$$\tilde{C}_{r_{\mathrm{SCLD}}}(\tilde{\gamma};\tilde{\mathbf{f}})_{n,q} = a^n c_{s,n,q} T^{-1} e^{j(n-2q)\theta} e^{-j2\pi\tilde{\beta}\varepsilon T} \prod_{p=1}^{n-1} H^{(*)_p}((-)_p \tilde{f}_p - \Delta f_c) G^{(*)_p}((-)_p \tilde{f}_p - \Delta f_c)$$

$$\times H^{(*)_n}((-)_n(\tilde{\beta} - \sum_{p=1}^{n-1}(-)_p((-)_p \tilde{f}_p - \Delta f_c))$$

$$\times G^{(*)_n}((-)_n(\tilde{\beta} - \sum_{p=1}^{n-1}(-)_p((-)_p \tilde{f}_p - \Delta f_c)) + \tilde{C}_w(\tilde{\gamma};\tilde{\mathbf{f}})_{n,q}, \tag{4.9}$$

and

$$\tilde{\kappa}_{n,q}^{\mathrm{SCLD}} = \{\tilde{\gamma} \mid \tilde{\gamma} = \tilde{\beta} + (n-2q)\Delta f_c,\ \tilde{\beta} = lT^{-1},\ l \text{ integer}\}. \tag{4.10}$$

A necessary and sufficient condition on the oversampling factor, ρ, to eliminate cycle aliasing is derived in Appendix F, which will be presented in Section 4.3. Under the assumption of no aliasing, the expressions for the nth-order (q-conjugate) CC, CCP, and CFs for the discrete-time SCLD signal, $r_{\mathrm{SCLD}}(u)$, can be easily derived based on (4.8)-(4.10) and by using (2.11)-(2.13).

4.2.3. Cyclostationarity of OFDM Signals

Results derived in Appendices D, E and F for the nth-order cyclostationarity of the OFDM signal are presented as follows. The nth-order (q-conjugate) time-varying cumulant at delay vector $\tilde{\boldsymbol{\tau}}$ (see Appendix D for comments on the delay values) for the continuous-time baseband received OFDM signal, $r_{\mathrm{OFDM}}(t)$, is given by

$$\tilde{c}_{r_{\mathrm{OFDM}}}(t;\tilde{\boldsymbol{\tau}})_{n,q} = a^n c_{s,n,q} e^{j(n-2q)\theta} e^{j2\pi\Delta f_c \sum_{p=1}^{n}(-)_p \tilde{\tau}_p} e^{j2\pi(n-2q)\Delta f_c t} \sum_{k=0}^{K-1} e^{j2\pi k\Delta f_K \sum_{p=1}^{n}(-)_p \tilde{\tau}_p}$$

$$\times e^{j2\pi(n-2q)k\Delta f_K t} \prod_{p=1}^{n} \sum_{m_p=1}^{M} h^{(*)_p}(\tilde{\zeta}_{m_p}) g^{(*)_p}(t - \tilde{\zeta}_{m_p} + \tilde{\tau}_p) e^{-j2\pi k\Delta f_K \sum_{p=1}^{n}(-)_p \tilde{\zeta}_{m_p}}$$

$$\otimes \sum_{l=-\infty}^{\infty} \delta(t - lT - \varepsilon T) + \tilde{c}_{w'}(t;\tilde{\boldsymbol{\tau}})_{n,q}. \tag{4.11}$$

The nth-order (q-conjugate) CC at CF $\tilde{\gamma}$ and delay vector $\tilde{\boldsymbol{\tau}}$, the nth-order (q-conjugate) CCP at CF $\tilde{\gamma}$ and spectral frequency vector $\tilde{\mathbf{f}}$, and the CFs for the continuous-time baseband received OFDM signal, $r_{\text{OFDM}}(t)$, are respectively given as

$$\begin{aligned}\tilde{c}_{r_{\text{OFDM}}}(\tilde{\gamma};\tilde{\boldsymbol{\tau}})_{n,q} &= a^n c_{s,n,q} T^{-1} e^{j(n-2q)\theta} e^{-j2\pi\tilde{\beta}\varepsilon T} e^{j2\pi\Delta f_c \sum_{p=1}^{n}(-)_p \tilde{\tau}_p} \sum_{k=0}^{K-1} e^{j2\pi k\Delta f_K \sum_{p=1}^{n}(-)_p \tilde{\tau}_p} \\ &\quad \times \int_{-\infty}^{\infty} \prod_{p=1}^{n} \sum_{m_p=1}^{M} h^{(*)_p}(\tilde{\zeta}_{m_p}) g^{(*)_p}(t - \tilde{\zeta}_{m_p} + \tilde{\tau}_p) e^{-j2\pi k\Delta f_K \sum_{p=1}^{n}(-)_p \tilde{\zeta}_{m_p}} e^{j2\pi(n-2q)k\Delta f_K t} e^{-j2\pi\tilde{\beta}t} dt \\ &\quad + \tilde{c}_w(\tilde{\gamma};\tilde{\boldsymbol{\tau}})_{n,q}, \end{aligned} \tag{4.12}$$

$$\begin{aligned}\tilde{C}_{r_{\text{OFDM}}}(\tilde{\gamma};\tilde{\mathbf{f}})_{n,q} &= a^n c_{s,n,q} T^{-1} e^{j(n-2q)\theta} e^{-j2\pi\tilde{\beta}\varepsilon T} \\ &\quad \times \sum_{k=0}^{K-1} \prod_{p=1}^{n-1} H^{(*)_p}((-)_p \tilde{f}_p - \Delta f_c) G^{(*)_p}((-)_p \tilde{f}_p - \Delta f_c - k\Delta f_K) \\ &\quad \times H^{(*)_n}((-)_n(\tilde{\beta} - \sum_{p=1}^{n-1}(-)_p((-)_p \tilde{f}_p - \Delta f_c - k\Delta f_K) - (n-2q)k\Delta f_K) + k\Delta f_K) \\ &\quad \times G^{(*)_n}((-)_n(\tilde{\beta} - \sum_{p=1}^{n-1}(-)_p((-)_p \tilde{f}_p - \Delta f_c - k\Delta f_K) - (n-2q)k\Delta f_K)) \\ &\quad + \tilde{C}_{w'}(\tilde{\gamma};\tilde{\mathbf{f}})_{n,q}, \end{aligned} \tag{4.13}$$

and

$$\tilde{\boldsymbol{\kappa}}_{n,q}^{\text{OFDM}} = \{\tilde{\gamma} \mid \tilde{\gamma} = \tilde{\beta} + (n-2q)\Delta f_c,\ \tilde{\beta} = lT^{-1},\ l \text{ integer}\}. \tag{4.14}$$

Note that (4.8) and (4.12), and (4.9) and (4.13) give the analytical expressions for the CC and CCP, respectively, only at CFs and certain delays (see Appendix D for comments on the delays). At other frequencies and delays, the CC and CCP equal to zero. It is also to be noted that (4.8)-(4.10) are particular cases of (4.12)-(4.14) for a single carrier ($K = 1$) and no cyclic prefix ($T_{cp} = 0$, $T = T_u$). This is expected from the comments on the signal model

(see Section 2.1). In addition, one can easily notice that if the channel is AWGN ($h(t)=\delta(t)$), then (3.4)-(3.6) and (3.12)-(3.14) are obtained as particular cases of (4.8)-(4.10) and (4.12)-(4.14) for SCLD and OFDM, respectively. From (4.8) and (4.12) one can notice that the *n*th-order (*q*-conjugate) CCs of both SCLD and OFDM signals depend on the *n*th power of the signal amplitude, the *n*th-order (*q*-conjugate) cumulant of the signal constellation, phase, timing and carrier frequency offsets, channel impulse response, pulse shape, and symbol period. In addition, the CCs of the OFDM signal depend on the frequency separation between two adjacent subcarriers, Δf_K, and the number of subcarriers, K. On the other hand, CC magnitude of the signal component does not depend on phase, timing and carrier frequency offsets. Owing to the nature of the noise, $\tilde{c}_w(\tilde{\gamma};\tilde{\boldsymbol{\tau}})_{n,q}$ is non-zero only for $n=2$ and $q=1$, at zero CF and for zero delay vector. From (4.9) and (4.13), one can notice that the *n*th-order (*q*-conjugate) CCPs of both SCLD and OFDM signals depend on the *n*th power of the signal amplitude, the *n*th-order (*q*-conjugate) cumulant of the signal constellation, phase, timing and carrier frequency offsets, symbol period, and the Fourier transform of the pulse shape and channel impulse response. In addition, the CCPs of the OFDM signal depend on the frequency separation between two adjacent subcarriers, Δf_K, and the number of subcarriers, K. According to (4.10) and (4.14), if $n=2q$, the CFs are integer multiples of the inverse of the SCLD and OFDM symbol period, respectively. Otherwise, there is a shift of these values due to the carrier frequency offset, Δf_c.

A necessary and sufficient condition on the oversampling factor per subcarrier, ρ, to eliminate cycle aliasing is derived in Appendix F, which will be presented in Section 4.3. Under the assumption of no aliasing, the expressions for the nth-order (q-conjugate) CC, CCP, and CFs for the discrete-time OFDM signal, $r_{\text{OFDM}}(u)$, can be easily derived based on (4.12)-(4.14) and by using (2.11)-(2.13).

4.3. A Necessary and Sufficient Condition on the Oversampling Factor (per Subcarrier) to Eliminate Cycle Aliasing for OFDM and SCLD Signals

In signal processing applications, cyclostationary continuous-time signals are subject to sampling operations. This can lead to aliasing in both cycle and spectral frequency domains [26]. In the application that we study here, the continuous-time signal is oversampled at the output of the receive low-pass filter. Therefore, it is important to find a condition to eliminate aliasing. As mentioned in Chapter 2, the Nyquist condition has to be fulfilled to eliminate spectral aliasing. A necessary and sufficient condition on the oversampling factor (per subcarrier), ρ, to eliminate cycle aliasing for both OFDM and SCLD signals is derived in Appendix F and presented here for good channels (there are no spectral nulls in the channel amplitude response). For bad channels (there exist spectral nulls in the channel amplitude response) the same reasoning can be applied to obtain a condition on the oversampling factor to eliminate cycle aliasing (see Appendix F).

For the SCLD signals, the condition on the oversampling factor in case of good channels is

$$\rho \geq \lceil 2nWT \rceil, \tag{4.15}$$

where W represents the one-sided bandwidth of the pulse shaped signal. One can easily notice that the oversampling factor, ρ, depends on the order n, symbol period, T, and the bandwidth (unless otherwise mentioned, the bandwidth is referred to as the one-sided bandwidth for both OFDM and SCLD signals) of the pulse shaped signal, W. For example, if $n = 2$ and the received SCLD signal is band-limited to $W = (1 + r_o)(2T)^{-1}$, with the roll-off factor $r_o = 0.35$, a necessary and sufficient condition on the oversampling factor, ρ, to eliminate cycle aliasing is $\rho \geq 3$. Note that for SCLD we use the term oversampling factor for ρ, as in this case there is a single carrier $(K = 1)$, and the oversampling factor per subcarrier simply becomes the oversampling factor.

For the OFDM signal and a good channel, a necessary and sufficient condition on the oversampling factor per subcarrier, ρ, to eliminate cycle aliasing is (see Appendix F for derivations):

$$\rho \geq \left\lceil T_u K^{-1} (2nW + |n - 2q|(K-1)\Delta f_K) \right\rceil. \tag{4.16}$$

One can easily notice that the oversampling factor per subcarrier, ρ, depends on the order n, number of conjugations, q, number of subcarriers, K, useful symbol duration, T_u, and the bandwidth of the pulse shaped signal, W. For example, if $n = 2$, $q = 1$, $K = 128$, and $W = T^{-1} = (1.25T_u)^{-1}$ $(T_{cp} = T_u / 4)$, the necessary and sufficient condition on the oversampling factor per subcarrier, ρ, given by (4.16), is $\rho \geq 1$.

Results presented here for both SCLD and OFDM signals are valid only for n even. For n odd we cannot derive such a condition, as the nth-order (q-conjugate) CCP equals zero.

To be noted that results obtained for SCLD and OFDM signals and good channels are the same as for the AWGN channel (for the latter see Chapter 3).

4.4. Recognition of OFDM Against SCLD by Exploiting Signal Cyclostationarity

Results presented in previous sections are employed here to develop an algorithm for the recognition of OFDM against SCLD, when affected by a time-dispersive channel, AWGN, carrier phase, and frequency and timing offsets. We extend the algorithm proposed in Chapter 3 for the recognition of OFDM against SCLD in the AWGN channel to time dispersive channels.

4.4.1. Discriminating Signal Features

We investigate the lowest-order non-zero CC to recognize OFDM against SCLD signals. This is of second-order (one-conjugate), as the first- and second-order (zero-conjugate) CCs for PSK and QAM signals with more than four points in the signal constellation equal zero due to zero values of $c_{s,1,0}$ and $c_{s,2,0}$, respectively [5], [11]. Under the assumption of no aliasing, with $n=2$, $q=1$, $\boldsymbol{\tau}=[\tau\ 0]^{\dagger}$, and by using (4.8), (4.10), (4.12), (4.14), (2.11), and (2.13) one can easily obtain the second-order (one-conjugate) CCs and sets of CFs for the discrete- time SCLD and OFDM signals respectively, as[3]

$$c_{r_{\mathrm{SCLD}}}(\beta;\tau)_{2,1} = a^2 c_{s,2,1}\rho^{-1}e^{-j2\pi\beta\varepsilon\rho}e^{j\frac{2\pi}{\rho}\Delta f_c T\tau} \times \sum_{u}\sum_{m_1=1}^{M} h(u_{m_1})g(u+\tau-u_{m_1})\sum_{m_2=1}^{M} h^*(u_{m_2})g^*(u-u_{m_2})e^{-j2\pi\beta u}$$

$$+ c_w(\beta;\tau)_{2,1}, \tag{4.17}$$

$$c_{r_{\text{OFDM}}}(\beta;\tau)_{2,1} = a^2 c_{s,2,1} D^{-1} e^{-j2\pi\beta\varepsilon D} e^{j\frac{2\pi}{\rho K}\Delta f_c T_u \tau} \times \sum_u \sum_{m_1=1}^{M} h(u_{m_1}) g(u+\tau-u_{m_1}) \sum_{m_2=1}^{M} h^*(u_{m_2}) g^*(u-u_{m_2}) \sum_{k=0}^{K-1} e^{j\frac{2\pi}{\rho K}k(\tau-u_{m_1}+u_{m_2})} e^{-j2\pi\beta u}$$

$$+ c_w(\beta;\tau)_{2,1}. \tag{4.18}$$

$$\kappa_{n,q}^{\text{SCLD}} = \{\beta \,|\, \beta = l\rho^{-1},\ l \ \text{integer}\}, \tag{4.19}$$

and

$$\kappa_{n,q}^{\text{OFDM}} = \{\beta \,|\, \beta = lD^{-1},\ l \ \text{integer}\}. \tag{4.20}$$

One can easily show that $\sum_{k=0}^{K-1} e^{j\frac{2\pi}{\rho K}k(\tau-u_{m_1}+u_{m_2})} = e^{j\frac{\pi}{\rho K}(K-1)(\tau-u_{m_1}+u_{m_2})} \frac{\sin(\pi(\tau-u_{m_1}+u_{m_2})/\rho)}{\sin(\pi(\tau-u_{m_1}+u_{m_2})/\rho K)}$, and by denoting this function $\Xi_K(\tau,u_{m_1},u_{m_2})$, (4.18) can be further expressed as,

$$c_{r_{\text{OFDM}}}(\beta;\tau)_{2,1} = a^2 c_{s,2,1} D^{-1} e^{-j2\pi\beta\varepsilon D} e^{j\frac{2\pi}{\rho K}\Delta f_c T_u \tau} \times \sum_u \sum_{m_1=1}^{M} h(u_{m_1}) g(u+\tau-u_{m_1}) \sum_{m_2=1}^{M} h^*(u_{m_2}) g^*(u-u_{m_2}) \Xi_K(\tau,u_{m_1},u_{m_2}) e^{-j2\pi\beta u}$$

$$+ c_w(\beta;\tau)_{2,1}. \tag{4.21}$$

According to the analysis carried out in Appendix D, these results are valid for specific ranges of the delay values. For SCLD and OFDM, these delay values belong to the interval zero to that corresponding to symbol period of SCLD and OFDM, respectively (for rectangular pulse shape). At zero delay, the second-order (one-conjugate) CC magnitude reaches maximum, and approaches zero at delay corresponding to the symbol period for both SCLD and OFDM signals (rectangular pulse shape). If the pulse shape is non-rectangular, non-zero CC magnitude values can appear also at delays beyond that corresponding to the symbol period. For the OFDM signal, a significant non-zero value of

the second-order (one-conjugate) CC magnitude can be noticed at delays corresponding to the useful symbol period, $\pm\rho K$. This is due to the existence of the cyclic prefix. At delays around zero and $\pm\rho K$, other peaks can appear (local maxima) in the second-order (one-conjugate) CC magnitude, depending on the location of the channel coefficients, u_m, $m=1,\ldots,M$ (here we assume that $u_M < T_{cp} f_s$). The magnitude of the second-order (one-conjugate) CC of SCLD and OFDM signals (in the absence of noise) is plotted versus CF and delay in Fig. 4.1 a) and b), respectively (for the parameter setting see Sections 3.5.1 and 4.5.1). In addition to the peak at zero delay, CC magnitude peaks are visible for the OFDM signal at $\tau=\pm\rho K$ and for different CFs. To be noted that other peaks (local maxima) appear around zero and $\pm\rho K$ delays; these are due to the time dispersive channel, and occur at delays τ , such that $\tau-u_{m_1}+u_{m_2}=0$ and $\tau-u_{m_1}+u_{m_2}=\pm\rho K,\quad m_1,m_2=1,\ldots,5$. To be noted that this is an extension of the results presented in Chapter 3 for the AWGN channel. If $h(u_1)=1$, with $u_1=0$, and $h(u_p)=0$, p=2,$\cdots M$, (4.17) and (4.19) give the expressions for the second-order (one-conjugate) CCs for SCLD and OFDM signals in AWGN channel, respectively. With sufficiently large K , the peaks in the CC magnitude at delays $\pm\rho K$ do not occur in the vicinity of zero, and the existence of such peaks represents a distinctive characteristic of the OFDM signal when compared with SCLD. The existence of such peaks in the second-order (one-conjugate) CC magnitude of the OFDM signal (at zero CF, $\beta=0$) is employed here as a discriminating feature to identify OFDM against SCLD.

4.4.2. Proposed Recognition Algorithm

At the receive-side, the bandwidth of the received-signal is roughly estimated, and a low-pass filter is used to remove the out-of-band noise. The signal is down-converted and (over)sampled at a rate equal to ρ times the signal bandwidth estimate. Discrimination between OFDM and SCLD signals is performed by applying the following algorithm, which consists of two steps.

Step 1:

Based on the observation interval available at the receive-side (L samples), the magnitude of the second-order (one-conjugate) CC of the baseband received signal is estimated at zero CF, $\beta = 0$, and over a range of positive delay values. This range is chosen to cover possible peaks at $\rho K_{\min}$ and $\rho K_{\max}$, with $K_{\min}$ and $K_{\max}$ as the minimum and maximum number of subcarriers that we consider (the number of subcarriers is assumed unknown at the receive-side and a range of possible values considered). The peak $\rho K_{\min}$ has to be far enough from zero delay to serve as an unambiguous discriminating feature between OFDM and SCLD signals. Over the considered delay range, we select that delay value for which the CC magnitude reaches a maximum.

Step 2:

With $n = 2$ and $q = 1$, the cyclostationarity test developed in [28] is used to check whether or not $\beta = 0$ is indeed a CF for the delay selected in Step 1. This test consists of comparing a statistic based on the second-order (one-conjugate) CC, against a threshold. This threshold corresponds to a certain probability of false alarm, P_f, which actually represents the probability to

decide that $\beta = 0$ is a CF for the delay selected in the Step 1 of the recognition algorithm, when it is actually not; in other words, that the received signal is OFDM, when this is SCLD (see Appendix G for the test description). We actually compare the test statistics with a thresholds, which correspond to $P_f = 10^{-5}$. If the test statistic exceeds the threshold, then we decide that the received signal is OFDM. Otherwise we declare the signal as SCLD.

As one can notice, the algorithm proposed here to recognize OFDM against SCLD does not require symbol timing, carrier and waveform recovery, or estimation of signal and noise powers.

4.4.3. Complexity Analysis of Proposed Recognition Algorithm

As previously presented, the proposed recognition algorithm consists of two steps. As such, the computational complexity of the algorithm is determined by the estimation of the second-order (one-conjugate) CC at zero CF and over the considered delay range, $\tau \in [\rho K_{min}, \rho K_{max}]$ (Step 1), and estimation of a covariance matrix used with the cyclostationarity test for decision making (Step 2).

In the following we investigate the computational complexity associated with both Step 1 and Step 2. In Step 1 we estimate the second-order (one-conjugate) CC at zero CF for a number of delays equal to $\tau_{max} - \tau_{min} + 1$, with $\tau_{max} = \rho K_{max}$ and $\tau_{min} = \rho K_{min}$ as integers. According to (2.14)[4], estimation of the second-order (one-conjugate) CC at zero CF, $\beta = 0$,

[4] For zero-mean processes, (2.14) gives the estimator for the second-order (n=2) /one-conjugate (q=1) CC.

and for a specific delay value, requires L complex multiplications and $L-1$ complex additions, where L is the total number of processed samples at the receive-side. Therefore, estimation of the second-order (one-conjugate) CCs at zero CF and for all delay values within the range $[\tau_{min}, \tau_{max}]$ requires $\rho L(K_{max}-K_{min})+L$ complex multiplications and $\rho(L-1)(K_{max}-K_{min})+(L-1)$ complex additions. Hence, the total number of complex multiplications and additions required for Step 1 of the recognition algorithm is $\rho(2L-1)(K_{max}-K_{min})+(2L-1)$. For an OFDM signal observed over T_{obs} seconds and sampled at a rate $f_s=\rho W_{\text{OFDM}}$, with W_{OFDM} as the bandwidth of the OFDM signal, the total number of complex computations (additions and multiplications) required in Step 1 can be easily expressed as $\rho(2\rho T_{obs}W_{\text{OFDM}}-1)(K_{max}-K_{min})+(2\rho T_{obs}W_{\text{OFDM}}-1)$. For the SCLD signal, this number can be similarly expressed as $\rho(2\rho T_{obs}W_{\text{SCLD}}-1)(K_{max}-K_{min})+(2\rho T_{obs}W_{\text{SCLD}}-1)$. Note that for the SCLD signal, the sampling frequency is $f_s=\rho W_{\text{SCLD}}$, with W_{SCLD} as the bandwidth of the SCLD signal.

For Step 2 we are interested in the computation of the covariance matrix $\Sigma_{2,1}$ needed for the cyclostationarity test (for details on the test and parameters that this involves, one can see Appendix G). This requires estimation of $Q_{2,0}$ and $Q_{2,1}$. Based on to (G.8) and (G.9), one can easily find that estimation of $Q_{2,0}$ requires $2(L+1)L_{sw}+(L+2)$ complex multiplications and $2(L-1)L_{sw}+(L_{sw}-1)$ complex additions, where L_{sw} is the length of spectral window, $W^{(L_{SW})}$. Furthermore, the estimation of $Q_{2,1}$ additionally requires $3L_{sw}+1$ complex multiplications and $L_{sw}-1$ complex additions. We can thus state that the total number of complex computations required in Step 2 is $(4L+5)L_{sw}+(L+1)$.

From the above results, one can notice that the computational complexity of the algorithm is mainly given by Step 1. For example, with the parameters setting as given under Section 3.5.1, $K_{min} = 32$, and $K_{max} = 1024$, the number of complex computations required in the Step 1 and Step 2 of the algorithm is as follows.

Table 4.1: Number of complex computations required in Step 1 and Step 2 of the algorithm

	Step 1		Step 2		Total number of complex computations
	Number of complex multiplications	Number of complex additions	Number of complex multiplications	Number of complex additions	
OFDM	1.2701×10^{9}	1.2700×10^{9}	3.9360×10^{7}	3.9039×10^{7}	2.6184×10^{9}
SCLD	6.3504×10^{7}	6.3500×10^{7}	1.9683×10^{6}	1.9519×10^{6}	1.3094×10^{8}

With a high performance digital signal processor, which is capable of executing 1500 million floating-point operations per second [30], the aforementioned number of computations will be performed in approximately 1.8 s and 87 ms for OFDM and SCLD, respectively.

4.5. Simulation Results

Simulations are performed to confirm theoretical developments, and results of these simulations are presented in the following.

4.5.1. Simulation Setup

Here we consider the simulations setup used in Section 3.3.2. In addition to that, the channel considered in simulations is a five-tap (M=5) time dispersive channel, with coefficients $h(\tilde{\zeta}_1)=0.227$, $h(\tilde{\zeta}_2)=0.460$, $h(\tilde{\zeta}_3)=0.688$, $h(\tilde{\zeta}_4)=0.460$, and $h(\tilde{\zeta}_5)=0.688$ [31], and $\tilde{\zeta}_i$, $i=1,\ldots,5$, uniformly distributed over $[0,\ \tilde{\zeta}_5]$, with $\tilde{\zeta}_5=25\ \mu s$. The threshold used for decision making is set to 23.0258 (see Appendix G for the description of the test and parameters involved in it). This threshold value corresponds to a probability of false alarm $P_f=10^{-5}$ [29]. The probability to correctly decide that the modulation format of the received signal is i, when indeed the modulation format i is transmitted, $P_{cr}^{(i|i)}$, $i=\text{OFDM, SCLD}$, is used to evaluate the performance of the proposed recognition algorithm. This is evaluated based on 100 trials.

4.5.2. Numerical Results

The estimated magnitude of the second-order (one-conjugate) CC of OFDM and SCLD signals is plotted versus cycle frequency and delay in Fig. 4.2 a) and b), respectively. These results are obtained for 20dB SNR and 0.1s observation interval. When comparing results presented in Figs. 4.1 and 4.2, one can notice the existence of non-zero spikes in the

estimated magnitude at frequencies different than CFs, and over the whole delay range. This is due to the finite length of the observation interval used for estimation.

The magnitude of the second-order (one-conjugate) CC at zero CF, $\beta = 0$, is plotted versus delay (positive values) in Fig. 4.3 a) and b), for OFDM and SCLD signals, respectively. These results are obtained by using (4.17) and (4.21) in the absence of noise, with signal parameters set as specified in Sections 3.5.1 and 4.5.1. Peaks at delays $\tau = \pm(\rho K + u_{m_1} - u_{m_2})$, $m_1, m_2 = 1,\ldots,5$, are to be noticed for OFDM; such peaks do not appear for SCLD.

Fig. 4.4 shows the estimated magnitude of the second-order (one-conjugate) CC of OFDM versus delay, for zero CF and at different SNRs. From Fig. 4.4 one can notice the peaks at delays $\tau = \pm(\rho K + u_{m_1} - u_{m_2})$, $m_1, m_2 = 1,\ldots,5$, which are specific to the OFDM signal. It is also to be noted that the CC value at zero delay increases with a decrease in the SNR, which can be explained by the noise contribution to the CC at zero CF and zero delay. Fig. 4.5 shows the estimated magnitude of the second-order (one-conjugate) CC of SCLD versus delay, for zero CF and at different SNRs. From Fig. 4.5 one can notice that there is no significant peak along the delay axis, even at lower SNR values. As the SNR decreases, the same behavior of the CC at zero CF and zero delay can be noticed for SCLD signals, as well.

Recognition performance of the proposed algorithm is shown in Fig. 4.6. The probability of correct recognition, $P_{cr}^{(i|i)}$, is plotted versus SNR, for $i = \text{OFDM, SCLD}$. It can be noticed that with 0.1 s and 0.05 s observation intervals, $P_{cr}^{(\text{OFDM}|\text{OFDM})}$ equals one for SNR above

–9 dB and –7 dB respectively. These results do not depend on the modulation type within the OFDM signal (4-PSK or 16-QAM). On the other hand, $P_{cr}^{(\mathrm{SCLD}|\mathrm{SCLD})}$ is always one for the whole investigated SNR range. These results hold regardless the SCLD modulation format.

In Fig. 4.7, the probability of correct recognition, $P_{cr}^{(i|i)}$, is plotted versus SNR for $i = \mathrm{OFDM}, \mathrm{SCLD}$, in time dispersive and AWGN channels, respectively. One can notice that the recognition performance in the time dispersive channel is close to that in the AWGN channel, with both 0.1 s and 0.05 s observation intervals.

In Fig. 4.8, the probability of correct recognition, $P_{cr}^{(i|i)}$, is plotted versus SNR for $i = \mathrm{OFDM}, \mathrm{SCLD}$, assuming that different observation intervals are available at the receive-side. As expected, the recognition performance depends on the observation interval. With sufficient observation interval (above 10 ms), the probability of correct recognition reaches one above a certain SNR; the longer the observation interval, the lower the SNR at which this performance is achieved. However, for a shorter sequence (see $T_{obs} = 7$ ms), the probability of correct recognition does not reach one even at higher SNR (the $P_{cr}^{(i|i)}$ reaches a floor); this is due to the inaccurate estimation when insufficient data are available at the receive-side.

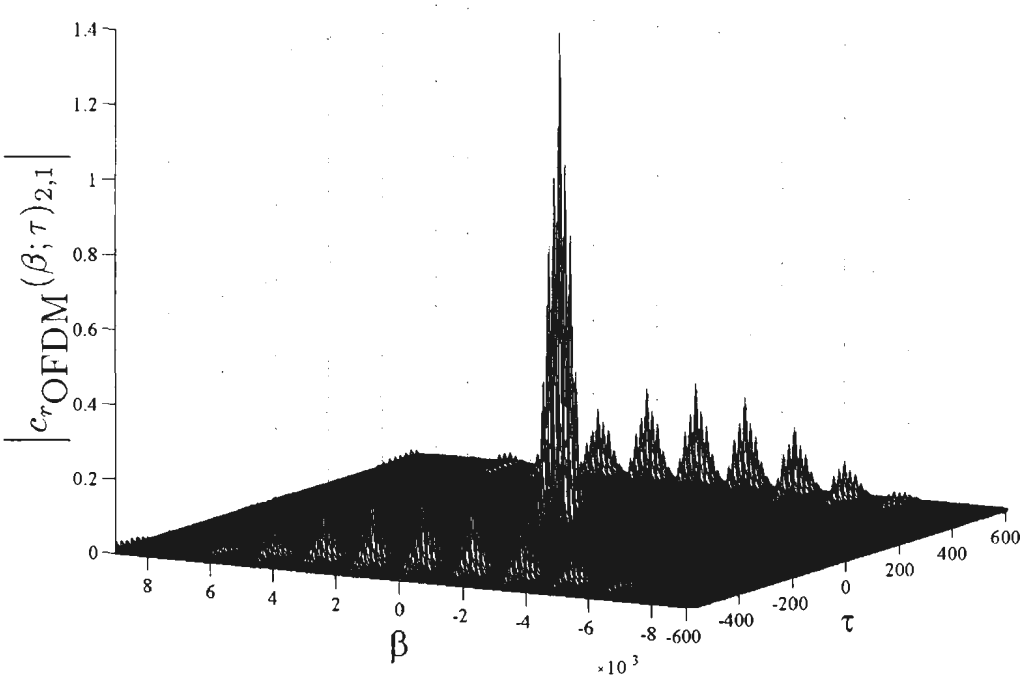

a)

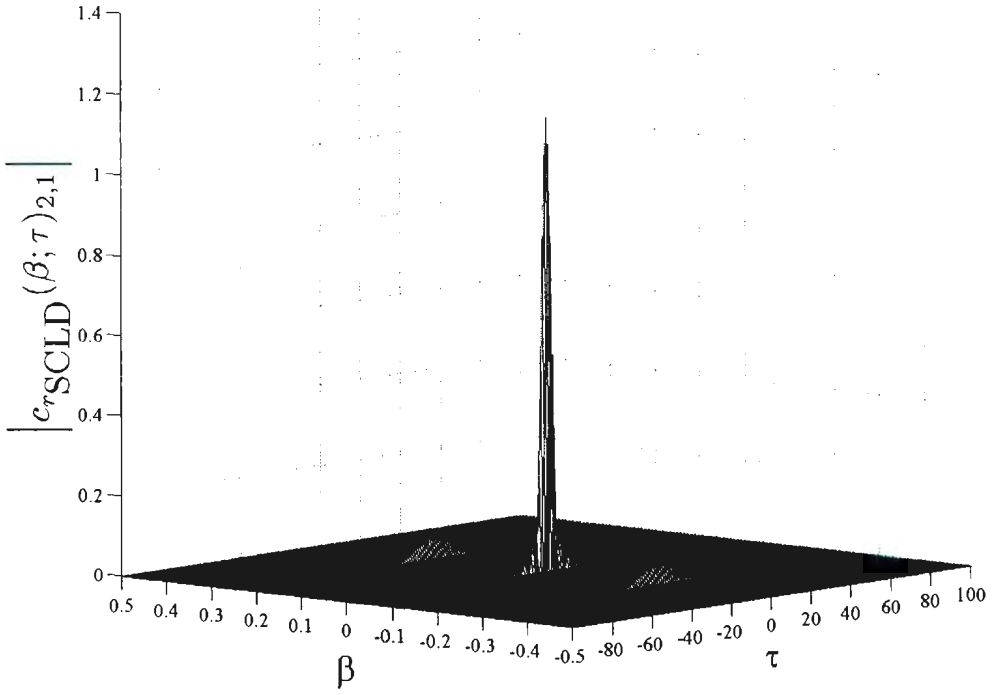

b)

Figure 4.1: The magnitude of second-order (one-conjugate) CC versus cycle frequency and delay (in absence of noise), for a) OFDM and b) SCLD signals in time dispersive channel

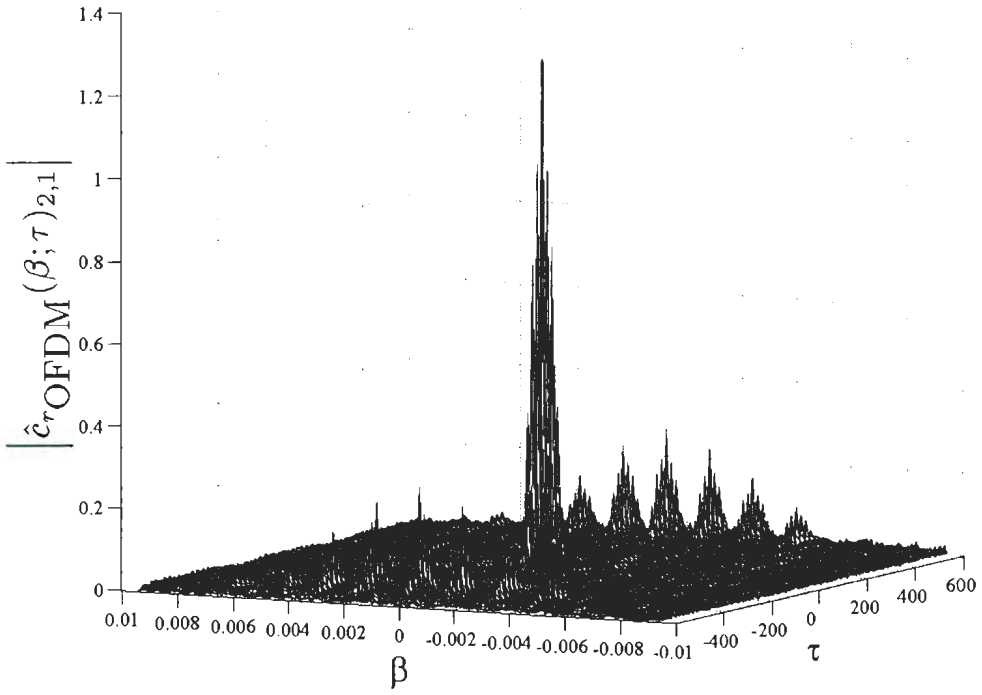

a)

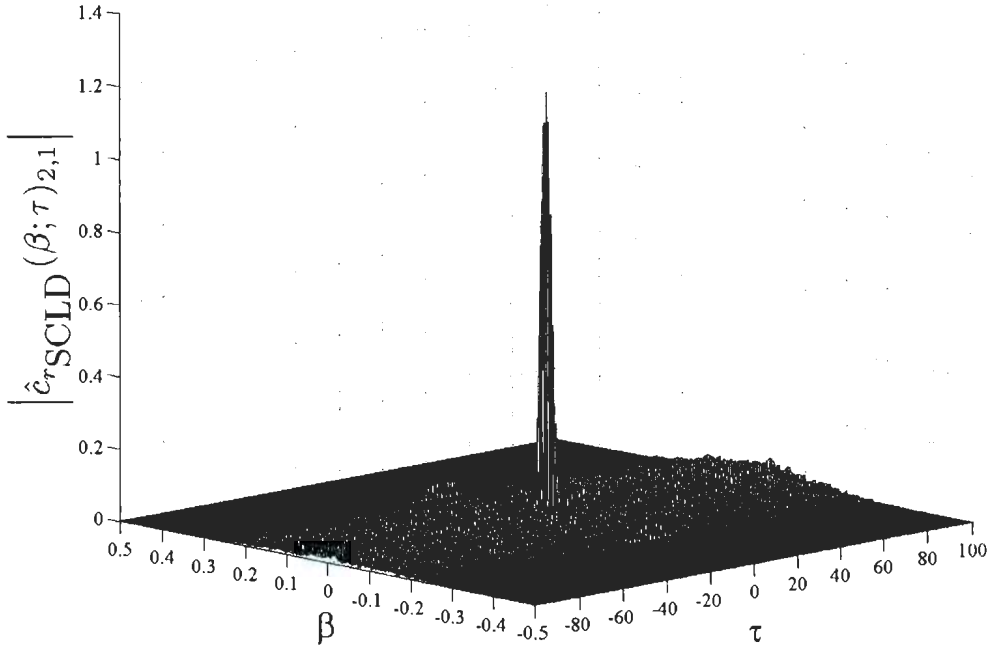

b)

Figure 4.2: The estimated second-order (one-conjugate) CC magnitude versus cycle frequency and delay (at 20 dB SNR), for a) OFDM and b) SCLD signals in time dispersive channel

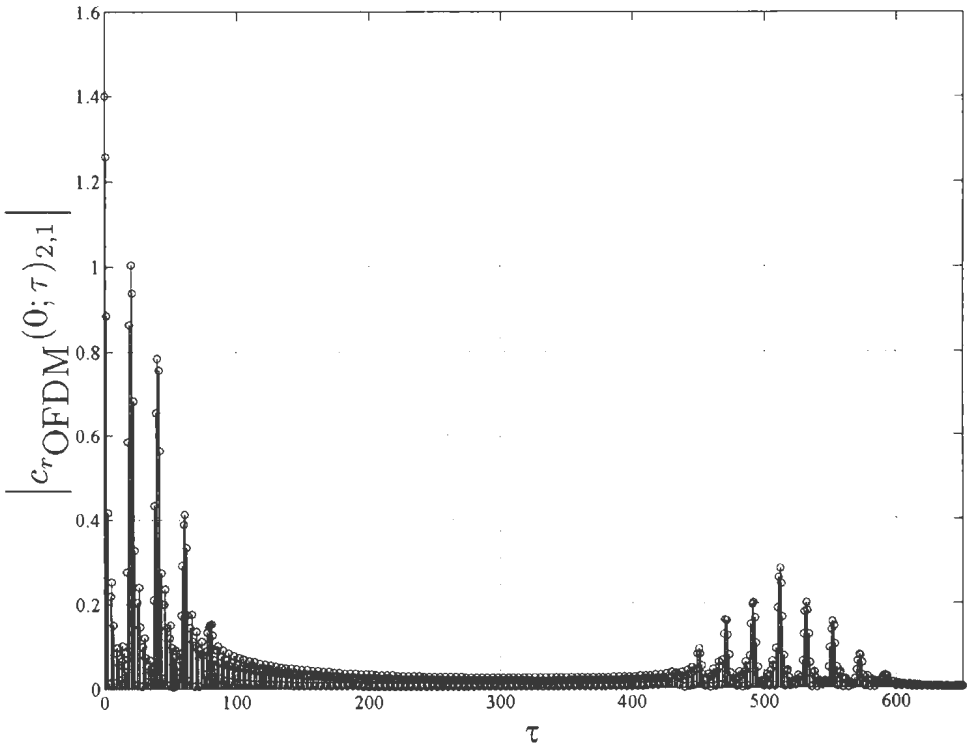

a)

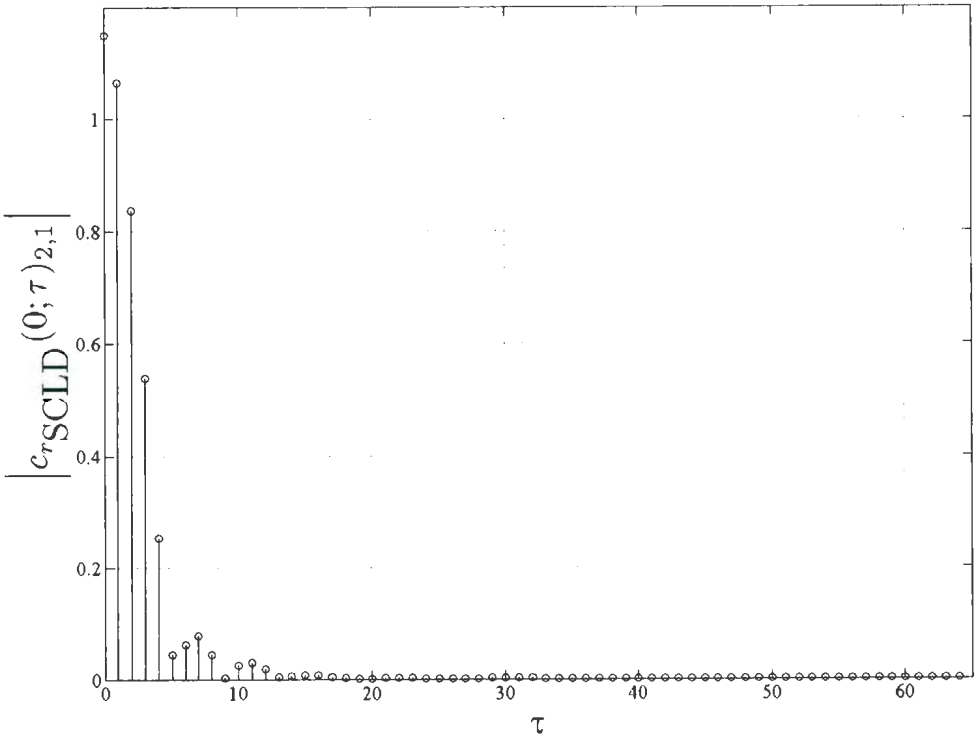

b)

Figure 4.3: The magnitude of second-order (one-conjugate) CC at zero CF versus positive delays (in absence of noise), for a) OFDM and b) SCLD signals in time dispersive channel

a)

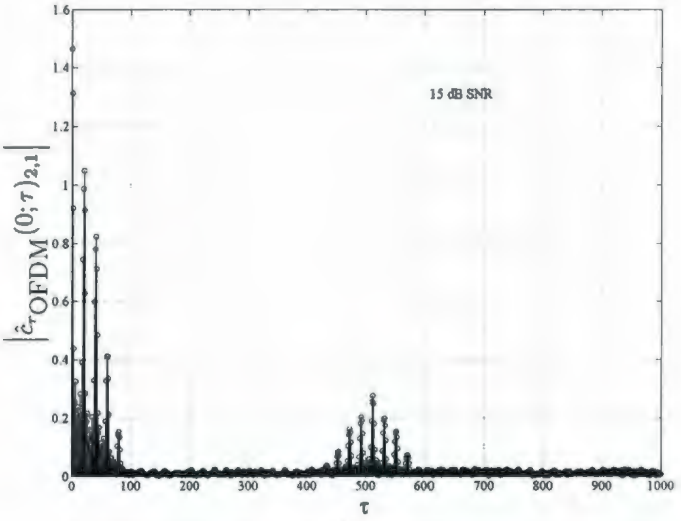

b)

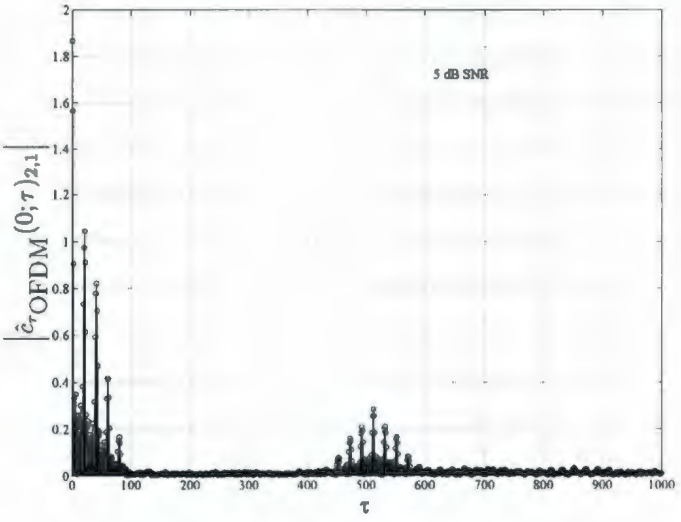

c)

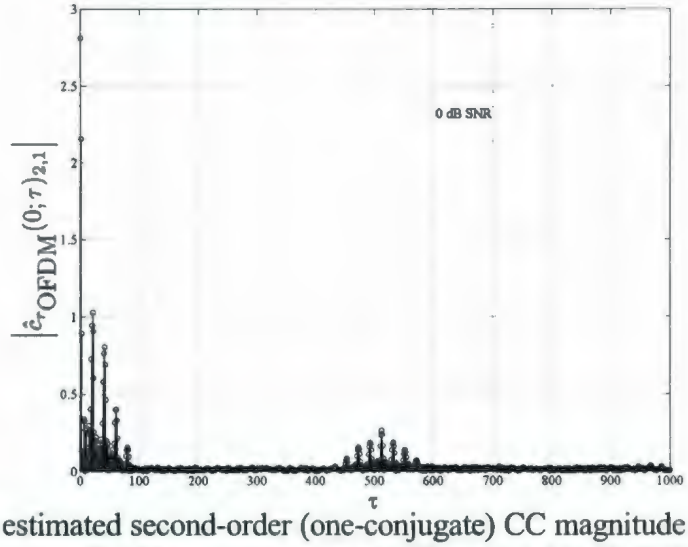

Figure 4.4: The estimated second-order (one-conjugate) CC magnitude of OFDM signals (in time dispersive channel) versus delay, at zero CF and a) 15 dB SNR, b) 5 dB SNR, and c) 0 dB SNR

a)

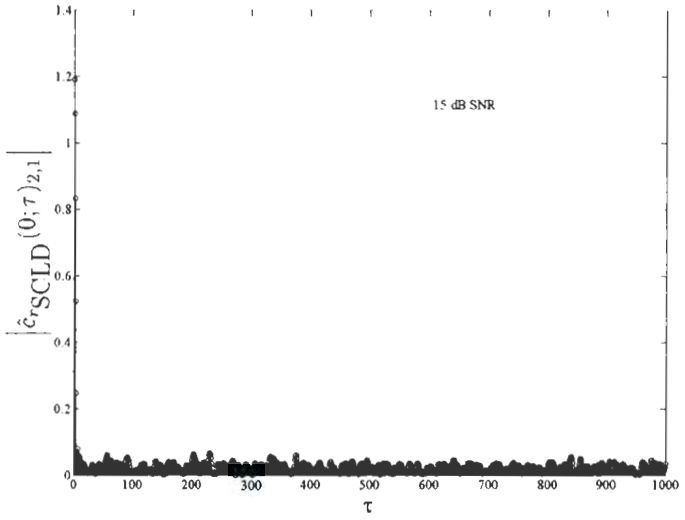

b)

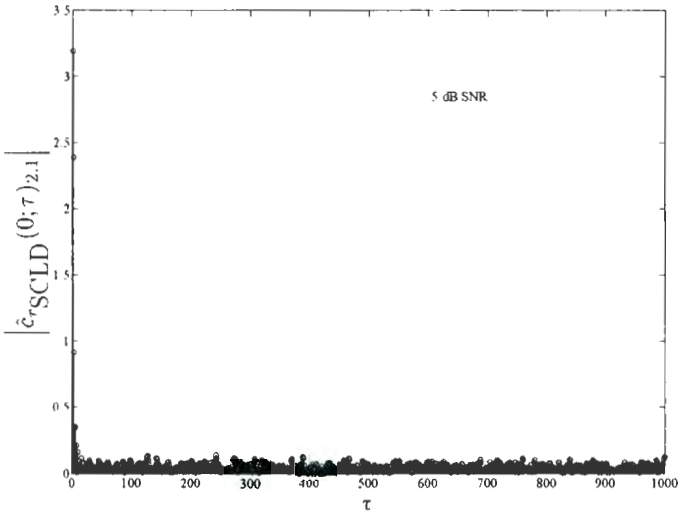

c)

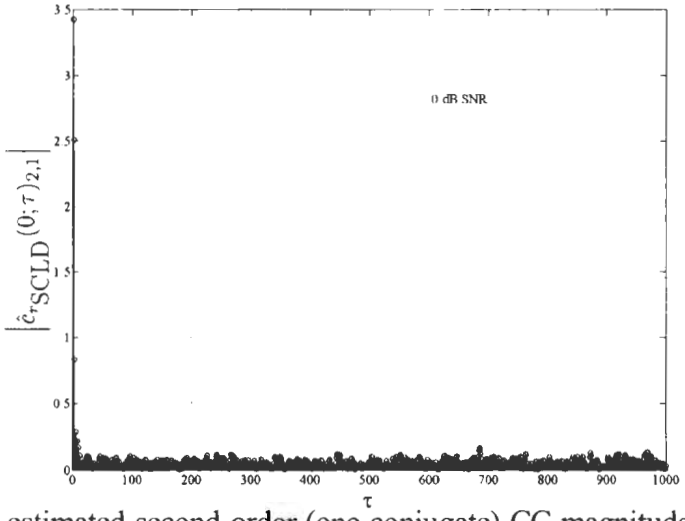

Figure 4.5: The estimated second-order (one-conjugate) CC magnitude of SCLD signals (in time dispersive channel) versus delay, at zero CF and a) 15 dB SNR, b) 5 dB SNR, and c) 0 dB SNR

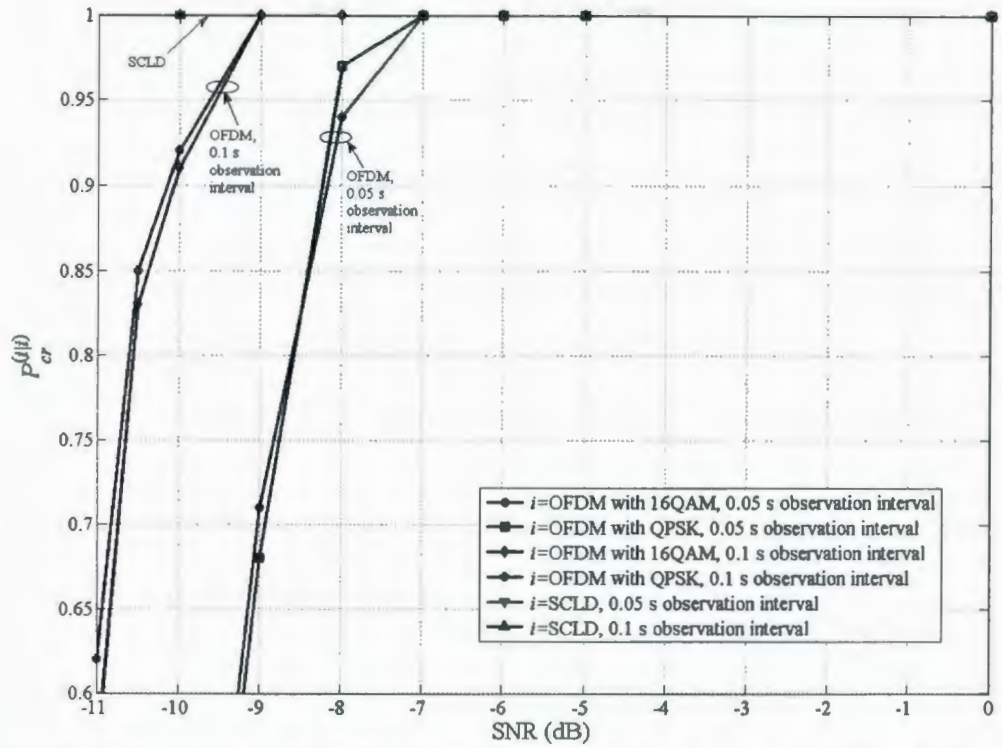

Figure 4.6: The average probability of correct recognition, $P_{cr}^{(i|i)}$, $i = \text{OFDM, SCLD}$, versus SNR, in time dispersive channel

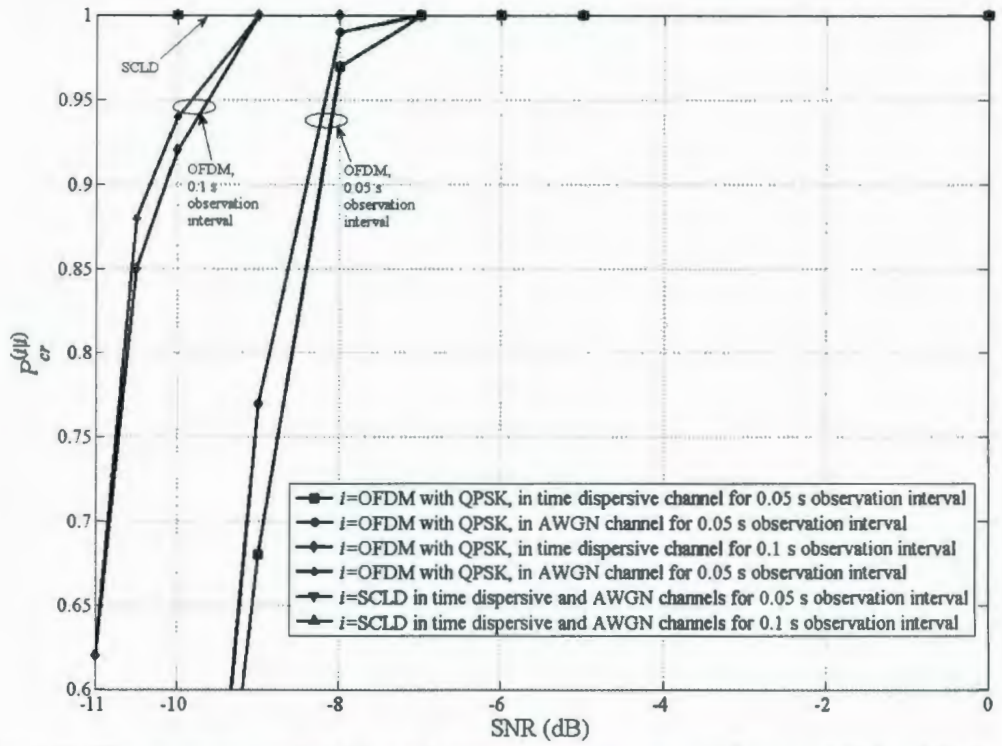

Figure 4.7: The average probability of correct recognition, $P_{cr}^{(i|i)}$, $i = \text{OFDM, SCLD}$, versus SNR, in AWGN and time dispersive channels, respectively

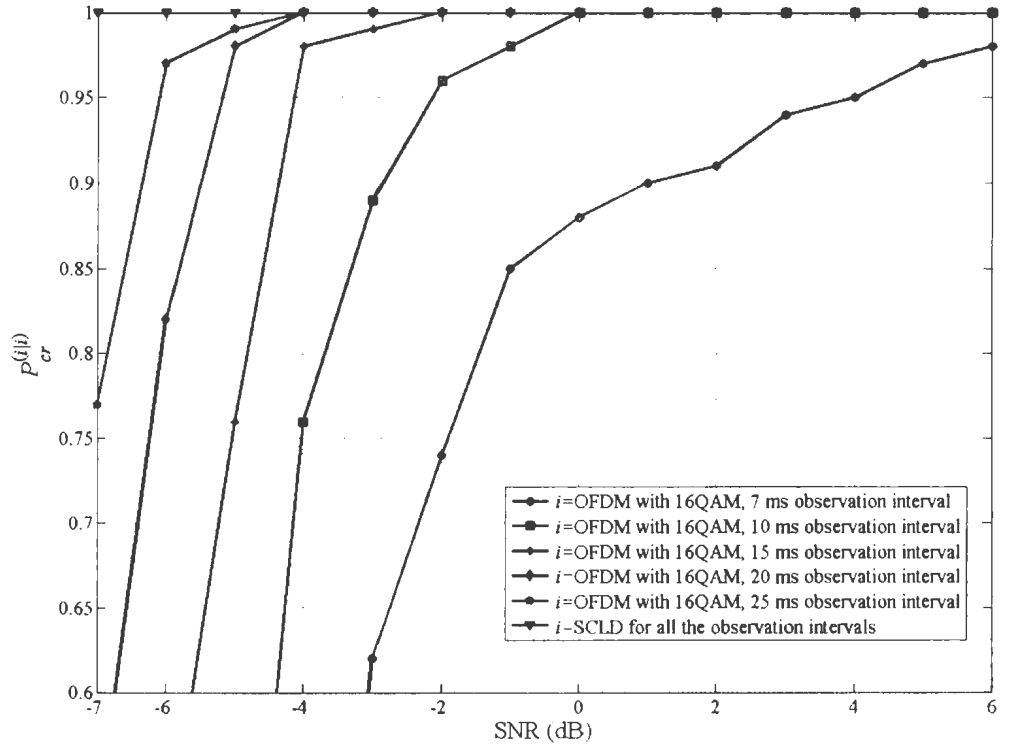

Figure 4.8: The average probability of correct recognition, $P_{cr}^{(i|i)}$, $i = \text{OFDM, SCLD}$, versus SNR in time dispersive channel, for different observation intervals

4. 6. Summary

In this Chapter, we investigate the cyclostationarity of OFDM and SCLD signals, when affected by a time dispersive channel, white Gaussian noise, carrier phase, frequency and timing offsets. We derive the analytical closed-form expressions for the *n*th-order (*q*-conjugate) CCs, *n*th-order (*q*-conjugate) CCPs, and *n*th-order (*q*-conjugate) CFs for OFDM and SCLD signals, and obtain a necessary and sufficient condition on the oversampling factor (per subcarrier) to avoid cycle aliasing. Furthermore, based on the second-order (one-conjugate) CC, we propose an algorithm to discriminate OFDM against SCLD modulations. The proposed recognition algorithm has the advantage that is devoid

of preprocessing tasks, such as symbol timing, carrier and waveform recovery, and signal and noise power estimation.

Chapter 5

Conclusions and Future Work

In this thesis, we investigate the *n*th-order cyclostationarity of orthogonal frequency division multiplexing (OFDM) and single carrier linearly digitally (SCLD) modulated signals affected by additive white Gaussian noise (AWGN) and time dispersive channel, with a view to recognizing OFDM against SCLD modulations. An algorithm is proposed based on a second-order cyclic cumulant to recognize OFDM against SCLD. The proposed recognition algorithm shows good recognition performance even at low signal-to-noise ratio (SNR).

The major contributions of this thesis includes the following:

We investigate the *n*th-order cyclostationarity of OFDM signal embedded in AWGN, and subject to phase, frequency and timing offsets. The analytical closed-form expressions for the *n*th-order (*q*-conjugate) cyclic cumulants (CCs), cycle frequencies (CFs), and cyclic cumulant polyspectra (CCPs) of OFDM signal are derived.

We obtain a necessary and sufficient condition on the oversampling factor (per subcarrier) to avoid cycle aliasing for OFDM signals, when these are affected by AWGN, phase and frequency and timing offsets.

An algorithm based on a second-order CC is proposed to recognize OFDM against SCLD modulations in AWGN channel as an application of signal cyclostationarity to the modulation recognition problem.

We further investigate the nth-order cyclostationarity of OFDM and SCLD modulated signal affected by a time dispersive channel, AWGN, carrier phase, and frequency and timing offsets. The analytical closed-form expressions for the nth-order (q-conjugate) CCs, CFs, and CCPs of such signals are derived.

A necessary and sufficient condition on the oversampling factor (per subcarrier) to eliminate cycle aliasing for both OFDM and SCLD signals are obtained for good and bad channels. It is shown that for good channels, this condition is same as in AWGN.

We extend the applicability of the proposed algorithm in AWGN channel to time dispersive channels. The proposed algorithm obviates that it does not require the preprocessing tasks; such as symbol timing, carrier and waveform recovery, and signal and noise power estimation. This is of practical significance, as algorithms that rely less on preprocessing are of crucial interest for receivers that operate with no prior information in a non-cooperative environment.

The performance of the proposed algorithm is evaluated through computer simulations. It can be noticed that the recognition performance of the proposed algorithm does not depend on the modulation type within the OFDM signal and modulation format used for SCLD in both AWGN and time dispersive channels. In addition, the recognition performance of the time dispersive channel is close to that in AWGN channel.

The computational complexity associated with the proposed recognition algorithm is also investigated. It is shown that the computational complexity mainly depend on the first step of the proposed recognition algorithm.

Suggested future work as follows:

Investigation of the applicability of the proposed algorithm to environment with different propagation characteristics, such as frequency-selective fading.

Study the applicability of signal cyclostatioanrity to blind parameter estimation, such as number of subcarriers, cyclic prefix period and useful symbol periods.

Exploitation of the OFDM signal cyclostationarity for modulation recognition within the OFDM signals.

We will improve the accuracy of the proposed recognitnio algorithm by appropriately choosing K_{min} .

References

[1] J. A. C. Bingham, "Multicarrier modulation for data transmission: an idea for whose time has come," *IEEE Commun. Mag.*, vol. 28, pp. 5-14, 1990.

[2] R. V. Nee and R. Prasad, *OFDM for Wireless Multimedia Communications*. Artech House, 2000.

[3] Part 11: Wireless LAN Medium Access Control (MAC) and Physical Layer (PHY) Specifications: High Speed Physical Layer in the 5GHz, IEEE Standard 802.11a-1999.

[4] Local and Metropolitan Area Networks-Part 16, Air Interface for Fixed Broadband Wireless Access Systems, IEEE Standard IEEE 802.16a-2001.

[5] O. A. Dobre, A. Abdi, Y. Bar-Nees, and W. Su, "A survey of automatic modulation classification techniques: classical approaches and new trends," *IET Commun.*, vol. 1, pp. 137-156, April 2007.

[6] M. Oner and F. Jondral, "Cyclostationarity based air interface recognition for software radio systems," in *Proc. IEEE Conf. on Radio and Wireless,* 2004, pp. 263-266.

[7] M. Oner and F. Jondral, "Air interface recognition for a software radio system exploiting cyclostationarity," in *Proc. IEEE PIMRC*, 2004, pp. 1947-1951.

[8] B. Wang and L. Ge, "A novel algorithm for identification of OFDM signal," in *Proc. IEEE WCNC,* 2005, pp. 261-264.

[9] D. Grimaldi, S. Rapunao, and G. Truglia, "An automatic digital modulation classifier for measurement on telecommunication networks," in *Proc. IEEE IMT*, 2002, pp. 957-962.

[10] W. Akmouche, "Detection of multicarrier modulations using 4th order cumulants," in *Proc. IEEE MILCOM,* 1999, pp. 432-436.

[11] O. A. Dobre, Y. Bar-Nees, and W. Su, "Higher-order cyclic cumulants for high order modulation classification," in *Proc. IEEE MILCOM,* 2003, pp. 112-117.

[12] P. Marchand, J. L. Lacoume, and C. Martret, "Classification of linear modulations by a combination of different orders cyclic cumulants," in *Proc. Workshop on HOS,* 1997, pp. 47-51.

[13] C. M. Spooner, "Classification of co-channel communication signal using cyclic cumulants," in *Proc. IEEE ASILOMAR,* 1995, pp. 531-536.

[14] C. M. Spooner, W. A. Brown, and G. K. Yeung, "Automatic radio frequency environment analysis," in *Proc. IEEE ASILOMAR*, 2000, pp.1181-1186.

[15] O. A. Dobre, Y. Bar-Nees, and W. Su, "Robust qam modulation classification algorithm based on cyclic cumulants," in *Proc. IEEE WCNC,* 2004, pp. 745-748.

[16] O. A. Dobre, Y. Bar-Nees, and W. Su, "Selection combining for modulation recognition in fading channels," in *Proc. IEEE MILCOM,* 2005, pp. 1-7.

[17] F. Gini and G. B. Giannakis, "Frequency offset and symbol timing recovery in flat-fading channels: A cyclostationary approach," *IEEE Trans. Commun.*, vol. 46, pp. 400-411, 1998.

[18] H. Bolcskei, "Blind estimation of symbol timing and carrier frequency offset in wireless OFDM systems," *IEEE Trans. Commun.*, vol. 49, pp. 988-999, 2001.

[19] M. Oner and F. Jondral, "Cyclostationary-based methods for the extraction of the channel allocation information in a spectrum poling system," in *Proc. IEEE Conf. on Radio and Wireless,* 2004, pp. 279-282.

[20] R. W. Heath and G. B. Giannakis, "Exploiting input cyclostationarity for blind channel identification in OFDM systems," *IEEE Trans. Sig. Proc.*, vol. 47, no. 3, pp. 848-856, 1999.

[21] O. A. Dobre, S. Rajan, and R. Inkol, "A Novel Algorithm for Blind Recognition of M-ary Frequency Shift Keying Modulation," in *Proc. IEEE WCNC*, 2007, Hong Kong.

[22] W. A. Gardner, *Cyclostationarity in Communication and Signal Processing.* IEEE Press, 1994.

[23] A. V. Dandawate and G. B. Giannakis, "Nonparametric polyspectral estimators for kth-order (almost) cyclostationary processes," *IEEE Trans. Inform. Theory*, vol. 40, pp. 67-84, 1994.

[24] A. V. Dandawate and G. B. Giannakis, "Asymptotic theory of mixed time averages and kth-order cyclic moment and cumulant statistics," *IEEE Trans. Inform. Theory,* vol. 41, pp. 216-232, 1995.

[25] C. M. Spooner and W. A. Gardner, "The cumulant theory of cyclostationary time-series, part I: foundation and part II: development and applications," *IEEE Trans. Sig. Proc.*, vol. 42, pp. 3387-3429, 1994.

[26] A. Napolitano, "Cyclic higher-order statistics: input/output relations for discrete- and continuous-time MIMO linear almost-periodically time-variant systems," *IEEE Trans. Sig. Proc.*, vol. 42, pp. 147-166, 1995.

[27] J. G. Proakis, *Digital Communications*, 4th ed. McGraw Hill, 2000.

[28] A. V. Dandawate and G. B. Giannakis, "Statistical test for presence of cyclostationarity," *IEEE Trans. Sig. Proc.*, vol. 42, pp. 2355-2369, 1994.

[29] M. Abramowitz and I. A. Stegun, *Handbook of Mathematical Functions.* Dover Publications, 1972.

[30] http://focus.ti.com/docs/prod/folders/print/tms320c6711d.html

[31] S. K. Mak and A. H. Aghvami, "Detection of trellis-coded modulation on time-dispersive channels," in *Proc. IEEE GLOBECOM,* 1996, pp. 18-22.

[32] L. Nikias and A. P. Petropulu, *Higher-Order Spectra Analysis: A Nonlinear Signal Processing Framework.* Prentice Hall, 1993.

Appendix A

Cyclic Cumulants and Cycle Frequencies of Received OFDM Signal in AWGN Channel

The expressions for the nth-order (q-conjugate) CC and CFs for the received baseband OFDM signal are derived here. With the received baseband OFDM signal as in (3.9), and by using the multi-linearity property of the cumulants [32], the time-varying nth-order (q-conjugate) cumulant of $r_{\text{OFDM}}(t)$ at delay vector $\tilde{\tau}$ can be expressed as follows[2],

$$\tilde{c}_{r_{\text{OFDM}}}(t;\tilde{\boldsymbol{\tau}})_{n,q} = \text{Cum}[r_{\text{OFDM}}(t+\tilde{\tau}_1),\ldots,r_{\text{OFDM}}(t+\tilde{\tau}_{n-q-1}),r^*_{\text{OFDM}}(t+\tilde{\tau}_{n-q}),\ldots,r^*_{\text{OFDM}}(t+\tilde{\tau}_n)], \quad \text{(A.1)}$$

$$\begin{aligned}
&= a^n e^{j(n-2q)\theta} e^{j2\pi(n-2q)\Delta f_c t} e^{j2\pi\Delta f_c \sum_{p=1}^{n}(-)_p \tilde{\tau}_p} \sum_{k_1}\sum_{l_1}\cdots\sum_{k_{n-q-1}}\sum_{l_{n-q-1}}\sum_{k_{n-q}}\sum_{l_{n-q}}\sum_{k_n}\sum_{l_n} \\
&\times \text{Cum}[s_{k_1,l_1},\ldots,s_{k_{n-q-1},l_{n-q-1}},s^*_{k_{n-q},l_{n-q}},\ldots,s^*_{k_n,l_n}] e^{j2\pi k\Delta f_K(t+\tilde{\tau}_1-l_1T-\varepsilon T)}\cdots \\
&\times e^{j2\pi k\Delta f_K(t+\tilde{\tau}_{n-q-1}-l_{n-q-1}T-\varepsilon T)} e^{-j2\pi k\Delta f_K(t+\tilde{\tau}_{n-q}-l_{n-q}T-\varepsilon T)}\cdots e^{-j2\pi k\Delta f_K(t+\tilde{\tau}_n-l_nT-\varepsilon T)} \\
&\times g(t+\tilde{\tau}_1-l_1T-\varepsilon T)\ldots g(t+\tilde{\tau}_{n-q-1}-l_{n-q-1}T-\varepsilon T) \\
&\times g^*(t+\tilde{\tau}_{n-q}-l_{n-q}T-\varepsilon T)\ldots g^*(t+\tilde{\tau}_n-l_nT-\varepsilon T)+\tilde{c}_w(t;\tilde{\boldsymbol{\tau}})_{n,q}, \quad \text{(A.2)}
\end{aligned}$$

where $*$ denotes conjugation.

In the following derivations we consider only the cumulant of the signal component[5]. As the data symbols $\{s_{k,l}\}$ on each subcarrier k, $k=1,\ldots,K$, are i.i.d. and mutually independent for different subcarriers, $\text{Cum}[s_{k_1,l_1},\ldots,s_{k_{n-q-1},l_{n-q-1}},s^*_{k_{n-q},l_{n-q}},\ldots,s^*_{k_n,l_n}]$ equals zero, unless $k_1=\cdots=k_n=k$ and $l_1=\cdots=l_n=l$. This occurs for certain delays, $\tilde{\tau}_p$, $p=1,\ldots,n$.

[5] The cumulant of the noise component has to be added to the final result.

For the OFDM signal, the values of these delays belong to the interval zero to the OFDM symbol period, T (for a rectangular pulse shape). For a non-rectangular pulse shape, this interval exceeds the symbol period. At zero delays, the cumulant magnitude reaches a maximum, as this is calculated for the signal and its identical replicas. At delays equal to the useful symbol period, T_u, the cumulant magnitude reaches a local maximum, due to the existence of the cyclic prefix. Non-zero cumulant magnitudes at delays over the symbol period (for rectangular pulse shape) or beyond (for non-rectangular pulse shape), other than those previously mentioned, are due to the inverse Fast Fourier transform (IFFT) operation. Under such conditions, ($k_1 = \cdots = k_n = k$ and $l_1 = \cdots = l_n = l$), the cumulant $\mathrm{Cum}[s_{k,l},\ldots,s_{k,l},s^*_{k,l},\ldots,s^*_{k,l}]$ is non-zero and equals the nth-order (q-conjugate) cumulant for the signal constellation, $c_{s,n,q}$. With $k_1 = \cdots = k_n = k$, $l_1 = \cdots = l_n = l$, the cumulant $\mathrm{Cum}[s_{k,l},\ldots,s_{k,l},s^*_{k,l},\ldots,s^*_{k,l}] = c_{s,n,q}$ and (A.2) can be further written as,

$$\begin{aligned}\tilde{c}_{r_{\mathrm{OFDM}}}(t;\tilde{\boldsymbol{\tau}})_{n,q} &= a^n c_{s,n,q} e^{j(n-2q)\theta} e^{j2\pi\Delta f_c \sum_{p=1}^{n}(-)_p \tilde{\tau}_p} e^{j2\pi(n-2q)\Delta f_c t} \sum_{k=0}^{K-1} e^{j2\pi k\Delta f_K \sum_{p=1}^{n}(-)_p \tilde{\tau}_p} \\ &\times \sum_{l=-\infty}^{\infty} e^{j2\pi(n-2q)k\Delta f_K (t-lT-\varepsilon T)} \prod_{p=1}^{n} g^{(*)_p}(t+\tilde{\tau}_p - lT - \varepsilon T), \\ &= a^n c_{s,n,q} e^{j(n-2q)\theta} e^{j2\pi\Delta f_c \sum_{p=1}^{n}(-)_p \tilde{\tau}_p} e^{j2\pi(n-2q)\Delta f_c t} \sum_{k=0}^{K-1} e^{j2\pi k\Delta f_K \sum_{p=1}^{n}(-)_p \tilde{\tau}_p} \\ &\times e^{j2\pi(n-2q)k\Delta f_K t} \prod_{p=1}^{n} g^{(*)_p}(t+\tilde{\tau}_p) \otimes \sum_{l=-\infty}^{\infty} \delta(t-lT-\varepsilon T). \end{aligned} \quad \text{(A.3)}$$

The Fourier transform of the nth-order (q-conjugate) time-varying cumulant of the received baseband OFDM signal can be expressed as

$$\Im\{\tilde{c}_{r_{\mathrm{OFDM}}}(t;\tilde{\boldsymbol{\tau}})_{n,q}\} = \int_{-\infty}^{\infty} \tilde{c}_{r_{\mathrm{OFDM}}}(t;\tilde{\boldsymbol{\tau}})_{n,q} e^{-j2\pi\tilde{\gamma}t} dt$$

$$= a^n c_{s,n,q} e^{j(n-2q)\theta} e^{j2\pi\Delta f_c \sum_{p=1}^{n}(-)_p \tilde{\tau}_p} \int_{-\infty}^{\infty} [e^{j2\pi(n-2q)\Delta f_c t} \sum_{k=0}^{K-1} e^{j2\pi k\Delta f_K \sum_{p=1}^{n}(-)_p \tilde{\tau}_p}$$

$$\times e^{j2\pi(n-2q)k\Delta f_K t} \prod_{p=1}^{n} g^{(*)_p}(t+\tilde{\tau}_p) \otimes \sum_{l=-\infty}^{\infty} \delta(t-lT-\varepsilon T)] e^{-j2\pi\tilde{\gamma}t} dt, \qquad \text{(A.4)}$$

where $\Im\{\cdot\}$ denotes the Fourier transform.

By using the convolution theorem, (A.4) can be written as

$$\Im\{\tilde{c}_{r_{\mathrm{OFDM}}}(t;\tilde{\boldsymbol{\tau}})_{n,q}\} = a^n c_{s,n,q} e^{j(n-2q)\theta} e^{j2\pi\Delta f_c \sum_{p=1}^{n}(-)_p \tilde{\tau}_p} \sum_{k=0}^{K-1} e^{j2\pi k\Delta f_K \sum_{p=1}^{n}(-)_p \tilde{\tau}_p} \int_{-\infty}^{\infty} e^{j2\pi(n-2q)\Delta f_c t}$$

$$\times \int_{-\infty}^{\infty} e^{j2\pi(n-2q)k\Delta f_K u} \prod_{p=1}^{n} g^{(*)_p}(u+\tilde{\tau}_p) \sum_{l=-\infty}^{\infty} \delta(t-u-lT-\varepsilon T) e^{-j2\pi\tilde{\gamma}t} du dt. \quad \text{(A.5)}$$

With the change of variables $t-u-\varepsilon T=v$ and $u=u$, and by using the identity $\Im\{\sum_l \delta(t-lT)\} = T^{-1}\sum_l \delta(\tilde{\gamma}-lT^{-1})$, one can easily show that

$$\Im\{\tilde{c}_{r_{\mathrm{OFDM}}}(t;\tilde{\boldsymbol{\tau}})_{n,q}\} = a^n c_{s,n,q} T^{-1} e^{j(n-2q)\theta} e^{j2\pi\Delta f_c \sum_{p=1}^{n}(-)_p \tilde{\tau}_p} e^{-j2\pi(\tilde{\gamma}-(n-2q)\Delta f_c)\varepsilon T} \sum_{k=0}^{K-1} e^{j2\pi k\Delta f_K \sum_{p=1}^{n}(-)_p \tilde{\tau}_p}$$

$$\times \int_{-\infty}^{\infty} e^{j2\pi(n-2q)k\Delta f_K u} \prod_{p=1}^{n} g^{(*)_p}(u+\tilde{\tau}_p) e^{-j2\pi(\tilde{\gamma}-(n-2q)\Delta f_c)u} du$$

$$\times \sum_l \delta(\tilde{\gamma}-(n-2q)\Delta f_c - lT^{-1}). \qquad \text{(A.6)}$$

It can be seen that $\Im\{\tilde{c}_{r_{\mathrm{OFDM}}}(t;\tilde{\boldsymbol{\tau}})_{n,q}\} \neq 0$ only if $\tilde{\gamma} = lT^{-1} + (n-2q)\Delta f_c$, with l as an integer.

By using the notations $\tilde{\beta} = lT^{-1}$ and $u=t$, (A.6) can be written as

$$\Im\{\tilde{c}_{r_{\mathrm{OFDM}}}(t;\tilde{\boldsymbol{\tau}})_{n,q}\} = a^n c_{s,n,q} T^{-1} e^{j(n-2q)\theta} e^{j2\pi\Delta f_c \sum_{p=1}^{n}(-)_p \tilde{\tau}_p} e^{-j2\pi\tilde{\beta}\varepsilon T} \sum_{k=0}^{K-1} e^{j2\pi k\Delta f_K \sum_{p=1}^{n}(-)_p \tilde{\tau}_p}$$
$$\times \int_{-\infty}^{\infty} e^{j2\pi(n-2q)k\Delta f_K t} \prod_{p=1}^{n} g^{(*)_p}(t+\tilde{\tau}_p) e^{-j2\pi\tilde{\beta}t} dt$$
$$\times \sum_{l} \delta(\tilde{\gamma} - (n-2q)\Delta f_c - lT^{-1}). \tag{A.7}$$

By taking the inverse Fourier transform of (A.7) one can easily show that $\tilde{c}_{r_{\mathrm{OFDM}}}(t;\tilde{\boldsymbol{\tau}})_{n,q}$ can be expressed as[5]

$$\tilde{c}_{r_{\mathrm{OFDM}}}(t;\tilde{\boldsymbol{\tau}})_{n,q} = \sum_{\{\tilde{\gamma}\}} B_{\tilde{\gamma}} e^{j2\pi\tilde{\gamma}t}, \tag{A.8}$$

where $\{\tilde{\gamma}\}$ denotes the set $\{\tilde{\gamma} \mid \tilde{\gamma} = \tilde{\beta} + (n-2q)\Delta f_c,\ \tilde{\beta} = lT^{-1}, l \text{ integer}\}$, and $B_{\tilde{\gamma}}$ is the coefficient corresponding to frequency $\tilde{\gamma}$ in the Fourier series expansion of the time-varying cumulant. This implies that the cycle frequency domain is discrete, and the spectrum consists of a set of finite-strength additive components. By using (2.2) and (A.8), one can easily notice that the *n*th-order (*q*-conjugate) CC at CF $\tilde{\gamma}$ [5], and the CFs are respectively given as

$$\tilde{c}_{r_{\mathrm{OFDM}}}(\tilde{\gamma};\tilde{\tau})_{n,q} = a^n c_{s,n,q} T^{-1} e^{j(n-2q)\theta} e^{-j2\pi\tilde{\beta}\varepsilon T} e^{j2\pi\Delta f_c \sum_{p=1}^{n}(-)_p \tilde{\tau}_p} \sum_{k=0}^{K-1} e^{j2\pi k\Delta f_K \sum_{p=1}^{n}(-)_p \tilde{\tau}_p}$$
$$\times \int_{-\infty}^{\infty} \prod_{p=1}^{n} g^{(*)_p}(t+\tilde{\tau}_p) e^{j2\pi(n-2q)k\Delta f_K t} e^{-j2\pi\tilde{\beta}t} dt, \tag{A.9}$$

and

$$\tilde{\kappa}_{n,q}^{\mathrm{OFDM}} = \{\tilde{\gamma} \mid \tilde{\gamma} = \tilde{\beta} + (n-2q)\Delta f_c,\ \tilde{\beta} = lT^{-1},\ l \text{ integer}\}. \tag{A.10}$$

Note that $\tilde{\kappa}_{n,q}^{\mathrm{OFDM}}$ is used here to denote the CFs which corresponds to the *n*th-order (*q*-conjugate) CC of the continuous-time OFDM signal.

Appendix B

Cyclic Cumulant Polyspectrum of Received OFDM Signal in AWGN Channel

The expression for the nth-order (q-conjugate) CCP of the received baseband OFDM signal is derived here. In this derivation, we consider only the signal component (no noise). By replacing (A.9) into (2.9), the nth-order (q-conjugate) CCP of $r_{\mathrm{OFDM}}(t)$ can be expressed as

$$\begin{aligned}
\tilde{C}_{r_{\mathrm{OFDM}}}(\tilde{\gamma};\tilde{\mathbf{f}})_{n,q} &= \int_{-\infty}^{\infty}\cdots\int_{-\infty}^{\infty} c_{r_{\mathrm{OFDM}}}(\tilde{\gamma};\tilde{\boldsymbol{\tau}})_{n,q} e^{-j2\pi\tilde{f}_1\tilde{\tau}_1}\cdots e^{-j2\pi\tilde{f}_{n-1}\tilde{\tau}_{n-1}} d\tilde{\tau}_1\cdots d\tilde{\tau}_{n-1} \\
&= a^n c_{s,n,q} T^{-1} e^{j(n-2q)\theta} e^{-j2\pi\tilde{\beta}\varepsilon T} \int_{-\infty}^{\infty}\cdots\int_{-\infty}^{\infty} e^{j2\pi\Delta f_c \sum_{p=1}^{n}(-)_p\tilde{\tau}_p} \sum_{k=0}^{K-1} e^{j2\pi k\Delta f_K \sum_{p=1}^{n}(-)_p\tilde{\tau}_p} \\
&\times \int_{-\infty}^{\infty} e^{j2\pi(n-2q)k\Delta f_K t} \prod_{p=1}^{n} g^{(*)_p}(t+\tilde{\tau}_p) e^{-j2\pi\tilde{\beta}t} e^{-j2\pi\tilde{f}_1\tilde{\tau}_1}\cdots e^{-j2\pi\tilde{f}_{n-1}\tilde{\tau}_{n-1}} d\tilde{\tau}_1\cdots d\tilde{\tau}_{n-1} dt \\
&= a^n c_{s,n,q} T^{-1} e^{j(n-2q)\theta} e^{-j2\pi\tilde{\beta}\varepsilon T} \sum_{k=0}^{K-1} \int_{-\infty}^{\infty} g^{(*)_n}(t) e^{j2\pi(n-2q)k\Delta f_K t} e^{-j2\pi\tilde{\beta}t} \\
&\times \int_{-\infty}^{\infty} g^{(*)_1}(t+\tilde{\tau}_1) e^{(-)_1 j2\pi\Delta f_c\tilde{\tau}_1} e^{(-)_1 j2\pi k\Delta f_K\tilde{\tau}_1} e^{-j2\pi\tilde{f}_1\tilde{\tau}_1} d\tilde{\tau}_1\cdots \\
&\times \int_{-\infty}^{\infty} g^{(*)_{n-1}}(t+\tilde{\tau}_{n-1}) e^{(-)_{n-1} j2\pi\Delta f_c\tilde{\tau}_{n-1}} e^{(-)_{n-1} j2\pi k\Delta f_K\tilde{\tau}_{n-1}} e^{-j2\pi\tilde{f}_{n-1}\tilde{\tau}_{n-1}} d\tilde{\tau}_{n-1} dt. \qquad \text{(B.1)}
\end{aligned}$$

With a change of variables, i.e., $t = t$, $u_1 = t + \tau_1$, $\cdots$, $u_{n-1} = t + \tau_{n-1}$, (B.1) becomes

$$\tilde{C}_{r_{\mathrm{OFDM}}}(\tilde{\gamma};\tilde{\mathbf{f}})_{n,q} = a^n c_{s,n,q} T^{-1} e^{j(n-2q)\theta} e^{-j2\pi\tilde{\beta}\varepsilon T}$$

$$\times \sum_{k=0}^{K-1} \int_{-\infty}^{\infty} g^{(*)_n}(t) e^{j2\pi(n-2q)k\Delta f_K t} e^{-j2\pi\tilde{\beta}t} e^{j2\pi\sum_{p=1}^{n-1}(-)_p((-)_p\tilde{f}_p-\Delta f_c-k\Delta f_K)t} dt$$

$$\times \int_{-\infty}^{\infty} g^{(*)_1}(u_1) e^{-j2\pi(\tilde{f}_1-(-)_1\Delta f_c-(-)_1 k\Delta f_K)u_1} du_1 \cdots$$

$$\times \int_{-\infty}^{\infty} g^{(*)_{n-1}}(u_{n-1}) e^{-j2\pi(\tilde{f}_{n-1}-(-)_{n-1}\Delta f_c-(-)_{n-1}k\Delta f_K)u_{n-1}} du_{n-1}. \qquad \text{(B.2)}$$

By using that $\int_{-\infty}^{\infty} g(\tilde{\tau}) e^{-j2\pi\tilde{f}\tilde{\tau}} e^{j2\pi\Delta f\tilde{\tau}} d\tilde{\tau} = G(\tilde{f}-\Delta f)$ and $\int_{-\infty}^{\infty} g^{(*)}(\tilde{\tau}) e^{-j2\pi\tilde{f}\tilde{\tau}} e^{j2\pi\Delta f\tilde{\tau}} d\tilde{\tau} = G^*(-\tilde{f}+\Delta f)$,

with $G(\tilde{f})$ as the Fourier transform of $g(t)$ and Δf as a frequency shift, (B.2) can be rewritten as

$$\tilde{C}_{r_{\mathrm{OFDM}}}(\tilde{\gamma};\tilde{\mathbf{f}})_{n,q} = a^n c_{s,n,q} T^{-1} e^{j(n-2q)\theta} e^{-j2\pi\tilde{\beta}\varepsilon T} \sum_{k=0}^{K-1} \prod_{p=1}^{n-1} G^{(*)_p}((-)_p\tilde{f}_p - \Delta f_c - k\Delta f_K)$$

$$\times G^{(*)_n}((-)_n(\tilde{\beta}-(\sum_{p=1}^{n-1}(-)_p((-)_p\tilde{f}_p-\Delta f_c-k\Delta f_K))-(n-2q)k\Delta f_K)). \qquad \text{(B.3)}$$

Appendix C

A Necessary and Sufficient Condition on the Oversampling Factor (per Subcarrier) to Eliminate Cycle Aliasing for OFDM Signals in AWGN Channel

As mentioned in Chapter 2, the *n*th-order (*q*-conjugate) CCP of a discrete-time signal is the periodic extension of the *n*th-order (*q*-conjugate) CCP of the original continuous-time signal, in both spectral and cycle frequency domains. This periodic extension of CCP of the original continuous-time signal leads to two kinds of aliasing, i.e., spectral and cycle aliasing. When sampling is carried out, both spectral and cycle aliasing have to be eliminated. As mentioned in Chapter 2, the Nyquist condition has to be fulfilled in order to eliminate aliasing in the spectral frequency domain. To derive a condition to eliminate cycle aliasing when sampling an OFDM signal, the domain of $\tilde{\gamma}$ for which $\tilde{C}_{r_{\text{OFDM}}}(\tilde{\gamma};\mathbf{f})_{n,q}$ is non-zero has to be first obtained. Here we start with the derivation of this domain for particular values of *n*, *q*, and *K*, i.e., $n=2$, $q=0$, and $K=4$ (Example 1), $n=2$, $q=2$, and $K=4$ (Example 2), $n=2$, $q=1$, and $K=4$ (Example 3), and then we generalize the results to any *n*, *q*, and *K*.

Example 1: $n=2$, $q=0$, and $K=4$.

For these particular values of *n*, *q*, and *K*, (B.3) becomes

$$\tilde{C}_{r_{OFDM}}(\tilde{\gamma};\tilde{f}_1)_{2,0} = a^2 c_{s,2,0} T^{-1} e^{j2\theta} e^{-j2\pi\tilde{\beta}\varepsilon T} [G(\tilde{f}_1 - \Delta f_c) G(\tilde{\beta} - \tilde{f}_1 + \Delta f_c)$$
$$+ G(\tilde{f}_1 - \Delta f_c - \Delta f_K) G(\tilde{\beta} - \tilde{f}_1 + \Delta f_c - \Delta f_K)$$
$$+ G(\tilde{f}_1 - \Delta f_c - 2\Delta f_K) G(\tilde{\beta} - \tilde{f}_1 + \Delta f_c - 2\Delta f_K)$$
$$+ G(\tilde{f}_1 - \Delta f_c - 3\Delta f_K) G(\tilde{\beta} - \tilde{f}_1 + \Delta f_c - 3\Delta f_K)]. \quad \text{(C.1)}$$

By using that $G(\tilde{f}) = |G(\tilde{f})| e^{-j2\pi\tilde{f}\tau_g}$, with τ_g as a time delay, (C.1) can be rewritten as

$$\tilde{C}_{r_{OFDM}}(\tilde{\gamma};\tilde{f}_1)_{2,0} = a^2 c_{s,2,0} T^{-1} e^{j2\theta} e^{-j2\pi\tilde{\beta}\varepsilon T} [|G(\tilde{f}_1 - \Delta f_c)||G(\tilde{\beta} - \tilde{f}_1 + \Delta f_c)|$$
$$+ |G(\tilde{f}_1 - \Delta f_c - \Delta f_K)||G(\tilde{\beta} - \tilde{f}_1 + \Delta f_c - \Delta f_K)| e^{j4\pi\Delta f_K \tau_g}$$
$$+ |G(\tilde{f}_1 - \Delta f_c - 2\Delta f_K)||G(\tilde{\beta} - \tilde{f}_1 + \Delta f_c - 2\Delta f_K)| e^{j8\pi\Delta f_K \tau_g}$$
$$+ |G(\tilde{f}_1 - \Delta f_c - 3\Delta f_K)||G(\tilde{\beta} - \tilde{f}_1 + \Delta f_c - 3\Delta f_K)| e^{j12\pi\Delta f_K \tau_g}] e^{-j2\pi\tilde{\beta}\tau_g}. \quad \text{(C.2)}$$

We seek to find the range of $\tilde{\gamma}$ for which $|\tilde{C}_{r_{OFDM}}(\tilde{\gamma};\tilde{f}_1)_{2,0}| \neq 0$. Based on (C.2), one can identify different cases for which $|\tilde{C}_{r_{OFDM}}(\tilde{\gamma};\tilde{f}_1)_{2,0}|$ is non-zero, as follows:

<u>*Case 1:*</u> (one term out of four, i.e., the first term, from the summation in (C.2) is non-zero):

$$|\tilde{C}_{r_{OFDM}}(\tilde{\gamma};\tilde{f}_1)_{2,0}| \neq 0 \text{ if } \begin{cases} c_{s,2,0} \neq 0 \quad \text{(C 1.1), and} \\ |G(\tilde{f}_1 - \Delta f_c)| \neq 0 \quad \text{(C 1.2), and} \\ |G(\tilde{\beta} - \tilde{f}_1 + \Delta f_c)| \neq 0 \quad \text{(C 1.3), and} \\ |G(\tilde{f}_1 - \Delta f_c - \Delta f_K)| = 0 \quad \text{(C 1.4), and} \\ |G(\tilde{f}_1 - \Delta f_c - 2\Delta f_K)| = 0 \quad \text{(C 1.5), and} \\ |G(\tilde{f}_1 - \Delta f_c - 3\Delta f_K)| = 0 \quad \text{(C 1.6).} \end{cases} \quad \text{(C.3)}$$

Let us consider that $g(t)$ is band-limited to W, with $W = T^{-1}$ (this is valid in our case, in which we use a raised cosine window function [2] and a low-pass receive filter).

Based on the conditions (C 1.2), (C 1.4), (C 1.5), and (C 1.6), and by taking into account that $\Delta f_K = T_u^{-1} > W = T^{-1}$, one can easily show that

$$-W + \Delta f_c < \tilde{f}_1 < -W + \Delta f_c + \Delta f_K. \quad \text{(C.4)}$$

In addition, based on (C 1.3), one can write that

$$-W - \Delta f_c < \tilde{\beta} - \tilde{f}_1 < W - \Delta f_c. \tag{C.5}$$

By using (C.4) and (C.5), it is straightforward that $\tilde{\beta}$ takes values in the range

$$-2W < \tilde{\beta} < \Delta f_K. \tag{C.6}$$

Case 2: (one term out of four, i.e., the second term, from the summation in (C.2) is non-zero):

$$|\tilde{C}_{r_{\text{OFDM}}}(\tilde{\gamma};\tilde{f}_1)_{2,0}| \neq 0 \text{ if } \begin{cases} c_{s,2,0} \neq 0 \quad \text{(C 2.1)}, \quad \text{and} \\ |G(\tilde{f}_1 - \Delta f_c - \Delta f_K)| \neq 0 \quad \text{(C 2.2)}, \quad \text{and} \\ |G(\tilde{\beta} - \tilde{f}_1 + \Delta f_c - \Delta f_K)| \neq 0 \quad \text{(C 2.3)}, \quad \text{and} \\ |G(\tilde{f}_1 - \Delta f_c)| = 0 \quad \text{(C 2.4)}, \quad \text{and} \\ |G(\tilde{f}_1 - \Delta f_c - 2\Delta f_K)| = 0 \quad \text{(C 2.5)}, \quad \text{and} \\ |G(\tilde{f}_1 - \Delta f_c - 3\Delta f_K)| = 0 \quad \text{(C 2.6)}. \end{cases} \tag{C.7}$$

Based on the conditions (C 2.2), (C 2.4), (C 2.5), and (C 2.6), and by taking into account that $\Delta f_K = T_u^{-1} > W = T^{-1}$, one can easily show that

$$W + \Delta f_c < \tilde{f}_1 < -W + \Delta f_c + 2\Delta f_K. \tag{C.8}$$

In addition, based on the condition (C 2.3), one can write that

$$-W - \Delta f_c + \Delta f_K < \tilde{\beta} - \tilde{f}_1 < W - \Delta f_c + \Delta f_K. \tag{C.9}$$

By using (C.8) and (C.9), it is straightforward that $\tilde{\beta}$ takes values in the range

$$\Delta f_K < \tilde{\beta} < 3\Delta f_K. \tag{C.10}$$

Case 3: (one term out of four, i.e., the third term, from the summation in (C.2) is non-zero):

$$|\tilde{C}_{r_{\text{OFDM}}}(\tilde{\gamma};\tilde{f}_1)_{2,0}|\neq 0 \text{ if } \begin{cases} c_{s,2,0}\neq 0 \quad \text{(C 3.1)}, \quad \text{and} \\ |G(\tilde{f}_1-\Delta f_c-2\Delta f_K)|\neq 0 \quad \text{(C 3.2)}, \quad \text{and} \\ |G(\tilde{\beta}-\tilde{f}_1+\Delta f_c-2\Delta f_K)|\neq 0 \quad \text{(C 3.3)}, \quad \text{and} \\ |G(\tilde{f}_1-\Delta f_c)|=0 \quad \text{(C 3.4)}, \quad \text{and} \\ |G(\tilde{f}_1-\Delta f_c-\Delta f_K)|=0 \quad \text{(C 3.5)}, \quad \text{and} \\ |G(\tilde{f}_1-\Delta f_c-3\Delta f_K)|=0 \quad \text{(C 3.6)}. \end{cases} \tag{C.11}$$

Based on the conditions (C 3.2), (C 3.4), (C 3.5), and (C 3.6), and by taking into account that $\Delta f_K = T_u^{-1} > W = T^{-1}$, one can easily show that

$$W+\Delta f_c+\Delta f_K < \tilde{f}_1 < -W+\Delta f_c+3\Delta f_K. \tag{C.12}$$

In addition, based on (C 3.3), one can write that

$$-W-\Delta f_c+2\Delta f_K < \tilde{\beta}-\tilde{f}_1 < W-\Delta f_c+2\Delta f_K. \tag{C.13}$$

By using (C.12) and (C.13), it is straightforward that $\tilde{\beta}$ takes values in the range

$$3\Delta f_K < \tilde{\beta} < 5\Delta f_K. \tag{C.14}$$

Case 4: (one term out of four, i.e., the fourth term, from the summation in (C.2) is non-zero):

$$|\tilde{C}_{r_{\text{OFDM}}}(\tilde{\gamma};\tilde{f}_1)_{2,0}|\neq 0 \text{ if } \begin{cases} c_{s,2,0}\neq 0 \quad \text{(C 4.1)}, \quad \text{and} \\ |G(\tilde{f}_1-\Delta f_c-3\Delta f_K)|\neq 0 \quad \text{(C 4.2)}, \quad \text{and} \\ |G(\tilde{\beta}-\tilde{f}_1+\Delta f_c-3\Delta f_K)|\neq 0 \quad \text{(C 4.3)}, \quad \text{and} \\ |G(\tilde{f}_1-\Delta f_c)|=0 \quad \text{(C 4.4)}, \quad \text{and} \\ |G(\tilde{f}_1-\Delta f_c-\Delta f_K)|=0 \quad \text{(C 4.5)}, \quad \text{and} \\ |G(\tilde{f}_1-\Delta f_c-2\Delta f_K)|=0 \quad \text{(C 4.6)}. \end{cases} \tag{C.15}$$

Based on the conditions (C 4.2), (C 4.4), (C 4.5), and (C 4.6), and by taking into account that $\Delta f_K = T_u^{-1} > W = T^{-1}$, one can easily show that

$$W + \Delta f_c + 2\Delta f_K < \tilde{f}_1 < W + \Delta f_c + 3\Delta f_K . \quad \text{(C.16)}$$

In addition, based on (C 4.3), one can write that

$$-W - \Delta f_c + 3\Delta f_K < \tilde{\beta} - \tilde{f}_1 < W - \Delta f_c + 3\Delta f_K . \quad \text{(C.17)}$$

By using (C.16) and (C.17), it is straightforward that $\tilde{\beta}$ takes values in the range

$$5\Delta f_K < \tilde{\beta} < 2W + 6\Delta f_K . \quad \text{(C.18)}$$

Other cases in which only one term in the summation in (C.2) is non-zero can be identified. Derivations are not shown here, but these can be similarly performed. Results are taken into account when determining the overall range of $\tilde{\beta}$.

In order for $|\tilde{C}_{r_{\text{OFDM}}}(\tilde{\gamma}; \tilde{f}_1)_{2,0}|$ to be non-zero, two terms in the summation in (C.2) can be non-zero. It can be easily shown that only consecutive terms can be non-zero simultaneously (there is no spectral frequency range for which two non-consecutive terms are non-zero). For the case when the first and the second terms are non-zero in the summation in (C.2), one obtains

$$\tilde{C}_{r_{\text{OFDM}}}(\tilde{\gamma}; \tilde{f}_1)_{2,0} = a^2 c_{s,2,0} T^{-1} e^{j2\theta} e^{-j2\pi\tilde{\beta}\varepsilon T} [|G(\tilde{f}_1 - \Delta f_c)||G(\tilde{\beta} - \tilde{f}_1 + \Delta f_c)| + |G(\tilde{f}_1 - \Delta f_c - \Delta f_K)||G(\tilde{\beta} - \tilde{f}_1 + \Delta f_c - \Delta f_K)| e^{j4\pi\Delta f_K \tau_g}] e^{-j2\pi\tilde{\beta}\tau_g} . \quad \text{(C.19)}$$

By using that $|G(\tilde{f}_1 - \Delta f_c)| = |G(\tilde{\beta} - \tilde{f}_1 + \Delta f_c)| = |G(\tilde{f}_1 - \Delta f_c - \Delta f_K)| = |G(\tilde{\beta} - \tilde{f}_1 + \Delta f_c - \Delta f_K)| = |G(\tilde{f}_1)|$ for the whole range of $\tilde{f}_1$, (C.19) can be expressed as

$$\begin{aligned}\tilde{C}_{r_{\text{OFDM}}}(\tilde{\gamma}; \tilde{f}_1)_{2,0} &= a^2 c_{s,2,0} T^{-1} e^{j2\theta} e^{-j2\pi\tilde{\beta}\varepsilon T} |G(\tilde{f}_1)|^2 [1 + e^{j4\pi\Delta f_K \tau_g}] e^{-j2\pi\tilde{\beta}\tau_g} \\ &= a^2 c_{s,2,0} T^{-1} e^{j2\theta} e^{-j2\pi\tilde{\beta}\varepsilon T} |G(\tilde{f}_1)|^2 \frac{\sin(4\pi\Delta f_K \tau_g)}{\sin(2\pi\Delta f_K \tau_g)} e^{j2\pi\Delta f_K \tau_g} e^{-j2\pi\tilde{\beta}\tau_g} . \quad \text{(C.20)}\end{aligned}$$

Note that the identity $1+r=(1-r^2)/(1-r)$ is used in (C.20). Based on (C.20), $|\tilde{C}_{r_{\text{OFDM}}}(\tilde{\gamma};\tilde{f}_1)_{2,0}|$ can be written as follows

$$|\tilde{C}_{r_{\text{OFDM}}}(\tilde{\gamma};\tilde{f}_1)_{2,0}|=|a^2 c_{s,2,0}T^{-1}||G(\tilde{f}_1)|^2|\frac{\sin(4\pi\Delta f_K\tau_g)}{\sin(2\pi\Delta f_K\tau_g)}|. \qquad \text{(C.21)}$$

From (C.21) one can easily notice that $|\frac{\sin(4\pi\Delta f_K\tau_g)}{\sin(2\pi\Delta f_K\tau_g)}|\neq 0$, if $4\pi\Delta f_K\tau_g \neq l\pi$, with l as an odd integer.

This additional condition has also to be satisfied in order for $|\tilde{C}_{r_{\text{OFDM}}}(\tilde{\gamma};\tilde{f}_1)_{2,0}|\neq 0$. Examples of such cases, in which two consecutive terms are non-zero in the summation in (C.2), are given in the following.

Case 5: (two consecutive terms are non-zero in the summation in (C.2), i.e., the first and second terms):

$$|\tilde{C}_{r_{\text{OFDM}}}(\tilde{\gamma};\tilde{f}_1)_{2,0}|\neq 0 \text{ if } \begin{cases} c_{s,2,0}\neq 0 \quad \text{(C 5.1), and} \\ 4\pi\Delta f_K\tau_g \neq l\pi, \quad \text{with } l \text{ as an odd integer} \quad \text{(C 5.2), and} \\ |G(\tilde{f}_1-\Delta f_c)|\neq 0 \quad \text{(C 5.3), and} \\ |G(\tilde{f}_1-\Delta f_c-\Delta f_K)|\neq 0 \quad \text{(C 5.4), and} \\ |G(\tilde{\beta}-\tilde{f}_1+\Delta f_c)|\neq 0 \quad \text{(C 5.5), and} \\ |G(\tilde{\beta}-\tilde{f}_1+\Delta f_c-\Delta f_K)|\neq 0 \quad \text{(C 5.6), and} \\ |G(\tilde{f}_1-\Delta f_c-2\Delta f_K)|=0 \quad \text{(C 5.7), and} \\ |G(\tilde{f}_1-\Delta f_c-3\Delta f_K)|=0 \quad \text{(C 5.8).} \end{cases} \qquad \text{(C.22)}$$

Based on the conditions, (C 5.3), (C 5.4), (C 5.7), and (C 5.8), and by taking into account that $\Delta f_K = T_u^{-1} > W = T^{-1}$, one can easily show that

$$-W + \Delta f_c + \Delta f_K < \tilde{f}_1 < W + \Delta f_c. \tag{C.23}$$

In addition, based on (C 5.5) and (C 5.6), one can write that

$$-W - \Delta f_c + \Delta f_K < \tilde{\beta} - \tilde{f}_1 < W - \Delta f_c. \tag{C.24}$$

By using (C.23) and (C.24), it is straightforward that $\tilde{\beta}$ takes values in the range

$$-2W + 2\Delta f_K < \tilde{\beta} < 2W. \tag{C.25}$$

Other similar cases can be identified, for which the first and second consecutive terms in the summation in (C.2) are non-zero. These are not shown here, but derivation of the range of $\tilde{\beta}$ can be similarly done; note that results are included when determining the overall range of $\tilde{\beta}$.

Case 6: (two consecutive terms are non-zero in the summation in (C.2), i.e., the second and third terms):

$$|\tilde{C}_{r_{\text{OFDM}}}(\tilde{\gamma};\tilde{f}_1)_{2,0}| \neq 0 \text{ if } \begin{cases} c_{s,2,0} \neq 0 \quad \text{(C 6.1), and} \\ 4\pi\Delta f_K \tau_g \neq l\pi, \quad \text{with } l \text{ as an odd integer} \quad \text{(C 6.2), and} \\ |G(\tilde{f}_1 - \Delta f_c - \Delta f_K)| \neq 0 \quad \text{(C 6.3), and} \\ |G(\tilde{f}_1 - \Delta f_c - 2\Delta f_K)| \neq 0 \quad \text{(C 6.4), and} \\ |G(\tilde{\beta} - \tilde{f}_1 + \Delta f_c - \Delta f_K)| \neq 0 \quad \text{(C 6.5), and} \\ |G(\tilde{\beta} - \tilde{f}_1 + \Delta f_c - 2\Delta f_K)| \neq 0 \quad \text{(C 6.6), and} \\ |G(\tilde{f}_1 - \Delta f_c)| = 0 \quad \text{(C 6.7), and} \\ |G(\tilde{f}_1 - \Delta f_c - 3\Delta f_K)| = 0 \quad \text{(C 6.8).} \end{cases} \tag{C.26}$$

Based on the conditions (C 6.3), (C 6.4), (C 6.7), and (C 6.8), and by taking into account that $\Delta f_K = T_u^{-1} > W = T^{-1}$, one can easily show that

$$-W + \Delta f_c + 2\Delta f_K < \tilde{f}_1 < W + \Delta f_c + \Delta f_K. \tag{C.27}$$

In addition, based on (C 5.5) and (C 5.6), one can write that

$$-W-\Delta f_c+2\Delta f_K<\tilde{\beta}-\tilde{f}_1<W-\Delta f_c+\Delta f_K. \tag{C.28}$$

By using (C.27) and (C.28), it is straightforward that $\tilde{\beta}$ takes values in the range

$$-2W+4\Delta f_K<\tilde{\beta}<2W+2\Delta f_K. \tag{C.29}$$

Other similar cases can be identified, for which the second and third consecutive terms in the summation in (C.2) are non-zero. These are not shown here, but derivation of the range of $\tilde{\beta}$ can be similarly done; note that results are included when determining the overall range of $\tilde{\beta}$.

Case 7: (two consecutive terms are non-zero in the summation in (C.2), i.e., the third and fourth terms):

$$|\tilde{C}_{r_{\text{OFDM}}}(\tilde{\gamma};\tilde{f}_1)_{2,0}|\neq 0 \text{ if } \begin{cases} c_{s,2,0}\neq 0 \quad \text{(C 7.1), and} \\ 4\pi\Delta f_K\tau_g\neq l\pi, \quad \text{with } l \text{ as an odd integer} \quad \text{(C 7.2), and} \\ |G(\tilde{f}_1-\Delta f_c-2\Delta f_K)|\neq 0 \quad \text{(C 7.3), and} \\ |G(\tilde{f}_1-\Delta f_c-3\Delta f_K)|\neq 0 \quad \text{(C 7.4), and} \\ |G(\tilde{\beta}-\tilde{f}_1+\Delta f_c-2\Delta f_K)|\neq 0 \quad \text{(C 7.5), and} \\ |G(\tilde{\beta}-\tilde{f}_1+\Delta f_c-3\Delta f_K)|\neq 0 \quad \text{(C 7.6), and} \\ |G(\tilde{f}_1-\Delta f_c)|=0 \quad \text{(C 7.7), and} \\ |G(\tilde{f}_1-\Delta f_c-\Delta f_K)|=0 \quad \text{(C 7.8).} \end{cases} \tag{C.30}$$

Based on the conditions (C 7.3), (C 7.4), (C 7.7), and (C 7.8), and by taking into account that $\Delta f_K=T_u^{-1}>W=T^{-1}$, one can easily show that

$$-W+\Delta f_c+3\Delta f_K<\tilde{f}_1<W+\Delta f_c+2\Delta f_K. \tag{C.31}$$

In addition, based on (C 7.5) and (C 7.6), one can write that

$$-W-\Delta f_c+3\Delta f_K<\tilde{\beta}-\tilde{f}_1<W-\Delta f_c+2\Delta f_K. \tag{C.32}$$

By using (C.31) and (C.32), it is straightforward that $\tilde{\beta}$ takes values in the range

$$-2W+6\Delta f_K<\tilde{\beta}<2W+4\Delta f_K. \tag{C.33}$$

Other similar cases can be identified for which consecutive terms in the summation in (C.2) are

non-zero. These are not shown here, but derivation of the range of $\tilde{\beta}$ can be similarly done. Note that results are included when determining the overall range of $\tilde{\beta}$.

It can be easily shown that three or more consecutive terms in the summation in (C.2) cannot be non-zero simultaneously (there is no spectral frequency range for which three terms are non-zero).

By considering all possible cases for which CPP is non-zero, one can find the range of values for $\tilde{\beta}$ as

$$-2W<\tilde{\beta}<2W+6\Delta f_N. \tag{C.34}$$

Example 2: $n=2$, $q=2$, and $K=4$.

For these particular values of n, q, and K, (B.3) becomes

$$\begin{aligned}\tilde{C}_{r_{\text{OFDM}}}(\tilde{\gamma};\tilde{f}_1)_{2,2}=a^2c_{s,2,2}T^{-1}e^{-j2\theta}e^{-j2\pi\tilde{\beta}\varepsilon T}[&G^{(*)}(-\tilde{f}_1-\Delta f_c)G^{(*)}(-\tilde{\beta}+\tilde{f}_1+\Delta f_c)\\&+G^{(*)}(-\tilde{f}_1-\Delta f_c-\Delta f_K)G^{(*)}(-\tilde{\beta}+\tilde{f}_1+\Delta f_c-\Delta f_K)\\&+G^{(*)}(-\tilde{f}_1-\Delta f_c-2\Delta f_K)G^{(*)}(-\tilde{\beta}+\tilde{f}_1+\Delta f_c-2\Delta f_K)\\&+G^{(*)}(-\tilde{f}_1-\Delta f_c-3\Delta f_K)G^{(*)}(-\tilde{\beta}+\tilde{f}_1+\Delta f_c-3\Delta f_K)].\end{aligned} \tag{C.35}$$

By using that $G^{(*)}(-\tilde{f})=G(\tilde{f})$, (C.35) can be written as

$$\tilde{C}_{r_{\text{OFDM}}}(\tilde{\gamma};\tilde{f}_1)_{2,2} = a^2 c_{s,2,2} T^{-1} e^{-j2\theta} e^{-j2\pi\tilde{\beta}\varepsilon T} [|G(\tilde{f}_1+\Delta f_c)||G(\tilde{\beta}-\tilde{f}_1-\Delta f_c)|$$
$$+|G(\tilde{f}_1+\Delta f_c+\Delta f_K)||G(\tilde{\beta}-\tilde{f}_1-\Delta f_c+\Delta f_K)|e^{-j4\pi\Delta f_K\tau_g}$$
$$+|G(\tilde{f}_1+\Delta f_c+2\Delta f_K)||G(\tilde{\beta}-\tilde{f}_1-\Delta f_c+2\Delta f_K)|e^{-j8\pi\Delta f_K\tau_g}$$
$$+|G(\tilde{f}_1+\Delta f_c+3\Delta f_K)||G(\tilde{\beta}-\tilde{f}_1-\Delta f_c+3\Delta f_K)|e^{-j12\pi\Delta f_K\tau_g}]e^{-j2\pi\tilde{\beta}\tau_g}. \quad \text{(C.36)}$$

By performing a similar analysis as in Example 1, one can show that $\tilde{\beta}$ takes values in the range

$$-2W-6\Delta f_K<\tilde{\beta}<2W. \quad \text{(C.37)}$$

Example 3: $n=2$, $q=1$, $K=4$.

For these particular values of n, q, and K, (B.3) becomes

$$\tilde{C}_{r_{\text{OFDM}}}(\tilde{\gamma};\tilde{f}_1)_{2,1} = a^2 c_{s,2,1} T^{-1} e^{-j2\pi\tilde{\beta}\varepsilon T} [|G(\tilde{f}_1-\Delta f_c)||G(\tilde{\beta}-\tilde{f}_1+\Delta f_c)|$$
$$+|G(\tilde{f}_1-\Delta f_c-\Delta f_K)||G(\tilde{\beta}-\tilde{f}_1+\Delta f_c+\Delta f_K)|$$
$$+|G(\tilde{f}_1-\Delta f_c-2\Delta f_K)||G(\tilde{\beta}-\tilde{f}_1+\Delta f_c+2\Delta f_K)|$$
$$+|G(\tilde{f}_1-\Delta f_c-3\Delta f_K)||G(\tilde{\beta}-\tilde{f}_1+\Delta f_c+3\Delta f_K)|]e^{-j2\pi\tilde{\beta}\tau_g}. \quad \text{(C.38)}$$

By performing a similar analysis as in Example 1, one can show that $\tilde{\beta}$ takes values in the range

$$-2W<\tilde{\beta}<2W. \quad \text{(C.39)}$$

Results obtained for the range of $\tilde{\beta}$ for $n=2,4,6,8$, $q=0,\ldots,n$, and $K=4$ are shown in Table C.1.

Table C.1: The range of $\tilde{\beta}$ values for which CPP is non-zero, with $n = 2,4,6,8$, $q = 0,\ldots,n$, and $K = 4$ (for AWGN channel)

Order, n	Number of conjugations, q	Range of $\tilde{\beta}$ values
2	0	$-2W < \tilde{\beta} < 2W + 6\Delta f_K$
2	1	$-2W < \tilde{\beta} < 2W$
2	2	$-2W - 6\Delta f_K < \tilde{\beta} < 2W$
4	0	$-4W < \tilde{\beta} < 4W + 12\Delta f_K$
4	1	$-4W < \tilde{\beta} < 4W + 6\Delta f_K$
4	2	$-4W < \tilde{\beta} < 4W$
4	3	$-4W - 6\Delta f_K < \tilde{\beta} < 4W$
4	4	$-4W - 12\Delta f_K < \tilde{\beta} < 4W$
6	0	$-6W < \tilde{\beta} < 6W + 18\Delta f_K$
6	1	$-6W < \tilde{\beta} < 6W + 12\Delta f_K$
6	2	$-6W < \tilde{\beta} < 6W + 6\Delta f_K$
6	3	$-6W < \tilde{\beta} < 6W$
6	4	$-6W - 6\Delta f_K < \tilde{\beta} < 6W$
6	5	$-6W - 12\Delta f_K < \tilde{\beta} < 6W$
6	6	$-6W - 18\Delta f_K < \tilde{\beta} < 6W$

Order, n	Number of conjugations, q	Range of $\tilde{\beta}$ values
8	0	$-8W < \tilde{\beta} < 8W + 24\Delta f_K$
8	1	$-8W < \tilde{\beta} < 8W + 18\Delta f_K$
8	2	$-8W < \tilde{\beta} < 8W + 12\Delta f_K$
8	3	$-8W < \tilde{\beta} < 8W + 6\Delta f_K$
8	4	$-8W < \tilde{\beta} < 8W$
8	5	$-8W - 6\Delta f_K < \tilde{\beta} < 8W$
8	6	$-8W - 12\Delta f_K < \tilde{\beta} < 8W$
8	7	$-8W - 18\Delta f_K < \tilde{\beta} < 8W$
8	8	$-8W - 24\Delta f_K < \tilde{\beta} < 8W$

The same procedure can be applied for any n, q and K. Note that if n is odd, the CCP is zero, as $c_{s,n,q} = 0$ [11]. With n even, by using the mathematical induction, one can obtain the range of $\tilde{\gamma} = \tilde{\beta} + (n-2q)\Delta f_c$ as

$$\begin{aligned} &-nW + (n-2q)\Delta f_c < \tilde{\gamma} < nW + (n-2q)\Delta f_c + (n-2q)(K-1)\Delta f_K, \quad \text{if} \quad n-2q > 0, \\ &-nW + (n-2q)\Delta f_c + (n-2q)(K-1)\Delta f_K < \tilde{\gamma} < nW + (n-2q)\Delta f_c, \quad \text{if} \quad n-2q < 0, \\ &-nW < \tilde{\gamma} < nW, \quad \text{if} \quad n = 2q. \end{aligned} \tag{C.40}$$

By knowing the possible range of $\tilde{\gamma}$, a necessary and sufficient condition on the oversampling factor per subcarrier, ρ, to eliminate cycle aliasing can be derived for any order n, number of conjugations, q, and number of subcarriers, K. For example, if $n-2q>0$, then, according to (C.40), the range of $\tilde{\gamma}$ values is

$-nW+(n-2q)\Delta f_c < \tilde{\gamma} < nW+(n-2q)\Delta f_c+(n-2q)(K-1)\Delta f_K$. By using this domain of $\tilde{\gamma}$ values with (2.10), one can easily see that f_s has to satisfy the following condition to avoid cycle aliasing

$$f_s - nW+(n-2q)\Delta f_c > nW+(n-2q)\Delta f_c+(n-2q)(K-1)\Delta f_K. \qquad \text{(C.41)}$$

By replacing $f_s = \rho K T_u^{-1}$, $W = T^{-1}$ and $\Delta f_K = T_u^{-1}$ in (C.41), one can obtain the necessary and sufficient condition on the oversampling factor per subcarrier, ρ, to eliminate cycle aliasing as

$$\rho \geq (n-2q)+\left\lceil K^{-1}(2nT_uT^{-1}-(n-2q))\right\rceil \quad \text{if } n-2q>0. \qquad \text{(C.42)}$$

Similarly, for $n-2q<0$ and $n-2q=0$, one can respectively obtain the following necessary and sufficient conditions on ρ as

$$\begin{aligned} &\rho \geq -(n-2q)+\left\lceil K^{-1}(2nT_uT^{-1}+(n-2q))\right\rceil, \quad \text{if} \quad n-2q<0, \\ &\text{and} \\ &\rho \geq \left\lceil 2nT_uK^{-1}T^{-1}\right\rceil, \quad \text{if} \quad n-2q=0. \end{aligned} \qquad \text{(C.43)}$$

Appendix D

Cyclic Cumulants and Cycle Frequencies of OFDM and SCLD Signals in Time Dispersive Channel

The expressions for the nth-order (q-conjugate) CC and CFs for the received baseband OFDM and SCLD signals in time dispersive channel are derived here. We obtain the results for the SCLD as a particular case of OFDM ($K=1$ and $T_{cp}=0$). In the following, we consider only the cumulant of the signal component[5]. With the received baseband OFDM signal as in (4.5) and by using the multi-linearity property of the cumulants [32], the time-varying nth-order (q-conjugate) cumulant of $r_{\mathrm{OFDM}}(t)$ at delay vector $\tilde{\boldsymbol{\tau}}$ can be expressed as[5],

$$
\begin{aligned}
\tilde{c}_{r_{\mathrm{OFDM}}}(t;\tilde{\boldsymbol{\tau}})_{n,q} &= \mathrm{Cum}[r_{\mathrm{OFDM}}(t+\tilde{\tau}_1),\ldots,r_{\mathrm{OFDM}}(t+\tilde{\tau}_{n-q-1}),r^*_{\mathrm{OFDM}}(t+\tilde{\tau}_{n-q}),\ldots,r^*_{\mathrm{OFDM}}(t+\tilde{\tau}_n)] \\
&= a^n e^{j(n-2q)\theta} e^{j2\pi(n-2q)\Delta f_c t} e^{j2\pi\Delta f_c \sum_{p=1}^{n}(-)_p \tilde{\tau}_p} \sum_{k_1=0}^{K-1}\sum_{l_1}\cdots\sum_{k_{n-q-1}=0}^{K-1}\sum_{l_{n-q-1}}\sum_{k_{n-q}=0}^{K-1}\sum_{l_{n-q}}\cdots\sum_{k_n=0}^{K-1}\sum_{l_n} \\
&\times \mathrm{Cum}[s_{k_1,l_1},\ldots,s_{k_{n-q-1},l_{n-q-1}},s^*_{k_{n-q},l_{n-q}},\ldots,s^*_{k_n,l_n}] \\
&\times \sum_{m_1=1}^{M} h(\tilde{\zeta}_{m_1}) e^{j2\pi k\Delta f_K (t-\tilde{\zeta}_{m_1}+\tilde{\tau}_1-l_1T-\varepsilon T)} g(t-\tilde{\zeta}_{m_1}+\tilde{\tau}_1-l_1T-\varepsilon T)\cdots \\
&\times \sum_{m_{n-q-1}=1}^{M} h(\tilde{\zeta}_{m_{n-q-1}}) e^{j2\pi k\Delta f_K (t-\tilde{\zeta}_{m_{n-q-1}}+\tilde{\tau}_{n-q-1}-l_{n-q-1}T-\varepsilon T)} g(t-\tilde{\zeta}_{m_{n-q-1}}+\tilde{\tau}_{n-q-1}-l_{n-q-1}T-\varepsilon T) \\
&\times \sum_{m_{n-q}=1}^{M} h^*(\tilde{\zeta}_{m_{n-q}}) e^{-j2\pi k\Delta f_K (t-\tilde{\zeta}_{m_{n-q}}+\tilde{\tau}_{n-q}-l_{n-q}T-\varepsilon T)} g^*(t-\tilde{\zeta}_{m_{n-q}}+\tilde{\tau}_{n-q}-l_{n-q}T-\varepsilon T)\cdots \\
&\times \sum_{m_n=1}^{M} h^*(\tilde{\zeta}_{m_n}) e^{-j2\pi k\Delta f_K (t-\tilde{\zeta}_{m_n}+\tilde{\tau}_n-l_nT-\varepsilon T)} g^*(t-\tilde{\zeta}_{m_n}+\tilde{\tau}_n-l_nT-\varepsilon T). \qquad \text{(D.1)}
\end{aligned}
$$

As the data symbols $\{s_{k,l}\}$ on each subcarrier k, $k=1,\ldots,K$, are i.i.d. and mutually independent for different subcarriers, the cumulant $\mathrm{Cum}[s_{k_1,l_1},\ldots,s_{k_{n-q-1},l_{n-q-1}},s^*_{k_{n-q},l_{n-q}},\ldots,s^*_{k_n,l_n}]$ equals zero, unless $k_1=\cdots=k_n=k$ and $l_1=\cdots=l_n=l$. This occurs for certain delays, $\tilde{\tau}_p$, $p=1,\ldots,n$. For the OFDM signal, the values of these delays belong to the interval zero to the OFDM symbol period, T (for rectangular pulse shape). For a non-rectangular pulse shape, this interval exceeds the symbol period. At zero delays, the cumulant value reaches a maximum, as this is calculated for the signal and identical replicas. At delays equal to the useful symbol period, T_u, the cumulant value reaches a local maximum, due to the existence of the cyclic prefix. Under the assumption that $\tilde{\zeta}_M < T_{cp}$, local maxima appear at delays around zero and T_u, due to the calculation of the cumulant of the signal and its identical replicas and the existence of the cyclic prefix, respectively; these delay values depend on the channel delays $\tilde{\zeta}_m$, $m=1,\ldots,M$. Non-zero cumulant values at delays over the symbol period (for rectangular pulse shape) or beyond (for non-rectangular pulse shape), other than those previously mentioned, are due to the inverse Fast Fourier transform (IFFT) operation. Under such conditions ($k_1=\cdots=k_n=k$, $l_1=\cdots=l_n=l$), the cumulant $\mathrm{Cum}[s_{k,l},\ldots,s_{k,l},s^*_{k,l},\ldots,s^*_{k,l}]$ is non-zero and equals the nth-order (q-conjugate) cumulant for the signal constellation, $c_{s,n,q}$. With $k_1=\cdots=k_n=k$, $l_1=\cdots=l_n=l$, and $\mathrm{Cum}[s_{k,l},\ldots,s_{k,l},s^*_{k,l},\ldots,s^*_{k,l}]=c_{s,n,q}$, (D.1) can be further written as,

$$\tilde{c}_{r_{\mathrm{OFDM}}}(t;\tilde{\boldsymbol{\tau}})_{n,q} = a^n c_{s,n,q} e^{j(n-2q)\theta} e^{j2\pi\Delta f_c \sum_{p=1}^{n}(-)_p \tilde{\tau}_p} e^{j2\pi(n-2q)\Delta f_c t}$$

$$\times \sum_{k=0}^{K-1} e^{j2\pi k\Delta f_K \sum_{p=1}^{n}(-)_p \tilde{\tau}_p} \sum_{l=-\infty}^{\infty} e^{j2\pi(n-2q)k\Delta f_K (t-lT-\varepsilon T)}$$

$$\times \prod_{p=1}^{n} \sum_{m_p=1}^{M} h^{(*)_p}(\tilde{\zeta}_{m_p}) g^{(*)_p}(t-\tilde{\zeta}_{m_p}+\tilde{\tau}_p-lT-\varepsilon T) e^{-j2\pi k\Delta f_K \sum_{p=1}^{n}(-)_p \tilde{\zeta}_{m_p}}$$

$$= a^n c_{s,n,q} e^{j(n-2q)\theta} e^{j2\pi\Delta f_c \sum_{p=1}^{n}(-)_p \tilde{\tau}_p} e^{j2\pi(n-2q)\Delta f_c t} \sum_{k=0}^{K-1} e^{j2\pi k\Delta f_K \sum_{p=1}^{n}(-)_p \tilde{\tau}_p}$$

$$\times (e^{j2\pi(n-2q)k\Delta f_K t} \prod_{p=1}^{n} \sum_{m_p=1}^{M} h^{(*)_p}(\tilde{\zeta}_{m_p}) g^{(*)_p}(t-\tilde{\zeta}_{m_p}+\tilde{\tau}_p) e^{-j2\pi k\Delta f_K \sum_{p=1}^{n}(-)_p \tilde{\zeta}_{m_p}})$$

$$\otimes \sum_{l=-\infty}^{\infty} \delta(t-lT-\varepsilon T). \qquad \text{(D.2)}$$

The Fourier transform of the nth-order (q-conjugate) time-varying cumulant of the received baseband OFDM signal can be expressed as,

$$\Im\{\tilde{c}_{r_{\mathrm{OFDM}}}(t;\tilde{\boldsymbol{\tau}})_{n,q}\} = \int_{-\infty}^{\infty} \tilde{c}_{r_{\mathrm{OFDM}}}(t;\tilde{\boldsymbol{\tau}})_{n,q} e^{-j2\pi\tilde{\gamma}t} dt$$

$$= a^n c_{s,n,q} e^{j(n-2q)\theta} e^{j2\pi\Delta f_c \sum_{p=1}^{n}(-)_p \tilde{\tau}_p} \int_{-\infty}^{\infty} [e^{j2\pi(n-2q)\Delta f_c t} \sum_{k=0}^{K-1} e^{j2\pi k\Delta f_K \sum_{p=1}^{n}(-)_p \tilde{\tau}_p}$$

$$\times (e^{j2\pi(n-2q)k\Delta f_K t} \prod_{p=1}^{n} \sum_{m_p=1}^{M} h^{(*)_p}(\tilde{\zeta}_{m_p}) g^{(*)_p}(t-\tilde{\zeta}_{m_p}+\tilde{\tau}_p) e^{-j2\pi k\Delta f_K \sum_{p=1}^{n}(-)_p \tilde{\zeta}_{m_p}})$$

$$\otimes \sum_{l=-\infty}^{\infty} \delta(t-lT-\varepsilon T)] e^{-j2\pi\tilde{\gamma}t} dt. \qquad \text{(D.3)}$$

By using the convolution theorem, (D.3) can be written as,

$$\Im\{\tilde{c}_{r_{\mathrm{OFDM}}}(t;\tilde{\boldsymbol{\tau}})_{n,q}\} = a^n c_{s,n,q} e^{j(n-2q)\theta} e^{j2\pi\Delta f_c \sum_{p=1}^{n}(-)_p \tilde{\tau}_p} \sum_{k=0}^{K-1} e^{j2\pi k\Delta f_K \sum_{p=1}^{n}(-)_p \tilde{\tau}_p} \int_{-\infty}^{\infty} e^{j2\pi(n-2q)\Delta f_c t}$$

$$\times \int_{-\infty}^{\infty} e^{j2\pi(n-2q)k\Delta f_K y} \prod_{p=1}^{n} \sum_{m_p=1}^{M} h^{(*)_p}(\tilde{\zeta}_{m_p}) g^{(*)_p}(y - \tilde{\zeta}_{m_p} + \tilde{\tau}_p) e^{-j2\pi k\Delta f_K \sum_{p=1}^{n}(-)_p \tilde{\zeta}_{m_p}}$$

$$\times \sum_{l=-\infty}^{\infty} \delta(t - y - lT - \varepsilon T) e^{-j2\pi\tilde{\gamma}t} dy dt. \qquad \text{(D.4)}$$

With the change of variables $t - y - \varepsilon T = v$ and $y = y$, and by using the identity $\Im\{\sum_l \delta(t - lT)\} = T^{-1}\sum_l \delta(\tilde{\gamma} - lT^{-1})$, one can easily show that

$$\Im\{\tilde{c}_{r_{\mathrm{OFDM}}}(t;\tilde{\boldsymbol{\tau}})_{n,q}\} = a^n c_{s,n,q} T^{-1} e^{j(n-2q)\theta} e^{j2\pi\Delta f_c \sum_{p=1}^{n}(-)_p \tilde{\tau}_p} e^{-j2\pi(\tilde{\gamma}-(n-2q)\Delta f_c)\varepsilon T} \sum_{k=0}^{K-1} e^{j2\pi k\Delta f_K \sum_{p=1}^{n}(-)_p \tilde{\tau}_p}$$

$$\times \int_{-\infty}^{\infty} e^{j2\pi(n-2q)k\Delta f_K y} \prod_{p=1}^{n} \sum_{m_p=1}^{M} h^{(*)_p}(\tilde{\zeta}_{m_p}) g^{(*)_p}(u - \tilde{\zeta}_{m_p} + \tilde{\tau}_p) e^{-j2\pi k\Delta f_K \sum_{p=1}^{n}(-)_p \tilde{\zeta}_{m_p}}$$

$$\times e^{-j2\pi(\tilde{\gamma}-(n-2q)\Delta f_c)y} dy \sum_l \delta(\tilde{\gamma} - (n-2q)\Delta f_c - lT^{-1}). \qquad \text{(D.5)}$$

It can be seen that $\Im\{\tilde{c}_{r_{\mathrm{OFDM}}}(t;\tilde{\boldsymbol{\tau}})_{n,q}\} \neq 0$ only if $\tilde{\gamma} = lT^{-1} + (n-2q)\Delta f_c$, with l as an integer. By using the notations $\tilde{\beta} = lT^{-1}$ and $y = t$, (D.5) can be written as,

$$\Im\{\tilde{c}_{r_{\mathrm{OFDM}}}(t;\tilde{\boldsymbol{\tau}})_{n,q}\} = a^n c_{s,n,q} T^{-1} e^{j(n-2q)\theta} e^{j2\pi\Delta f_c \sum_{p=1}^{n}(-)_p \tilde{\tau}_p} e^{-j2\pi\tilde{\beta}\varepsilon T} \sum_{k=0}^{K-1} e^{j2\pi k\Delta f_K \sum_{p=1}^{n}(-)_p \tilde{\tau}_p}$$

$$\times \int_{-\infty}^{\infty} e^{j2\pi(n-2q)k\Delta f_K t} \prod_{p=1}^{n} \sum_{m_p=1}^{M} h^{(*)_p}(\tilde{\zeta}_{m_p}) g^{(*)_p}(t - \tilde{\zeta}_{m_p} + \tilde{\tau}_p) e^{-j2\pi k\Delta f_K \sum_{p=1}^{n}(-)_p \tilde{\zeta}_{m_p}} e^{-j2\pi\tilde{\beta}t} dt$$

$$\times \sum_l \delta(\tilde{\gamma} - (n-2q)\Delta f_c - lT^{-1}). \qquad \text{(D.6)}$$

By taking the inverse Fourier transform of (D.6) one can easily show that $\tilde{c}_{r_{\mathrm{OFDM}}}(t;\tilde{\boldsymbol{\tau}})_{n,q}$ can be expressed as[5]

$$\tilde{c}_{r_{\text{OFDM}}}(t;\tilde{\boldsymbol{\tau}})_{n,q} = \sum_{\{\tilde{\gamma}\}} B_{\tilde{\gamma}} e^{j2\pi\tilde{\gamma}t}, \tag{D.7}$$

where $\{\tilde{\gamma}\}$ denotes the set $\{\tilde{\gamma} \mid \tilde{\gamma} = \tilde{\beta} + (n-2q)\Delta f_c,\ \tilde{\beta} = lT^{-1}, l \text{ integer}\}$, and $B_{\tilde{\gamma}}$ is the coefficient corresponding to frequency $\tilde{\gamma}$ in the Fourier series expansion of the time-varying cumulant, given by

$$B_{\tilde{\gamma}} = a^n c_{s,n,q} T^{-1} e^{j(n-2q)\theta} e^{-j2\pi\tilde{\beta}\varepsilon T} e^{j2\pi\Delta f_c \sum_{p=1}^{n}(-)_p \tilde{\tau}_p} \sum_{k=0}^{K-1} e^{j2\pi k\Delta f_K \sum_{p=1}^{n}(-)_p \tilde{\tau}_p} \int_{-\infty}^{\infty} \prod_{p=1}^{n} \sum_{m_p=1}^{M} h^{(*)_p}(\tilde{\zeta}_{m_p}) g^{(*)_p}(t - \tilde{\zeta}_{m_p} + \tilde{\tau}_p)$$

$$\times e^{-j2\pi k\Delta f_K \sum_{p=1}^{n}(-)_p \tilde{\zeta}_{m_p}} e^{j2\pi(n-2q)k\Delta f_K t} e^{-j2\pi\tilde{\beta}t} dt .$$

This implies that the cycle frequency domain is discrete, and the spectrum consists of a finite-strength additive components. By using (2.2) and (D.7), one can easily notice that the nth-order (q-conjugate) CC at CF $\tilde{\gamma}$ and delay $\tilde{\tau}$ (see previous comments on the delay values), and the CFs are respectively given as

$$\tilde{c}_{r_{\text{OFDM}}}(\tilde{\gamma};\tilde{\boldsymbol{\tau}})_{n,q} = a^n c_{s,n,q} T^{-1} e^{j(n-2q)\theta} e^{-j2\pi\tilde{\beta}\varepsilon T} e^{j2\pi\Delta f_c \sum_{p=1}^{n}(-)_p \tilde{\tau}_p} \sum_{k=0}^{K-1} e^{j2\pi k\Delta f_K \sum_{p=1}^{n}(-)_p \tilde{\tau}_p}$$

$$\times \int_{-\infty}^{\infty} \prod_{p=1}^{n} \sum_{m_p=1}^{M} h^{(*)_p}(\tilde{\zeta}_{m_p}) g^{(*)_p}(t - \tilde{\zeta}_{m_p} + \tilde{\tau}_p) e^{-j2\pi k\Delta f_K \sum_{p=1}^{n}(-)_p \tilde{\zeta}_{m_p}} e^{j2\pi(n-2q)k\Delta f_K t} e^{-j2\pi\tilde{\beta}t} dt, \tag{D.8}$$

and

$$\tilde{\kappa}_{n,q}^{\text{OFDM}} = \{\tilde{\gamma} \mid \tilde{\gamma} = \tilde{\beta} + (n-2q)\Delta f_c,\ \tilde{\beta} = lT^{-1},\ l \text{ integer}\}. \tag{D.9}$$

For the OFDM signal in AWGN channel, the analytical closed-form expressions for the nth-order (q-conjugate) CC can be obtained form (D.8), when $h(\tilde{\zeta}_{m_1}) = 1$, with $\tilde{\zeta}_{m_1} = 0$, and $h(\tilde{\zeta}_{m_p}) = 0$, $m_p = 2,\ldots,M$, $p = 1,\ldots,n$. Note this is in agreement with results presented in Chapter 3.

As mentioned under the Signal Model Section, SCLD can be obtained as a particular case of OFDM, with K=1 and $T_{cp}=0$ $(T=T_u)$. In such case, the cumulant $\mathrm{Cum}[s_{k_1,l_1},\ldots,s_{k_{n-q-1},l_{n-q-1}},s^*_{k_{n-q},l_{n-q}},\ldots,s^*_{k_n,l_n}]$ reduces to $\mathrm{Cum}[s_{l_1},\ldots,s_{l_{n-q-1}},s^*_{l_{n-q}},\ldots,s^*_{l_n}]$, which equals $c_{s,n,q}$ if $l_1=\cdots=l_n=l$. This occurs for delay values within the symbol interval (for rectangular pulse shape). At zero-delays, the cumulant magnitude reaches a maximum, and as the delay values increase towards the symbol duration, the cumulant value reduces to zero. The delay values for which the CCs are non-zero can exceed the symbol period for a non-rectangular pulse shape. With (D.2), (D.8), and (D.9), the analytical closed-form expressions for the *n*th-order (*q*-conjugate) time varying cumulant, *n*th-order (*q*-conjugate) CC at CF $\tilde{\gamma}$ and delay $\tilde{\tau}$, and CFs for the SCLD signal are respectively given as,

$$\tilde{c}_{r_{\mathrm{SCLD}}}(t;\tilde{\boldsymbol{\tau}})_{n,q}=a^n c_{s,n,q}e^{j(n-2q)\theta}e^{j2\pi(n-2q)\Delta f_c t}e^{j2\pi\Delta f_c\sum_{p=1}^{n}(-)_p\tilde{\tau}_p}$$
$$\times\prod_{p=1}^{n}\sum_{m_p=1}^{M}h^{(*)_p}(\tilde{\zeta}_{m_p})g^{(*)_p}(t-\tilde{\zeta}_{m_p}+\tilde{\tau}_p)\otimes\sum_{l=-\infty}^{\infty}\delta(t-lT-\varepsilon T), \quad \text{(D.10)}$$

$$\tilde{c}_{r_{\mathrm{SCLD}}}(\tilde{\gamma};\tilde{\boldsymbol{\tau}})_{n,q}=a^n c_{s,n,q}T^{-1}e^{j(n-2q)\theta}e^{-j2\pi\tilde{\beta}\varepsilon T}e^{j2\pi\Delta f_c\sum_{p=1}^{n}(-)_p\tilde{\tau}_p}$$
$$\times\int_{-\infty}^{\infty}\prod_{p=1}^{n}\sum_{m_p=1}^{M}h^{(*)_p}(\tilde{\zeta}_{m_p})g^{(*)_p}(t-\tilde{\zeta}_{m_p}+\tilde{\tau}_p)e^{-j2\pi\tilde{\beta}t}dt, \quad \text{(D.11)}$$

and

$$\tilde{\kappa}^{\mathrm{SCLD}}_{n,q}=\{\tilde{\gamma}\,|\,\tilde{\gamma}=\tilde{\beta}+(n-2q)\Delta f_c,\ \tilde{\beta}=lT^{-1},\ l\ \text{integer}\}. \quad \text{(D.12)}$$

Note that $\tilde{\kappa}^{\mathrm{SCLD}}_{n,q}$ is used here to denote the CFs which correspond to the *n*th-order (*q*-conjugate) CC of the continuous-time SCLD signal. For the SCLD signal in AWGN channel, the analytical closed-form expressions for the *n*th-order (*q*-conjugate) CC can be

obtained from (D.11), when $h(\tilde{\zeta}_{m_1}) = 1$, with $\tilde{\zeta}_{m_1} = 0$, and $h(\tilde{\zeta}_{m_p}) = 0$, $m_p = 2,\ldots,M$, $p = 1,\ldots,n$.

Note this is in agreement with results presented in Chapter 3.

Appendix E

Cyclic Cumulant Polyspectrum of OFDM and SCLD Signals in Time Dispersive Channel

The expressions for the nth-order (q-conjugate) CCP of the received baseband OFDM and SCLD signals in a time dispersive channel are derived here. In this derivation, we consider only the signal component (no noise). We obtain the CCP of the SCLD signal as a particular case of OFDM, for $K=1$ and $T_{cp}=0$ $(T=T_u)$. By taking the Fourier transform of (D.8) with respect to $\tilde{\tau}$, the nth-order (q-conjugate) CCP of $r_{\text{OFDM}}(t)$ can be expressed as

$$\tilde{C}_{r_{\text{OFDM}}}(\tilde{\gamma};\tilde{\mathbf{f}})_{n,q} = \int_{-\infty}^{\infty}\cdots\int_{-\infty}^{\infty}\tilde{c}_{r_{\text{OFDM}}}(\tilde{\gamma};\tilde{\boldsymbol{\tau}})_{n,q}\, e^{-j2\pi\tilde{f}_1\tilde{\tau}_1}\cdots e^{-j2\pi\tilde{f}_{n-1}\tilde{\tau}_{n-1}}\, d\tilde{\tau}_1\cdots d\tilde{\tau}_{n-1}$$

$$= a^n c_{s,n,q} T^{-1} e^{j(n-2q)\theta} e^{-j2\pi\tilde{\beta}\varepsilon T} \int_{-\infty}^{\infty}\cdots\int_{-\infty}^{\infty} e^{j2\pi\Delta f_c \sum_{p=1}^{n}(-)_p\tilde{\tau}_p} \sum_{k=0}^{K-1} e^{j2\pi k\Delta f_K \sum_{p=1}^{n}(-)_p\tilde{\tau}_p}$$

$$\times \int_{-\infty}^{\infty}\prod_{p=1}^{n}\sum_{m_p=1}^{M} h^{(*)_p}(\tilde{\zeta}_{m_p}) g^{(*)_p}(t-\tilde{\zeta}_{m_p}+\tilde{\tau}_p)\, e^{-j2\pi k\Delta f_K \sum_{p=1}^{n}(-)_p\tilde{\zeta}_{m_p}} e^{j2\pi(n-2q)k\Delta f_K t}$$

$$\times e^{-j2\pi\tilde{\beta}t} e^{-j2\pi\tilde{f}_1\tilde{\tau}_1}\cdots e^{-j2\pi\tilde{f}_{n-1}\tilde{\tau}_{n-1}}\, d\tilde{\tau}_1\cdots d\tilde{\tau}_{n-1}dt,$$

$$= a^n c_{s,n,q} T^{-1} e^{j(n-2q)\theta} e^{-j2\pi\tilde{\beta}\varepsilon T}$$

$$\times \sum_{k=0}^{K-1}\int_{-\infty}^{\infty}\int_{-\infty}^{\infty}\sum_{m_1=1}^{M} h^{(*)_1}(\tilde{\zeta}_{m_1}) g^{(*)_1}(t-\tilde{\zeta}_{m_1}+\tilde{\tau}_1)$$

$$\times\ e^{-(-)_1 j2\pi k\Delta f_K\tilde{\zeta}_{m_1}} e^{(-)_1 j2\pi k\Delta f_K\tilde{\tau}_1} e^{(-)_1 j2\pi\Delta f_c\tilde{\tau}_1} e^{-j2\pi\tilde{f}_1\tilde{\tau}_1}\, d\tilde{\tau}_1\cdots$$

$$\times \int_{-\infty}^{\infty}\sum_{m_{n-1}=1}^{M} h^{(*)_{n-1}}(\tilde{\zeta}_{m_{n-1}}) g^{(*)_{n-1}}(t-\tilde{\zeta}_{m_{n-1}}+\tilde{\tau}_{n-1})$$

$$\times e^{-(-)_{n-1} j2\pi k\Delta f_K\tilde{\zeta}_{m_{n-1}}} e^{(-)_{n-1} j2\pi k\Delta f_K\tilde{\tau}_{n-1}} e^{(-)_{n-1} j2\pi\Delta f_c\tilde{\tau}_{n-1}} e^{-j2\pi\tilde{f}_{n-1}\tilde{\tau}_{n-1}}\, d\tilde{\tau}_{n-1}$$

$$\times \sum_{m_n=1}^{M} h^{(*)_n}(\tilde{\zeta}_{m_n}) g^{(*)_n}(t-\tilde{\zeta}_{m_n}) e^{-(-)_n j2\pi k\Delta f_K \tilde{\zeta}_{m_n}} e^{j2\pi(n-2q)k\Delta f_K t} e^{-j2\pi\tilde{\beta}t} dt. \qquad \text{(E.1)}$$

With a change of variables, i.e., $t = t$, $v_1 = t + \tilde{\tau}_1$, $\cdots$, $v_{n-1} = t + \tilde{\tau}_{n-1}$, (E.1) becomes

$$\begin{aligned}
\tilde{C}_{r_{\text{OFDM}}}(\tilde{\gamma};\tilde{\mathbf{f}})_{n,q} &= a^n c_{s,n,q} T^{-1} e^{j(n-2q)\theta} e^{-j2\pi\tilde{\beta}\varepsilon T} \\
&\times \sum_{k=0}^{K-1} \int_{-\infty}^{\infty} \sum_{m_1=1}^{M} h^{(*)_1}(\tilde{\zeta}_{m_1}) e^{-(-)_1 j2\pi k\Delta f_K \tilde{\zeta}_{m_1}} g^{(*)_1}(v_1 - \tilde{\zeta}_{m_1}) e^{-j2\pi(\tilde{f}_1 - (-)_1 \Delta f_c - (-)_1 k\Delta f_K) v_1} dv_1 \cdots \\
&\times \int_{-\infty}^{\infty} \sum_{m_{n-1}=1}^{M} h^{(*)_{n-1}}(\tilde{\zeta}_{m_{n-1}}) e^{-(-)_{n-1} j2\pi k\Delta f_K \tilde{\zeta}_{m_{n-1}}} g^{(*)_{n-1}}(v_{n-1} - \tilde{\zeta}_{m_{n-1}}) \\
&\times e^{-j2\pi(\tilde{f}_{n-1} - (-)_{n-1}\Delta f_c - (-)_{n-1} k\Delta f_K) v_{n-1}} dv_{n-1} \\
&\times \int_{-\infty}^{\infty} \sum_{m_n=1}^{M} h^{(*)_n}(\tilde{\zeta}_{m_n}) e^{-(-)_n j2\pi k\Delta f_K \tilde{\zeta}_{m_n}} g^{(*)_n}(t - \tilde{\zeta}_{m_n}) \\
&\times e^{j2\pi \sum_{p=1}^{n-1} (-)_p ((-)_p \tilde{f}_p - \Delta f_c - k\Delta f_K) t} e^{-j2\pi(\tilde{\beta} - (n-2q)k\Delta f_K) t} dt. \qquad \text{(E.2)}
\end{aligned}$$

One can notice that the second, third, and fourth lines of (E.2) can be written as a Fourier transform of two convolved functions, and (E.2) becomes

$$\begin{aligned}
\tilde{C}_{r_{\text{OFDM}}}(\tilde{\gamma};\tilde{\mathbf{f}})_{n,q} &= a^n c_{s,n,q} T^{-1} e^{j(n-2q)\theta} e^{-j2\pi\tilde{\beta}\varepsilon T} \\
&\times \sum_{k=0}^{K-1} \int_{-\infty}^{\infty} (h^{(*)_1}(v_1) e^{-(-)_1 j2\pi k\Delta f_K v_1} \otimes g^{(*)_1}(v_1)) e^{-j2\pi(\tilde{f}_1 - (-)_1 \Delta f_c - (-)_1 k\Delta f_K) v_1} dv_1 \cdots \\
&\times \int_{-\infty}^{\infty} (h^{(*)_{n-1}}(v_{n-1}) e^{-(-)_{n-1} j2\pi k\Delta f_K v_{n-1}} \otimes g^{(*)_{n-1}}(v_{n-1})) e^{-j2\pi(\tilde{f}_{n-1} - (-)_{n-1}\Delta f_c - (-)_{n-1} k\Delta f_K) v_{n-1}} dv_{n-1} \\
&\times \int_{-\infty}^{\infty} (h^{(*)_n}(t) e^{-(-)_n j2\pi k\Delta f_K t} \otimes g^{(*)_n}(t)) e^{j2\pi \sum_{p=1}^{n-1} (-)_p ((-)_p \tilde{f}_p - \Delta f_c - k\Delta f_K) t} e^{-j2\pi(\tilde{\beta} - (n-2q)k\Delta f_K) t} dt.
\end{aligned}$$

(E.3)

By using that the Fourier transform of the convolution of two signals is multiplication of their Fourier transforms, and $\int_{-\infty}^{\infty} g(\tilde{\tau}) e^{-j2\pi\tilde{f}\tilde{\tau}} e^{j2\pi\Delta f\tilde{\tau}} d\tilde{\tau} = G(\tilde{f} - \Delta f)$,

$\int_{-\infty}^{\infty} g^{(*)}(\tilde{\tau}) e^{-j2\pi\tilde{f}\tilde{\tau}} e^{j2\pi\Delta f\tilde{\tau}} d\tilde{\tau} = G^*(-\tilde{f} + \Delta f)$, $\int_{-\infty}^{\infty} h(\tilde{\tau}) e^{-j2\pi\tilde{f}\tilde{\tau}} e^{j2\pi\Delta f\tilde{\tau}} d\tilde{\tau} = H(\tilde{f} - \Delta f)$, and

$\int_{-\infty}^{\infty} h^{(*)}(\tilde{\tau}) e^{-j2\pi\tilde{f}\tilde{\tau}} e^{j2\pi\Delta f\tilde{\tau}} d\tilde{\tau} = H^{*}(-\tilde{f}+\Delta f)$, with $G(\tilde{f})$ and $H(\tilde{f})$ as the Fourier transforms of $g(t)$ and $h(t)$ respectively, and Δf as a frequency shift, (E.3) becomes

$$\begin{aligned}\tilde{C}_{r_{\mathrm{OFDM}}}(\tilde{\gamma};\tilde{\mathbf{f}})_{n,q} = {} & a^{n} c_{s,n,q} T^{-1} e^{j(n-2q)\theta} e^{-j2\pi\tilde{\beta}\varepsilon T} \\ & \times \sum_{k=0}^{K-1} \prod_{p=1}^{n-1} H^{(*)_p}((-)_p \tilde{f}_p - \Delta f_c) G^{(*)_p}((-)_p \tilde{f}_p - \Delta f_c - k\Delta f_K) \\ & \times H^{(*)_n}((-)_n(\tilde{\beta} - \sum_{p=1}^{n-1}(-)_p((-)_p \tilde{f}_p - \Delta f_c - k\Delta f_K) - (n-2q)k\Delta f_K) + k\Delta f_K) \\ & \times G^{(*)_n}((-)_n(\tilde{\beta} - \sum_{p=1}^{n-1}(-)_p((-)_p \tilde{f}_p - \Delta f_c - k\Delta f_K) - (n-2q)k\Delta f_K)). \end{aligned} \quad \text{(E.4)}$$

Similarly, one an easily obtain the analytical closed-form expressions for the *n*th-order (*q*-conjugate) CCP of the SCLD signal. This can be also obtained as a particular case of (E.4), for $K=1$ and $T_{cp}=0$ ($T=T_u$), and is given by,

$$\begin{aligned}\tilde{C}_{r_{\mathrm{SCLD}}}(\tilde{\gamma};\tilde{\mathbf{f}})_{n,q} = {} & a^{n} c_{s,n,q} T^{-1} e^{j(n-2q)\theta} e^{-j2\pi\tilde{\beta}\varepsilon T} \prod_{p=1}^{n-1} H^{(*)_p}((-)_p \tilde{f}_p - \Delta f_c) G^{(*)_p}((-)_p \tilde{f}_p - \Delta f_c) \\ & \times H^{(*)_n}((-)_n(\tilde{\beta} - \sum_{p=1}^{n-1}(-)_p((-)_p \tilde{f}_p - \Delta f_c)) \\ & \times G^{(*)_n}((-)_n(\tilde{\beta} - \sum_{p=1}^{n-i}(-)_p((-)_p \tilde{f}_p - \Delta f_c)). \end{aligned} \quad \text{(E.5)}$$

Note that based on (E.4) and (E.5) one can easily obtain the analytical closed-form expressions for the *n*th-order (*q*-conjugate) CCPs of OFDM and SCLD signals in AWGN channel (with $h(t)=\delta(t)$ and $H(\tilde{f})=1$). These results are in agreement with those presented in Chapter 3 for OFDM and SCLD, respectively.

Appendix F

A Necessary and Sufficient Condition on the Oversampling Factor (per Subcarrier) to Eliminate Cycle Aliasing for OFDM and SCLD Signals in Time Dispersive Channel

Similar to the conditions defined in appendix C, here we have derived a necessary and sufficient condition on the oversampling factor (per subcarrier) to eliminate cycle aliasing for both OFDM and SCLD signals.

OFDM signals

First we derive the CF domain for which CPP is non-zero for $n=2$, $q=0$, and $K=4$ (Example 1), $n=2$, $q=2$, and $K=4$ (Example 2), and $n=2$, $q=1$, and $K=4$ (Example 3), and then we generalize the result to any *n*, *q*, and *K*.

Example 1: $n=2$, $q=0$, and $K=4$.

For these particular values of *n*, *q*, and *K*, (E.4) becomes

$$\begin{aligned}\tilde{C}_{r_{\text{OFDM}}}(\tilde{\gamma};\tilde{f}_1)_{2,0} = a^2 c_{s,2,0} T^{-1} e^{j2\theta} e^{-j2\pi\tilde{\beta}\varepsilon T} H(\tilde{f}_1-\Delta f_c)H(\tilde{\beta}-\tilde{f}_1+\Delta f_c)\\ \times[G(\tilde{f}_1-\Delta f_c)G(\tilde{\beta}-\tilde{f}_1+\Delta f_c)\\ + G(\tilde{f}_1-\Delta f_c-\Delta f_K)G(\tilde{\beta}-\tilde{f}_1+\Delta f_c-\Delta f_K)\\ + G(\tilde{f}_1-\Delta f_c-2\Delta f_K)G(\tilde{\beta}-\tilde{f}_1+\Delta f_c-2\Delta f_K)\\ + G(\tilde{f}_1-\Delta f_c-3\Delta f_K)G(\tilde{\beta}-\tilde{f}_1+\Delta f_c-3\Delta f_K)]. \qquad \text{(F.1)}\end{aligned}$$

By using that $G(\tilde{f}) = |G(\tilde{f})| e^{-j2\pi\tilde{f}\tau_g}$ and $H(\tilde{f}) = |H(\tilde{f})| e^{j\phi_H(\tilde{f})}$, with τ_g as a time delay (we assume linear phase for $g(t)$), and $\phi_H(\tilde{f})$ as the channel phase response, (F.1) can be rewritten as,

$$\begin{aligned}\tilde{C}_{r_{\text{OFDM}}}(\tilde{\gamma};\tilde{f}_1)_{2,0} = a^2 c_{s,2,0} T^{-1} e^{j2\theta} e^{-j2\pi\tilde{\beta}\varepsilon T} & |H(\tilde{f}_1 - \Delta f_c)||H(\tilde{\beta} - \tilde{f}_1 + \Delta f_c)| \\ \times [& |G(\tilde{f}_1 - \Delta f_c)||G(\tilde{\beta} - \tilde{f}_1 + \Delta f_c)| \\ & + |G(\tilde{f}_1 - \Delta f_c - \Delta f_K)||G(\tilde{\beta} - \tilde{f}_1 + \Delta f_c - \Delta f_K)| e^{j4\pi\Delta f_K \tau_g} \\ & + |G(\tilde{f}_1 - \Delta f_c - 2\Delta f_K)||G(\tilde{\beta} - \tilde{f}_1 + \Delta f_c - 2\Delta f_K)| e^{j8\pi\Delta f_K \tau_g} \\ & + |G(\tilde{f}_1 - \Delta f_c - 3\Delta f_K)||G(\tilde{\beta} - \tilde{f}_1 + \Delta f_c - 3\Delta f_K)| e^{j12\pi\Delta f_K \tau_g}] e^{j(\phi_{H_1} + \phi_{H_2})} e^{-j2\pi\tilde{\beta}\tau_g},\end{aligned} \tag{F.2}$$

where ϕ_{H_1} and ϕ_{H_2} represent the channel phase response at $\tilde{f}_1 - \Delta f_c$ and $\tilde{\beta} - \tilde{f}_1 + \Delta f_c$, respectively. We seek to find the range of $\tilde{\gamma}$ values for which $|\tilde{C}_{r_{\text{OFDM}}}(\tilde{\gamma};\tilde{f}_1)_{2,0}| \neq 0$. Based on (F.2), one can easily see that,

$$|\tilde{C}_{r_{\text{OFDM}}}(\tilde{\gamma};\tilde{f}_1)_{2,0}| \neq 0 \text{ if } \begin{cases} c_{s,2,0} \neq 0 \quad \text{(F 1.1), and} \\ |H(\tilde{f}_1 - \Delta f_c)| \neq 0 \quad \text{(F 1.2), and} \\ |H(\tilde{\beta} - \tilde{f}_1 + \Delta f_c)| \neq 0 \quad \text{(F 1.3), and} \\ |\tilde{C}^{\text{AWGN}}_{r_{\text{OFDM}}}(\tilde{\gamma};\tilde{f}_1)_{2,0}| \neq 0 \quad \text{(F 1.4),} \end{cases} \tag{F.3}$$

where $|\tilde{C}^{\text{AWGN}}_{r_{\text{OFDM}}}(\tilde{\gamma};\tilde{f}_1)_{2,0}| = a^2 |c_{s,2,0}| T^{-1} [|G(\tilde{f}_1 - \Delta f_c)||G(\tilde{\beta} - \tilde{f}_1 + \Delta f_c)|$

$+ |G(\tilde{f}_1 - \Delta f_c - \Delta f_K)||G(\tilde{\beta} - \tilde{f}_1 + \Delta f_c - \Delta f_K)| e^{j4\pi\Delta f_K \tau_g} + |G(\tilde{f}_1 - \Delta f_c - 2\Delta f_K)||G(\tilde{\beta} - \tilde{f}_1 + \Delta f_c - 2\Delta f_K)| e^{j8\pi\Delta f_K \tau_g}$
$+ |G(\tilde{f}_1 - \Delta f_c - 3\Delta f_K)||G(\tilde{\beta} - \tilde{f}_1 + \Delta f_c - 3\Delta f_K)| e^{j12\pi\Delta f_K \tau_g}]$ is the second-order (zero-conjugate) CCP of the OFDM signal in AWGN channel.

Let us assume that $g(t)$ is band-limited to W. In our case, $g(t) = g^{tr}(t) \otimes g^{rec}(t)$, with $g^{tr}(t)$ as a raised cosine window function [2] that is considered band-limited to T^{-1}, and

$g^{rr}(t)$ as the low-pass receive filter with bandwidth $K\Delta f_K$. As such, one can easily obtain that $W = T^{-1}$. In our discussion we consider two types of channels, i.e., a good channel (there are no spectral nulls in the channel amplitude response) and a bad channel (there are spectral nulls in the channel amplitude response) [27]. When the channel amplitude response has no spectral nulls, then infinite channel bandwidth can be assumed, and (F 1.2) and (F 1.3) are valid for any $\tilde{\beta}$. On the other hand, when the channel amplitude response has spectral nulls, one can easily show from (F 1.2) and (F 1.3) that $\tilde{\beta}$ belongs to a union of open intervals whose endpoints are sums of frequencies at which spectral nulls occur in the channel amplitude response, and this amplitude is non-zero above or below these frequencies. Let us denote the union of these intervals by $\kappa_H^{\tilde{\beta}}$. In addition, based on the condition (F 1.4) (see analysis performed in Appendix C for the AWGN channel), one can write that

$$-2W < \tilde{\beta} < 2W + 6\Delta f_K. \tag{F.4}$$

By using (F.4) and the remarks on the domain of $\tilde{\beta}$ values for good and bad channels, one can conclude the following:

- If the channel is good (there are no spectral nulls in the channel amplitude response), then the range of $\tilde{\beta}$ values is given by (F.4). Note that this also corresponds to the AWGN channel.

- If the channel is bad (there are spectral nulls), then the range of $\tilde{\beta}$ values is given by $\kappa_H^{\tilde{\beta}} \bigcap (-2W, 2W + 6\Delta f_K)$.

Example 2: $n=2$, $q=2$, and $K=4$.

For these particular values of n, q, and K, (E.4) becomes

$$\begin{aligned}\tilde{C}_{r_{\text{OFDM}}}(\tilde{\gamma};\tilde{f}_1)_{2,2} = a^2 c_{s,2,2} T^{-1} e^{-j2\theta} e^{-j2\pi\tilde{\beta}\varepsilon T} H^*(-\tilde{f}_1-\Delta f_c)H^*(-\tilde{\beta}+\tilde{f}_1+\Delta f_c)\\ \times[G^*(-\tilde{f}_1-\Delta f_c)G^*(-\tilde{\beta}+\tilde{f}_1+\Delta f_c)\\ + G^*(-\tilde{f}_1-\Delta f_c-\Delta f_K)G^*(-\tilde{\beta}+\tilde{f}_1+\Delta f_c-\Delta f_K)\\ + G^*(-\tilde{f}_1-\Delta f_c-2\Delta f_K)G^*(-\tilde{\beta}+\tilde{f}_1+\Delta f_c-2\Delta f_K)\\ + G^*(-\tilde{f}_1-\Delta f_c-3\Delta f_K)G^*(-\tilde{\beta}+\tilde{f}_1+\Delta f_c-3\Delta f_K)]. \qquad \text{(F.5)}\end{aligned}$$

By using that $G^{(*)}(-\tilde{f}) = G(\tilde{f})$ and $H^{(*)}(-\tilde{f}) = H(\tilde{f})$, (F.5) can be written as

$$\begin{aligned}\tilde{C}_{r_{\text{OFDM}}}(\tilde{\gamma};\tilde{f}_1)_{2,2} = a^2 c_{s,2,2} T^{-1} e^{-j2\theta} e^{-j2\pi\tilde{\beta}\varepsilon T} \,|H(\tilde{f}_1+\Delta f_c)||H(\tilde{\beta}-\tilde{f}_1-\Delta f_c)|\\ \times[|G(\tilde{f}_1+\Delta f_c)||G(\tilde{\beta}-\tilde{f}_1-\Delta f_c)|\\ + |G(\tilde{f}_1+\Delta f_c+\Delta f_K)||G(\tilde{\beta}-\tilde{f}_1-\Delta f_c+\Delta f_K)|e^{-j4\pi\Delta f_K\tau_g}\\ + |G(\tilde{f}_1+\Delta f_c+2\Delta f_K)||G(\tilde{\beta}-\tilde{f}_1-\Delta f_c+2\Delta f_K)|e^{-j8\pi\Delta f_K\tau_g}\\ + |G(\tilde{f}_1+\Delta f_c+3\Delta f_K)||G(\tilde{\beta}-\tilde{f}_1-\Delta f_c+3\Delta f_K)|e^{-j12\pi\Delta f_K\tau_g}]e^{j(\phi_{H_3}+\phi_{H_4})}e^{-j2\pi\tilde{\beta}\tau_g},\end{aligned}$$

(F.6)

where ϕ_{H_3} and ϕ_{H_4} represent the channel phase response at $\tilde{f}_1+\Delta f_c$ and $\tilde{\beta}-\tilde{f}_1-\Delta f_c$, respectively. By performing a similar analysis as in Example 1, one can show that

If the channel is good (there are no spectral nulls in the channel amplitude response), the range of $\tilde{\beta}$ values is $-2W-6\Delta f_K < \tilde{\beta} < 2W$. Note that this is the same as in the AWGN channel case.

If the channel is bad (there are spectral nulls in the channel amplitude response), then the range of $\tilde{\beta}$ values is $\kappa_H^{\tilde{\beta}} \cap (-2W-6\Delta f_K, 2W)$.

Example 3: $n=2$, $q=1$, $K=4$.

For these particular values of n, q, and K, (E.4) becomes

$$\tilde{C}_{r_{\text{OFDM}}}(\tilde{\gamma};\tilde{f}_1)_{2,1} = a^2 c_{s,2,1} T^{-1} e^{-j2\pi\tilde{\beta}\varepsilon T} \,|H(\tilde{f}_1-\Delta f_c)||H(\tilde{\beta}-\tilde{f}_1+\Delta f_c)|$$
$$\times[|G(\tilde{f}_1-\Delta f_c)||G(\tilde{\beta}-\tilde{f}_1+\Delta f_c)|$$
$$+|G(\tilde{f}_1-\Delta f_c-\Delta f_K)||G(\tilde{\beta}-\tilde{f}_1+\Delta f_c+\Delta f_K)|$$
$$+|G(\tilde{f}_1-\Delta f_c-2\Delta f_K)||G(\tilde{\beta}-\tilde{f}_1+\Delta f_c+2\Delta f_K)|$$
$$+|G(\tilde{f}_1-\Delta f_c-3\Delta f_K)||G(\tilde{\beta}-\tilde{f}_1+\Delta f_c+3\Delta f_K)|]e^{j(\phi_{H_1}+\phi_{H_5})}e^{-j2\pi\tilde{\beta}\tau_g}, \qquad \text{(F.7)}$$

where ϕ_{H_5} represents the channel phase response at $\tilde{\beta}-\tilde{f}_1+\Delta f_c$.

By performing a similar analysis as in Example 1, one can conclude the following:

If the channel is good (there are no spectral nulls in the channel amplitude response), the range of $\tilde{\beta}$ values is $-2W<\tilde{\beta}<2W$. Note that this is the same as in the AWGN channel case.

- If the channel is bad (there are spectral nulls in the channel amplitude response), then the range of $\tilde{\beta}$ values is $\kappa_H^{\tilde{\beta}} \bigcap (-2W, 2W)$.

Results obtained for the range of $\tilde{\beta}$ for $n=2,4,6,8$, $q=0,\ldots,n$, $K=4$, and a good time dispersive channel are the same for the AWGN channel (see Table C.1).

The same procedure can be applied for any *n*, *q* and *K*. Note that if *n* is odd, the *n* th-order CCP is zero, as $c_{s,n,q}=0$. With *n* even, by using the mathematical induction, one can obtain the range of $\tilde{\gamma}=\tilde{\beta}+(n-2q)\Delta f_c$ for the case of a good time dispersive channel, as follows:

If $n-2q>0$, then

$$-nW+(n-2q)\Delta f_c<\tilde{\gamma}<nW+(n-2q)\Delta f_c+(n-2q)(K-1)\Delta f_K, \qquad \text{(F.8)}$$

- If $n-2q<0$, then

$$-nW+(n-2q)\Delta f_c+(n-2q)(K-1)\Delta f_K<\tilde{\gamma}<nW+(n-2q)\Delta f_c, \qquad \text{(F.9)}$$

- If $n = 2q$, then

$$-nW < \tilde{\gamma} < nW. \tag{F.10}$$

Note that these results are identical to those derived for the AWGN channel, given in (3.15).

For a bad channel, the $\tilde{\gamma}$ range is given by the intersection of previous intervals with $\kappa_H^{\tilde{\gamma}}$, where $\kappa_H^{\tilde{\gamma}}$ represents the union of open intervals whose endpoints are the endpoints of the intervals in $\kappa_H^{\tilde{\beta}}$ shifted by $(n-2q)\Delta f_c$.

By knowing the range of CF values, a necessary and sufficient condition on the oversampling factor per subcarrier, ρ, can be derived to eliminate cycle aliasing for any order, *n,* number of conjugations, *q*, number of subcarriers, *K*, frequency separation Δf_K, and channel. Results will be presented here for good channels, i.e., without spectral nulls in the amplitude response. For such channels, with the range of $\tilde{\gamma}$ values as in (F.8)-(F.10), and by using (2.10), one can easily write the condition to avoid cycle aliasing as follows:

- If $n-2q>0$, then

$$f_s - nW + (n-2q)\Delta f_c > nW + (n-2q)\Delta f_c + (n-2q)(K-1)\Delta f_K. \tag{F.11}$$

By replacing $f_s = \rho K T_u^{-1}$ in (F.11), one can obtain the necessary and sufficient condition on the oversampling factor per subcarrier, ρ, to eliminate cycle aliasing as,

$$\rho \geq \left\lceil T_u K^{-1}(2nW + (n-2q)(K-1)\Delta f_K) \right\rceil. \tag{F.12}$$

- If $n-2q<0$, the necessary and sufficient condition on ρ to eliminate cycle aliasing is,

$$\rho \geq \left\lceil T_u K^{-1}(2nW-(n-2q)(K-1)\Delta f_K) \right\rceil. \quad \text{(F.13)}$$

- If $n-2q=0$, the condition can be written as

$$\rho \geq \left\lceil T_u K^{-1}(2nW) \right\rceil. \quad \text{(F.14)}$$

To be noted that these results are identical to those derived for the AWGN channel, given in (3.7). The same reasoning can be applied for bad channels to derive a necessary and sufficient condition on the oversampling factor per subcarrier to eliminate cycle aliasing, given the channel amplitude response.

SCLD signals

The same procedure can be applied to find a necessary and sufficient condition to eliminate cycle aliasing for SCLD signals. However, results for SCLD signals can be also obtained as a particular case of OFDM, with K=1 (single carrier) and T_{cp}=0 $(T=T_u)$. As such, from (F.8)-(F.10) one can obtain the range of $\tilde{\gamma}=\tilde{\beta}+(n-2q)\Delta f_c$ values for SCLD signals and good time dispersive channels as

$$-nW+(n-2q)\Delta f_c < \tilde{\gamma} < nW+(n-2q)\Delta f_c, \quad \text{(F.15)}$$

For any n and q. With $f_s=\rho T^{-1}$ and by using (2.10) and (F.15), a necessary and sufficient condition on the oversampling factor, ρ, to eliminate cycle aliasing can be easily obtained as,

$$\rho \geq \left\lceil T(2nW) \right\rceil. \quad \text{(F.16)}$$

The same reasoning can be applied for bad channels to obtain a condition on the oversampling factor to eliminate cycle aliasing, given the channel amplitude response.

Appendix G

Cyclostationarity Test Used for Decision Making

A cyclostationarity test, which is developed in [28], is presented here for n=2 and q=1. This is used in Step 2 of the proposed recognition algorithm, for decision making. With this test, the presence of a CF is formulated as a binary hypothesis-testing problem, i.e., under hypothesis H_0 the tested frequency β is not a CF at delay τ, and under hypothesis H_1 the tested frequency β is a CF at delay τ. The cyclostationarity test consists of the following three steps.

Step 1:

The second-order (one-conjugate) CC of the received signal $r_i(u)$ is estimated (from L samples) at tested frequency β and delay τ, and a vector $\hat{\mathbf{c}}_{2,1}$ is formed as

$$\hat{\mathbf{c}}_{2,1} = [\mathrm{Re}\{\hat{c}_{r_i}(\beta;\tau)_{2,1}\} \;\; \mathrm{Im}\{\hat{c}_{r_i}(\beta;\tau)_{2,1}\}], \tag{G.1}$$

where $\mathrm{Re}\{\cdot\}$ and $\mathrm{Im}\{\cdot\}$ are the real and imaginary parts, respectively.

Step 2:

A statistic $\Psi_{2,1}$ is computed for the tested frequency β and delay τ,

$$\Psi_{2,1} = L\, \hat{\mathbf{c}}_{2,1}\, \hat{\Sigma}_{2,1}^{-1}\, \hat{\mathbf{c}}_{2,1}^{\dagger}, \tag{G.2}$$

where -1 denotes the matrix inverse and $\hat{\Sigma}_{2,1}$ is an estimate of the covariance matrix

$$\Sigma_{2,1} = \begin{bmatrix} \mathrm{Re}\{(Q_{2,0}+Q_{2,1})/2\} & \mathrm{Im}\{(Q_{2,0}-Q_{2,1})/2\} \\ \mathrm{Im}\{(Q_{2,0}+Q_{2,1})/2\} & \mathrm{Re}\{(Q_{2,1}-Q_{2,0})/2\} \end{bmatrix}, \tag{G.3}$$

with

$$Q_{2,0} = \lim_{L\to\infty} L\mathrm{Cum}[\hat{c}_{r_i}(\beta;\tau)_{2,1}, \hat{c}_{r_i}(\beta;\tau)_{2,1}], \tag{G.4}$$

and

$$Q_{2,1} = \lim_{L\to\infty} L\mathrm{Cum}[\hat{c}_{r_i}(\beta;\tau)_{2,1}, \hat{c}^*_{r_i}(\beta;\tau)_{21}]. \tag{G.5}$$

The covariances $Q_{2,0}$ and $Q_{2,1}$ are given respectively by [28][6]

$$Q_{2,0} = \lim_{L\to\infty} L^{-1}\sum_{l=0}^{L-1}\sum_{\xi=-\infty}^{\infty} \mathrm{Cum}[f_{2,1}(l;\tau), f_{2,1}(l+\xi;\tau)]e^{-j2\pi 2\beta l}e^{-j2\pi\beta\xi}, \tag{G.6}$$

and

$$Q_{2,1} = \lim_{L\to\infty} L^{-1}\sum_{l=0}^{L-1}\sum_{\xi=-\infty}^{\infty} \mathrm{Cum}[f_{2,1}(l;\tau), f^*_{2,1}(l+\xi;\tau)]e^{-j2\pi(-\beta)l}, \tag{G.7}$$

where $f_{2,1}(l;\tau) = r_i(l+\tau)r_i^*(l)$ is the second-order (one-conjugate) lag product.

The estimators for the covariances $Q_{2,0}$ and $Q_{2,1}$ are given respectively by [28][6]

$$\hat{Q}_{2,0} = (LL_{sw})^{-1}\sum_{s=-(L_{sw}-1)/2}^{(L_{sw}-1)/2} W^{(L_{sw})}(s)F_\tau^{(L)}(\beta - sL^{-1})F_\tau^{(L)}(\beta + sL^{-1}), \tag{G.8}$$

and

$$\hat{Q}_{2,1} = (LL_{sw})^{-1}\sum_{s=-(L_{sw}-1)/2}^{(L_{sw}-1)/2} W^{(L_{sw})}(s)F_\tau^{*(L)}(\beta + sL^{-1})F_\tau^{(L)}(\beta + sL^{-1}), \tag{G.9}$$

where $W^{(L_{sw})}$ is a spectral window of length L_{sw} and $F_\tau^{(L)}(\gamma) = \sum_{l=0}^{L-1} r_i(l+\tau)r_i^*(l)e^{-j2\pi\gamma l}$.

Step 3:

The test statistic $\Psi_{2,1}$, calculated for the tested frequency β and delay τ, is compared against a threshold Γ. If $\Psi_{2,1} \geq \Gamma$, we decide that the tested frequency β is a CF at delay τ; otherwise not. The threshold Γ is set for a given probability of false alarm, P_f, which is

[6] These equations are valid for zero-mean processes.

defined as the probability to decide that the tested frequency β is a CF at tested delay τ, when this is actually not. This can be expressed as $P_f = \Pr\{\Psi_{2,1} \geq \Gamma \mid H_0\}$. By using that the statistic $\Psi_{2,1}$ has an asymptotic chi-square distribution with two degrees of freedom under the hypothesis H_0 [28], the threshold Γ is obtained from the tables of the chi-squared distribution for a given probability of false alarm, P_f.